

AD-781 547

THREE-DIMENSIONAL MEASUREMENTS OF THE
VELOCITY IN THE NEAR FLOW FIELD OF A FULL-
SCALE HOVERING ROTOR

Donald W. Boatwright

Mississippi State University

Prepared for:

Army Research Office

January 1974

DISTRIBUTED BY:

NTIS

National Technical Information Service
U. S. DEPARTMENT OF COMMERCE
5285 Port Royal Road, Springfield Va. 22151

COLLEGE OF ENGINEERING ADMINISTRATION

HARRY C. SIMRALL, M.S.
DEAN, COLLEGE OF ENGINEERING

WILLIE L. MCDANIEL, JR., PH.D.
ASSOCIATE DEAN

WALTER R. CARNES, PH.D.
ASSOCIATE DEAN

LAWRENCE J. HILL, M.S.
DIRECTOR, ENGINEERING EXTENSION

CHARLES B. CLIETT, M.S.
AEROPHYSICS & AEROSPACE ENGINEERING

WILLIAM R. FOX, PH.D.
AGRICULTURAL & BIOLOGICAL ENGINEERING

JOHN L. WEEKS, JR., PH.D.
CHEMICAL ENGINEERING

ROBERT M. SCHOLTES, PH.D.
CIVIL ENGINEERING

B. J. BALL, PH.D.
ELECTRICAL ENGINEERING

W. H. EUBANKS, M.ED.
ENGINEERING GRAPHICS

J. E. THOMAS, M.S.
INSTITUTE OF ENGINEERING TECHNOLOGY

FRANK E. COTTON, JR., PH.D.
INDUSTRIAL ENGINEERING

C. T. CARLEY, PH.D.
MECHANICAL ENGINEERING

JOHN I. PAULK, PH.D.
NUCLEAR ENGINEERING

WILLIAM D. MCCAIN, JR., PH.D.
PETROLEUM ENGINEERING

ACCESSION FOR		
NTIS	Write Section	<input checked="" type="checkbox"/>
DDC	Ref. Section	<input type="checkbox"/>
UNANNOUNCED		<input type="checkbox"/>
JUSTIFICATION		
BY		
DISTRIBUTION/AVAILABILITY CODES		
Dist.	AVAIL. and/or SPECIAL	
A		

For additional copies or information
address correspondence to:

ENGINEERING AND INDUSTRIAL RESEARCH STATION
DRAWER DE
MISSISSIPPI STATE UNIVERSITY
MISSISSIPPI STATE, MISSISSIPPI 39762

TELEPHONE (601) 325-2266

Unclassified

Security Classification

DOCUMENT CONTROL DATA - R & D

AD-781547

(Security classification of title, body of abstract and indexing annotation must be entered when the overall report is classified)

1. ORIGINATING ACTIVITY (Corporate author) Mississippi State University Department of Aerophysics and Aerospace Engineering Mississippi State, MS 39762		2a. REPORT SECURITY CLASSIFICATION Unclassified	
		2b. GROUP N/A	
3. REPORT TITLE Three-Dimensional Measurements of the Velocity in the Near Flow Field of a Full-Scale Hovering Rotor			
4. DESCRIPTIVE NOTES (Type of report and inclusive dates) ARO-D Interim Report			
5. AUTHOR(S) (First name, middle initial, last name) Donald W. Boatwright			
6. REPORT DATE January 1974		7a. TOTAL NO. OF PAGES 150	7b. NO. OF REFS 4
8a. CONTRACT OR GRANT NO. DAHC04-68-C-0003		8b. ORIGINATOR'S REPORT NUMBER(S) EIRS-ASE-74-4	
8c. PROJECT NO. Task No T-3-E		8d. OTHER REPORT NO(S) (Any other numbers that may be assigned this report)	
8d.			
10. DISTRIBUTION STATEMENT Approved for public release; Distribution unlimited			
Reproduced by NATIONAL TECHNICAL INFORMATION SERVICE U S Department of Commerce Springfield VA 22151			
11. SUPPLEMENTARY NOTES NONE		12. SPONSORING MILITARY ACTIVITY U. S. Army Research Office - Durham Box CM, Duke Station Durham, North Carolina 27706	
13. ABSTRACT An experimental investigation of the flow field of a hovering helicopter rotor was initiated at Mississippi State University in 1970. The initial results of this work were reported in USAAMRDL TR 72-33. The current report presents additional experimental results obtained during a continuation of the rotor flow study. The experimental measurements were performed on the Mississippi State University rotor whirl tower which was equipped with a 33.5-foot diameter, OH-23B two-bladed rotor. The measurements consisted primarily of velocity surveys of the rotor inflow and wake with measurements below the rotor being confined to the region just below the blades. Some experiments were also performed to determine boundary layer flow phenomena by use of the chemical sublimation technique. Radial distributions of the mean values of the inplane and axial velocity components of the flow at various levels above and below the rotor are presented in the current report in plotted and tabulated form for three test conditions and for blade azimuth increments of 45 degrees. Examples of instantaneous local flow phenomena are also presented with emphasis on local flow characteristics across the helical tip vortices. Analysis of the experimental data included investigations of the tip vortex structural characteristics and path coordinates for each test condition. The results of the blade sublimation tests were used to examine the three-dimensional spanwise characteristics of the boundary layer as affected by rotation, Reynolds number, and induced flow field. A scarcity of comparable experimental data emphasized a need for continued investigation of rotor flow fields and boundary layer phenomena for both large and small rotors of variable geometry and modes of operation.			

DD FORM 1473

REPLACES DD FORM 1473, 1 JAN 64, WHICH IS OBSOLETE FOR ARMY USE.

Unclassified

Security Classification

14.

KEY WORDS

LINK A

LINK 8

LINK C

[illegible]

WT

NAME	ROLE
Mr. J. Edgar Hoover	Director
Mr. Clegg	Chief Clerk
Mr. Glavin	Assistant Director
Mr. Ladd	Assistant Director
Mr. Nichols	Assistant Director
Mr. Rosen	Assistant Director
Mr. Tracy	Assistant Director
Mr. Egan	Assistant Director
Mr. Gurnea	Assistant Director
Mr. Harbo	Assistant Director
Mr. Hendon	Assistant Director
Mr. Pennington	Assistant Director
Mr. Quinn	Assistant Director
Mr. Nease	Assistant Director
Mr. Tamm	Assistant Director
Mr. Winterrowd	Assistant Director
Mr. Mohr	Assistant Director
Mr. Casper	Assistant Director
Mr. Callahan	Assistant Director
Mr. Connelley	Assistant Director
Mr. Felt	Assistant Director
Mr. Gale	Assistant Director
Mr. Rosen	Assistant Director
Mr. Sullivan	Assistant Director
Mr. Tavel	Assistant Director
Mr. Trotter	Assistant Director
Mr. Tele. Room	Telephone Room
Miss Gandy	Miss Gandy

WT

[illegible]

WT

Flow Visualization

ia

Task Number T-3-E
Contract DAHC04-68-C-0003
January 1974

THREE-DIMENSIONAL MEASUREMENTS OF THE
VELOCITY IN THE NEAR FLOW FIELD OF A
FULL-SCALE HOVERING ROTOR

ARO-D Interim Report
EIRS-ASE-74-4

By

Donald W. Boatwright

Prepared by

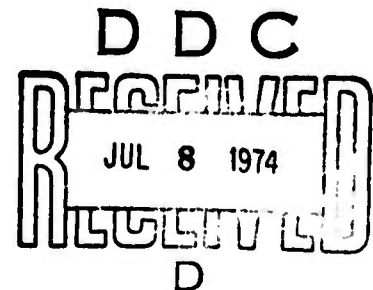
Engineering and Industrial Research Station
Department of Aerophysics and Aerospace Engineering
Mississippi State University
Mississippi State, Mississippi

for

U. S. Army Research Office - Durham
Durham, North Carolina

Approved for public release; distribution unlimited.

//



ABSTRACT

An experimental investigation of the flow field of a hovering helicopter rotor was initiated at Mississippi State University in 1970. The initial results of this work were reported in USAAMRDL TR 72-33. The current report presents additional experimental results obtained during a continuation of the rotor flow study. The experimental measurements were performed on the Mississippi State University rotor whirl tower which was equipped with a 33.5-foot diameter, OH-23B two-bladed rotor. The measurements consisted primarily of velocity surveys of the rotor inflow and wake with measurements below the rotor being confined to the region just below the blades. Some experiments were also performed to determine boundary layer flow phenomena by use of the chemical sublimation technique. Radial distributions of the mean values of the inplane and axial velocity components of the flow at various levels above and below the rotor are presented in the current report in plotted and tabulated form for three test conditions and for blade azimuth increments of 45 degrees. Examples of instantaneous local flow phenomena are also presented with emphasis on local flow characteristics across the helical tip vortices. Analysis of the experimental data included investigations of the tip vortex structural characteristics and path coordinates for each test condition. The results of the blade sublimation tests were used to examine the three-dimensional spanwise characteristics of the boundary layer as affected by rotation, Reynolds number, and induced flow field. A scarcity of comparable experimental data emphasized a need for continued investigation of rotor flow fields and boundary layer phenomena for both large and small rotors of variable geometry and modes of operation.

TABLE OF CONTENTS

	<u>Page</u>
ABSTRACT.	iii
LIST OF ILLUSTRATIONS	vii
LIST OF SYMBOLS	x
INTRODUCTION.	1
TEST FACILITY AND INSTRUMENTATION	3
Whirl Tower and Rotor Installation	3
Anemometer System.	4
Additional Data Acquisition and Reduction Instrumentation. . .	5
CALIBRATION OF INSTRUMENTATION AND ACCURACY OF DATA	6
Thrust Measurement	6
Blade Pitch and Angular Velocity	6
Probe Coordinates.	6
Anemometer System.	7
Accuracy of Test Variables	7
Accuracy of Velocity Measurements.	8
TEST CONDITIONS	10
Rotor Test Parameters.	10
Environmental Conditions	10
DESCRIPTION OF TESTS.	12
Velocity Measurements.	12
Sublimation Studies.	12
DATA REDUCTION.	14
DISCUSSION OF RESULTS	16
Rotor Inflow Measurements.	16
Near Wake Velocity Measurements.	17
Helical Vortex Measurements.	18
Boundary Layer Sublimation Study	20
RESULTS AND CONCLUSIONS	24
RECOMMENDATIONS	25

LITERATURE CITED.	61
APPENDIXES.	62
I. Distributions of Mean Inflow Velocity Components and Standard Deviation Parameters Computed from Experimental Inflow Data, OH-23B Rotor, Hover Condition	62
II. Distributions of Mean Wake Velocity Components and Standard Deviation Parameters Computed from Experimental Wake Survey Data, OH-23B Rotor, Hover Condition.	85

LIST OF ILLUSTRATIONS

<u>Figure</u>		<u>Page</u>
1	Whirl Tower Installation and Access Gantry.	26
2	Mounting Configuration of Total Vector Probe for Inflow Velocity Measurements.	27
3	Total Vector Anemometer System.	28
4	Block Diagram of Data Acquisition and Reduction System.	29
5	Sketch of the Test Installation Showing Vertical Measurement Stations Above and Below the Rotor.	30
6	Whirl Tower Fixed Coordinate System	31
7	Mean Distribution of Inflow Velocity Components and Total Velocity, Test Condition 1, $z/R = 0.1$, $\psi = 45$ deg.	32
8	Mean Distribution of Inflow Velocity Components and Total Velocity, Test Condition 2, $z/R = 0.1$, $\psi = 45$ deg.	33
9	Mean Distribution of Inflow Velocity Components and Total Velocity, Test Condition 3, $z/R = 0.1$, $\psi = 45$ deg.	34
10	Mean Distribution of Inflow Velocity Components and Total Velocity, Test Condition 2, $z/R = 0.2$, $\psi = 45$ deg.	35
11	Mean Distribution of Inflow Velocity Components and Total Velocity, Test Condition 2, $z/R = 0.3$, $\psi = 45$ deg.	36
12	Mean Distribution of Inflow Velocity Components and Total Velocity, Test Condition 2, $z/R = 0.4$, $\psi = 45$ deg.	37
13	Mean Distribution of Inflow Velocity Components and Total Velocity, Test Condition 2, $z/R = 0.1$, $\psi = 0$ deg.	38
14	Time-Dependent Inflow Characteristics at $x/R = 0.3$, Test Condition 2, $z/R = 0.1$	39

<u>Figure</u>		<u>Page</u>
15	Time-Dependent Inflow Characteristics at $x/R = 0.8$, Test Condition 2, $z/R = 0.1$	40
16	Mean Distribution of Wake Velocity Components and Total Velocity, Test Condition 2, $z/R = -0.045$, $\psi = 45$ deg.	41
17	Mean Distribution of Wake Velocity Components and Total Velocity, Test Condition 2, $z/R = -0.15$, $\psi = 0$ deg	42
18	Mean Distribution of Wake Velocity Components and Total Velocity, Test Condition 2, $z/R = -0.30$, $\psi = 90$ deg.	43
19	Mean Distribution of Wake Velocity Components and Total Velocity, Test Condition 2, $z/R = -0.045$, $\psi = 0$ deg	44
20	Extent of Vortex Scatter in the Wake Determined from Radial Velocity Surveys with Respect to Predicted Trajectories.	45
21	Time-Dependent Total Velocity (V_R) and Radial Velocity Component (v_x) Measured Near the Trailing Vortex, Test Condition 1, $z/R = 0$, $x/R = 0.944$	46
22	Time-Dependent Velocity Components v_y and v_z Measured near the Trailing Vortex, Test Condition 1, $z/R = 0$, $x/R = 0.944$	47
23	Distribution of the Instantaneous Velocity Components Across a Trailing Vortex, Test Condition 1, $z/R = 0$, $x/R = 0.944$	48
24	Distribution of the Instantaneous Velocity Components Across a Trailing Vortex, Test Condition 2, $z/R = 0$, $x/R = 0.931$	49
25	Distribution of the Instantaneous Velocity Components Across a Trailing Vortex, Test Condition 3, $z/R = 0$, $x/R = 0.913$	50
26	Distribution of the Instantaneous Velocity Components Across a Trailing Vortex, Test Condition 1, $z/R = -0.25$, $x/R = 0.788$	51

<u>Figure</u>		<u>Page</u>
27	Tip Vortex Coordinates, Test Condition 1.	52
28	Tip Vortex Coordinates, Test Condition 2.	53
29	Tip Vortex Coordinates, Test Condition 3.	54
30	Mean Values of the Vortex Core Radii Determined from Experimental Measurements at Various Distances Below the Rotor	55
31	Values of Tangential Velocity Measured at the Edge of the Vortex Cores.	56
32	Maximum Values of Axial Velocity Measured Near the Center of the Vortex Cores.	57
33	Photographs of the Rotor Blade Tip Section Showing Transition and Turbulent Wedges on the Upper Surface, $\theta_{75} = 2.5$ deg, $\Omega R = 429$ ft/sec.	58
34	Results of Sublimation Tests Using Fluorine on the (a) Upper and (b) Lower Surfaces of the 70-80 Percent Span Test Section, $\theta_{75} = 6.5$ deg, $\Omega R = 604$ ft/sec	59
35	Transition from Laminar to Turbulent Flow on the Test Blade as Determined from Chemical Sublimation Tests . . .	60

LIST OF SYMBOLS

C_T	rotor thrust coefficient; $C_T = \frac{T}{\rho \pi R^2 (\Omega R)^2}$
R	rotor radius, ft
r_c	vortex core radius, ft
T	rotor thrust, lb
v_a	axial velocity in the vortex core measured parallel to the y axis, ft/sec
V_R	instantaneous total velocity magnitude, ft/sec
\bar{V}_R	mean value of the total velocity at a point in the flow, ft/sec
v_t	tangential velocity of the vortex measured in the xz plane, ft/sec
v_x, v_y, v_z	instantaneous velocity components in the flow, ft/sec
$\bar{v}_x, \bar{v}_y, \bar{v}_z$	mean values of the velocity components at a point in the flow, ft/sec
x, y, z	fixed axes of the whirl tower
\bar{x}	radial tip vortex path coordinate, ft
\bar{z}	vertical tip vortex path coordinate measured from the blade tip, ft
ϵ	angle between the mean and instantaneous total velocity vector, deg or rad
θ_{75}	collective pitch angle measured at the three-quarter span station, deg or rad
v_o	absolute value of momentum induced velocity; $v_o = \Omega R \sqrt{\frac{C_T}{2}}$, ft/sec
ρ	density, lb-sec ² /ft ⁴
σ_{V_R}/v_o	standard deviation between instantaneous and mean total velocity magnitude
σ_ϵ	standard deviation of the angle between instantaneous and mean velocity vectors, deg or rad

ψ blade azimuth angle measured counterclockwise from
the positive x axis, deg or rad

Ω rotor angular velocity, rad/sec

INTRODUCTION

This report presents experimental results from an investigation of the flow about a hovering helicopter rotor. The investigation was initiated at Mississippi State University in September of 1970, with the results of the first year of study being reported in Reference 1. The results contained herein were obtained during a period of continued investigation which extended through August 1973.

The major effort of this work was directed toward the acquisition of three-dimensional velocity data in the flow surrounding the rotor. The work was considered of importance since experimental measurements of the wakes of both aircraft wings and rotors have been very limited in the past, and since recent developments in the helicopter and fixed-wing fields have indicated a need for better understanding of the wake properties of lifting aerodynamic surfaces. Also, the test data should be of value since current knowledge of helicopter wake characteristics is based to a large extent upon observed phenomena rather than direct measurements. Additionally, the lack of full-scale rotor wake data has in the past prohibited a full evaluation of the scale effects between model and full-scale rotors.

Because of the apparent need for full-scale wake data, it was the objective of the current study to obtain velocity measurements of the rotor inflow and wake which would provide definition of the major characteristics of flow in the near field of the rotor. Particular emphasis was to be placed upon obtaining a description of the trailing vortex properties. In addition, it was desired that experiments be conducted during the course of the investigation to determine the nature of the flow on the surface of the rotor blades by use of the chemical sublimation technique. In these tests, boundary layer transition phenomena would be observed, and various chemicals evaluated for this purpose. The effects of wind on the rotor wake were also of interest since previous measurements had shown the wake to be sensitive to small crosswinds.

The velocity data obtained during the current investigation are presented in tabular form in Appendixes I and II. These tables give the time-averaged values of total and component velocity magnitude for three test conditions of the rotor and for four blade azimuth angles. Standard deviations of total velocity magnitude and direction at each measurement station in the flow are also presented in the tables. Examples of these data are presented in plotted form as are samples of local instantaneous flow velocities measured at selected points in the flow above and below the rotor. Measured properties of the rotor tip vortices are also presented in addition to the results of the blade boundary layer investigation.

Evaluation of the vortex data obtained during the investigation with respect to data from other sources was limited to comparisons of the

tip vortex path coordinates with the generalized equations of Reference 2. The lack of comparable experimental data further emphasized the need for continued experimental research with rotors of various size, disk loading, and geometry.

The rotor flow investigation was the first performed on the rotor whirl tower at Mississippi State University. As a result, the tower and data acquisition instrumentation and data reduction systems were being used for the first time. The experience gained in this initial effort has indicated several ways in which the instrumentation, test procedures, and data reduction systems could be improved. Some modifications of the test procedure and computer program were made during the course of the investigation, but current results suggest that further refinements could be made to improve the quality of the data. For example, the time-averaged velocity data indicate that the time interval of measurement at each station in the wake should possibly be increased. Also, the velocity data obtained to determine the characteristics of the trailing tip vortices did not produce the quantity of data expected which was suitable for the analysis, thus indicating a need for further improvement of the test procedure. Another significant improvement in future programs will result by utilization of the UNIVAC 1106 computer for plotting of the data, a capability that became available during the course of the present investigation. Some uncertainty yet exists regarding the accuracy of the tower and anemometer instrumentation, but it is expected that these uncertainties can be resolved through modifications of the tower equipment and by the development of improved calibration techniques for the anemometer probe.

The current investigation was limited to the acquisition of the experimental data and presentation of the results. A theoretical analysis of the wake was beyond the scope of the present program.

TEST FACILITY AND INSTRUMENTATION

WHIRL TOWER AND ROTOR INSTALLATION

All tests were conducted on the Mississippi State University rotor whirl tower. This facility was equipped with an OH-13E helicopter engine and drive assembly which was mounted on a load cell arrangement at the top of the tower. The test rotor consisted of standard unmodified OH-23B blades which were adapted to the OH-13E hub. A gantry tower, mounted on railroad tracks, provided access to the upper tower structure and rotor blades. The facility was considered well-suited for the present investigation because its height and small upper diameter were expected to minimize interference effects of the ground plane and tower on the test data. Actual height of the test rotor above the ground plane was 67.92 ft. A photograph of the tower and gantry is shown in Figure 1.

Characteristics of the test rotor were as follows:

disk area	881.41 sq ft
number of blades	2.0
radius	16.75 ft
root chord	1.146 ft
tip chord	0.844 ft
airfoil section	(root) NACA 0018, (tip) NACA 0012
geometric twist	-4.0 deg
root cutout	0.056R
blade weight (each)	86.0 lbs
solidity	0.0357
blade area (each)	15.73 sq ft

The two test blades were matched with one exception. Although both blades were twisted -4 deg (tip down), the root incidence of one blade was 0.25 deg higher than the other. Compensation for this discrepancy was obtained by adjustment of the pitch links of the assembly until no discernable differences of tracking of the two blades could be detected. Tracking was accomplished by using a strobe flash unit at night with small reflectors attached to the blade tips.

The tower hardware included an instrumentation boom which was used to support the anemometer probe in the wake. For wake measurements, the

boom was attached to a vertical framework which was welded to the tower. The installation was designed so that the boom could be raised or lowered to a number of predetermined vertical locations below the rotor.

Measurements above the rotor required that the instrumentation boom be attached to the access gantry. In this case, the anemometer probe was fixed to the end of the boom as shown in Figure 2, and the boom was tilted in the vertical plane to position the probe at a desired height above the rotor disk. With this arrangement, the entire track-mounted gantry and boom assembly could be moved inward or outward with respect to the tower to locate the probe at a desired radial station in the flow.

The load cell arrangement upon which the engine and rotor assembly were mounted provided the means of measuring rotor thrust and torque. The control room of the tower was equipped with standard helicopter instrumentation, thrust and torque meters, a binary counter system for measuring rotor rpm, and a calibrated instrument for blade pitch measurement. The instrumentation also included a wind direction and velocity recorder.

ANEMOMETER SYSTEM

The anemometer used for velocity measurements was a Thermo-Systems, Inc. Model 1080 "total vector" system consisting of a single probe and a control circuit assembly. The velocity-sensitive elements of this anemometer consist of three sensor rods, each of which is a split-film sensor. The rods of the sensor head are orthogonally-mounted to form a cone containing a single temperature sensor. Diameter of the base of the sensor cone is approximately 0.3 in. The components of the anemometer system are shown in Figure 3.

The anemometer operates on 110 volts ac and provides six simultaneous velocity-dependent voltages and one 0-to-5-volt analog temperature signal. These voltages allow computation of the magnitude and direction of the instantaneous velocity vector over a solid angle of 360 deg in a three-dimensional flow field. Calibration constants and data reduction equations are supplied by the manufacturer. Advertised characteristics of the system are as follows:

frequency response	750 Hz
velocity range	0-to-300 ft/sec
sensitivity	0.1 ft/sec
spatial resolution	less than 0.5 in , spherical

For wake measurements, the probe was mounted vertically in the flow on a motor-driven traversing mechanism which was used to position the probe at selected radial stations across the wake.

ADDITIONAL DATA ACQUISITION AND REDUCTION INSTRUMENTATION

In addition to the anemometer, the data acquisition and reduction instrumentation consisted of a 7-channel magnetic tape recorder, two signal conditioners, the binary counter, a data relay box, an HP Model 5610A A/D converter, and an HP Model 2114A computer. A block diagram of the components of the system is shown in Figure 4.

Data signals from the anemometer probe were routed through one of the signal conditioners prior to the recording of these signals on magnetic tape. Signal conditioning consisted of adjusting the probe output voltages to values consistent with the acceptable voltage range of the tape recorder. After conditioning, the data signals were passed to the data relay control box which, in turn, passed the signals to the recorder. The data relay box automatically terminated recording of data after a pre-selected number of revolutions of the rotor. The purpose of the binary counter was to count the number of revolutions of the rotor and to provide the data cut-off signal. The counter also provided digital display of rotor rpm. The second signal conditioner was used to boost the voltage of the blade position reference signal obtained from a magnetic pick-up on the rotor shaft.

In the data reduction procedure, the recorded data signals were fed into the A/D converter and directly processed by the computer.

CALIBRATION OF INSTRUMENTATION AND ACCURACY OF DATA

THRUST MEASUREMENT

The thrust-measuring system of the whirl tower consisted of 4 load cells which supported the entire engine and rotor installation. The total thrust of the rotor was determined by summing the loads calculated from the output of these cells. Calibration data for each load cell were supplied by the manufacturer.

The overall accuracy of the system was checked prior to tests by a static calibration procedure consisting of the application of known vertical loads to the engine-rotor assembly. The results were used to correct indicated thrust values for system error.

A possible source of error was anticipated to be due to changes of mechanical friction in the system with the rotor operating. Since no feasible means of calibrating the system for dynamic error was available, measured performance of the rotor was compared to helicopter performance data from other sources for similar operating conditions of the rotor and engine. The results indicated that dynamic errors were relatively small, although some uncertainty remained because of the inability to determine these errors by direct calibration.

BLADE PITCH AND ANGULAR VELOCITY

Blade pitch measurements were made by use of a calibrated indicator connected to a potentiometer on the swashplate of the rotor. The indicator was calibrated by measuring the true blade collective pitch angles with a propeller protractor. Angular velocity of the rotor was obtained from the digital display of the binary counter output. Accuracy of the system was checked by comparing the indicated angular velocity of the counter with that of a rotating test assembly. An electronic strobe flash unit was utilized to determine the true angular velocity of the test assembly. A second check of the binary counter system could be obtained by comparing its output to the indicated rpm of the calibrated helicopter engine tachometer that was included in the standard instrumentation of the whirl tower. This latter instrument had previously been calibrated on a standard aircraft instrumentation test stand.

PROBE COORDINATES

Vertical positioning of the anemometer probe in the wake was accomplished by raising or lowering the instrumentation boom. The attachment points of the boom to the tower were predetermined by direct measurement. Prior to each test, the boom was leveled and probe alignment carefully checked.

Radial position of the probe was determined by two methods. The first of these utilized a potentiometer which was attached to the traversing

mechanism of the probe in a manner which would provide an indication of radial position. It was found, however, that precise positioning of the probe could be accomplished more readily by the use of a number of micro-switch actuators distributed along the track of the traverse system. Actuation of a micro-switch on the traversing carriage provided a signal (indicator light) that the probe was "on station".

In measuring the inflow velocity data, the vertical height of the probe was fixed by adjusting the orientation of the instrumentation boom with respect to the rotor. During these tests, however, the radial position of the anemometer probe was adjusted by moving the entire access gantry and boom installation either inboard or outboard with respect to the tower. Reference marks on the tracks of the access gantry provided a means of accurately positioning the probe at specific radial stations.

ANEMOMETER SYSTEM

Perhaps the largest source of error in the velocity measurements was associated with the anemometer system. Wind tunnel and other tests that were conducted to calibrate the system revealed that accuracy of the velocity data was strongly related to the orientation of the probe sensors with respect to the direction of the flow. Best accuracy was obtained when the probe shank was aligned with the flow direction. For other orientations, the errors associated with velocity magnitude and direction varied, and the tests conducted failed to produce a correlation between the magnitude of these errors and orientation of the probe.

In the calibration tests of the anemometer system, all of the equipment and procedures of data acquisition and reduction that were to be used in the whirl tower tests were utilized. As a result, it was possible to estimate the overall accuracy of the velocity data based on the largest errors obtained from the wind tunnel calibration tests.

Since the data signals of the anemometer probe were conditioned prior to the recording of these signals on magnetic tape, it was necessary to record calibration voltages for each data channel before the recording of test data. These calibration voltages were carefully measured with a digital voltmeter. Zero-velocity output of the probe was also checked and recorded prior to each test so that any change of the probe characteristics which might have occurred since the previous test could be detected.

On several occasions it was necessary to clean the sensor elements of the probe because of contamination. In the interval of time between the inflow measurements and wake survey measurements, the probe and control box were returned to the manufacturer for reconditioning and recalibration.

ACCURACY OF TEST VARIABLES

Estimates of the accuracy of the rotor test variables were obtained from calibration data and a series of tests that were conducted to

determine the repeatability of rotor thrust coefficient as affected by the degree of accuracy to which rotor speed and collective pitch could be set to specific values during repeated test runs. The results were as follows:

Thrust coefficient (C_T)

Dynamic repeatability	(Test Condition 1)	± 0.000011
	(Test Condition 2)	± 0.000019
	(Test Condition 3)	± 0.000009
Overall accuracy	(All Conditions)	$\pm 0.035C_T$
Collective pitch (θ)		± 0.25 deg
Tip speed (ΩR)		± 10.0 ft/sec

It should be noted that the effects of wind on measured thrust and rotor speed were appreciable at times. These effects were considered in estimating the accuracy of thrust coefficient and tip speed.

The degree of accuracy by which the anemometer probe could be positioned at a specific location in the flow was determined in terms of the non-dimensionalized probe coordinates. The results included the effects of vibration and oscillation of the instrumentation boom due to impingement of the non-steady wake on the cantilevered structure.

Probe position

x/R (radial coordinate)	± 0.00062
z/R (vertical coordinate)	± 0.0075

ACCURACY OF VELOCITY MEASUREMENTS

As mentioned previously, the accuracy of the anemometer system could be estimated only on the basis of available wind tunnel calibration data and from the advertised accuracy of the system. Also to be considered was the fact that probe characteristics were observed to vary somewhat during the test period because of contamination of the sensors and changes of environmental conditions, especially humidity. The advertised accuracy of the anemometer system is ± 3.0 percent of the resultant velocity magnitude and ± 3.0 deg with respect to the direction of the resultant velocity vector. Wind tunnel calibrations have shown agreement with these values when the three probe sensor rods are essentially at the same angle with respect to the resultant velocity vector. Other orientations of the probe produce larger errors. The accuracy of the velocity measurements is, therefore, a function of the direction of the field

velocity with respect to the probe. For the inflow measurements, the probe was positioned in the flow such that the sensor head was below the horizontal plane by 45 degrees as shown in Figure 2. While the accuracy of the velocity data was expected to be decreased with the probe in this position, it was necessary to angle the probe downward to obtain measurements close to the rotor. For wake measurements below the rotor, the probe was positioned upright, and the accuracy of the velocity measurements in the vortex sheet portion of the wake should have been somewhat better than that of the inflow data. In general, the overall accuracy of the inflow and wake velocity data - including the accuracy of all components of the data acquisition and reduction instrumentation - was estimated as shown below:

Inflow and Tip Vortex Measurements

Resultant velocity magnitude (V_R)	$\pm 0.05 V_R$
Angular accuracy	$\pm 8.0 \text{ deg}$

Wake Vortex Sheet

Resultant velocity magnitude (V_R)	$\pm 0.035 V_R$
Angular accuracy	$\pm 3.5 \text{ deg}$

Angular accuracy was based on standard deviations of the direction of the resultant velocity vector obtained from wind tunnel test results. Accuracy of the velocity data across the vortex trails should be considered only as an estimate, at best, since no actual test data for the probe were available for velocities of the magnitude measured near the vortex cores.

TEST CONDITIONS

ROTOR TEST PARAMETERS

Velocity data at each vertical station were obtained for three conditions of rotor operation. The test conditions consisted of three combinations of rotor angular velocity and collective pitch with two of these combinations producing essentially the same value of thrust coefficient. During each test run, the rotor was operated at specific values of indicated rpm and blade pitch, such that the velocity data of successive runs could be compared for the same test conditions of the rotor. Repeating tests at the same true values of the rotor operating parameters proved difficult during the extended course of the investigation, and control of rotor speed and blade pitch was not as good as anticipated. Even though tests were conducted when low wind conditions prevailed, the effects of low wind velocities were evident during test runs when attempting to maintain constant rotor operation. Also, occasional problems with the thrust-measuring load cells and pitch indicator resulted in variations of thrust coefficient which were quite significant. Since the velocity data are presented in non-dimensional form, however, the variations of thrust coefficient should not have significantly affected the validity of comparisons of data obtained from different test runs.

The range of values of the rotor test parameters and thrust coefficients at which the velocity data were obtained were as follows:

<u>Test Condition</u>	<u>ΩR, ft/sec</u>	<u>θ_{75}, deg</u>	<u>C_T</u>
1	628 \pm 6	6.11 \pm 0.16	0.0018 \pm 0.0004
2	444 \pm 10	9.77 \pm 0.19	0.0042 \pm 0.0004
3	452 \pm 8	6.20 \pm 0.16	0.0019 \pm 0.0004

The specific values of each of the above parameters are given for each set of velocity data presented in the Appendixes of this report.

ENVIRONMENTAL CONDITIONS

It was learned through experience that tests would have to be limited to conditions of very low wind velocity and conditions of low atmospheric humidity. The effect of wind in shifting the wake boundaries, i.e., the coordinates of the rotor tip vortices, had previously been observed from earlier tests of the rotor. It was also observed that the humidity of the air affected the zero-velocity output readings of the anemometer system. The most favorable test periods for low wind conditions were found to be just prior to sunrise or shortly after sunset. However, early morning tests were usually prohibited because of high humidity.

As a result, most of the tests were conducted during the early evening hours. In spite of the effort made to obtain velocity data under the most favorable conditions available, the effects of wind on the data were pronounced. This was especially evident when the locations of the tip vortices in the wake were determined from the velocity data. Recordings of wind magnitude and direction were made for each test run in an effort to evaluate the effects of wind on the wake characteristics. In no instances were test runs initiated when wind velocities in excess of 3.0 mph were occurring. During tests, however, wind gusts in excess of this value invariably occurred and in some instances required that the data be discarded. This was done in cases where wind velocity exceeded approximately 6.0 mph. The average wind velocity for all of the tests conducted was 3.1 mph or 4.55 ft/sec.

DESCRIPTION OF TESTS

VELOCITY MEASUREMENTS

The procedure for measuring the velocities in the flow field consisted of positioning the total vector probe at specific radial stations and then recording the 7-channel output of the anemometer system on magnetic tape. The analog data could then be played back into the A/D converter and computer to obtain a digital output of the wake velocity components at each measurement station in the flow.

Prior to each test, the instrumentation boom was positioned so that the probe sensors would be located at the desired vertical distance above or below the rotor. In wake tests, the probe was traversed along the boom to specific radial stations in the wake. Inflow measurements were made by fixing the probe to the boom, and then moving the entire boom and gantry assembly outboard on the gantry tracks. The tracks were calibrated in increments of radial distance equal to one tenth of the blade radius from $x/R = 0$ to $x/R = 1.5$. In contrast, a total of 52 radial stations was used during the velocity surveys below the rotor with radial measurement stations located 1.26 inch apart ($\Delta x/R = 0.00625$) from $x/R = 0.7$ to $x/R = 1.0$. The closely spaced stations in this region were intended to produce greater detail of the velocity distributions across the trailing tip vortices.

After installation of the probe on the instrumentation boom and prior to engine start, the zero-velocity output of each data channel of the probe was measured and checked to insure proper operation of the anemometer system. The engine was then started and calibration voltages were fed through the data system and recorded on the data tape. After smooth operation of the rotor was obtained at the desired values of blade pitch and rpm, the output of the anemometer system was recorded continuously for 25 revolutions of the rotor at each radial station in the flow. The time required to record the velocity data at the 52 radial stations in the wake was approximately 20 minutes. The primary difficulty encountered during these tests was that of maintaining constant rotor speed and thrust for the duration of each test. This difficulty was associated with small variations of wind direction and velocity, and engine operation factors. Because of these factors, thrust and rpm readings were recorded periodically throughout each velocity survey and averaged to obtain the mean values of each of these parameters.

SUBLIMATION STUDIES

Included as a part of the present investigation were tests with various chemicals to determine the boundary layer transition and flow direction characteristics on the rotor blades. This work also was concerned with an evaluation of the effectiveness of the different chemicals in revealing the boundary layer properties and the development of procedures to be used in testing with the sublimation technique. The chemical agents used

in these tests were naphthalene, acenaphthene, and fluorine, with the majority of the results obtained with the latter.

The test procedure consisted of applying a light coat of the chemical being used to the blade. The rotor was then started and brought to a condition of constant operation as quickly as possible. After a selected interval of operation, the rotor was stopped and the results inspected. Repeated tests with each of the chemicals evaluated at various conditions of rotor operation resulted in the development of procedures which produced the most favorable results.

The chemicals, when sprayed on the blade, were white or light gray in color. To provide good contrast, the blades were painted flat black so that traces of the chemicals remaining on the blade after each test could be seen easily. Four test sections of the blade were defined for tests of the sublimation rates of the chemicals at various rotor speeds.

The principle of the sublimation method is well known. (Reference 3). An organic chemical is first mixed with a volatile liquid and sprayed on the blade. The liquid evaporates quickly, leaving a deposit of the chemical on the surface. With the blade rotating, the chemical changes from a solid to gaseous state (sublimates) at a rate which is a function of turbulence, temperature, velocity, and humidity. The turbulence level of the boundary layer is a major factor in the sublimation process. Consequently, the chemical deposit will disappear on the portion of the blade over which the flow is turbulent before it disappears in the laminar region. After operation of the blade for the proper length of time, contrast between the laminar and turbulent regions becomes evident.

In the current investigation, petroleum ether was used as the evaporative agent. Because of high temperatures which occurred during the test period, most of the tests were conducted at night when the rotor blades were cool. Night tests were also more favorable for photographic purposes than daylight tests. The majority of tests were conducted at tip speeds of approximately 430 and 600 ft/sec and at blade pitch angles of $\theta_{75} = 2.5$ and 6.5 deg.

DATA REDUCTION

The recorded analog velocity data were processed by computer to obtain the velocity components of the flow at each measurement station. Using a reversed procedure of the data recording process, data were fed through the A/D converter directly into the computer which was programmed to compute the digital velocity information. The first step of the data reduction process involved computation of the calibration constants of the data system which were obtained from the recorded calibration data of each test run. Velocity information was then computed using a station-by-station procedure.

The computer was programmed to provide the mean velocity components (\bar{v}_x , \bar{v}_y , \bar{v}_z) and resultant velocity (\bar{V}_R) at each measurement station for four azimuth angles of the reference rotor blade ($\psi = 0, 45, 90, 135$ deg). The mean values of the velocity components were computed as the arithmetic mean of the 25 values of each component obtained from the data. The mean value of the resultant velocity vector was determined from the mean values of the velocity components. The standard deviations of the magnitude and direction of the resultant velocity vector were also computed and are presented with the mean velocity data in the Appendixes. The mean values of velocity were nondimensionalized by the momentum value of induced velocity v_0 to allow comparison of the data obtained at different values of thrust coefficient and rotor speed.

The computer could also be programmed to provide the instantaneous velocity components at a local station for any blade azimuth angle. By sampling the data at selected increments of time, plots of the velocity components versus time (or blade azimuth angle) could thus be obtained. This procedure provided a means of evaluating local flow variations with time, including assessment of the repeatability of the data per blade revolution.

Real-time distributions of velocity across the tip vortex trails were obtained by the data-sampling technique. Data obtained at each vertical level in the wake at outboard stations were scanned on an oscilloscope to locate the characteristic signals which indicated passage of the tip vortices near or across the anemometer probe sensors. Data at radial stations where the characteristic vortex signals were of largest amplitude were then fed into the computer and sampled to obtain a print-out of the velocity components at those stations. These data could then be visually searched for the characteristic velocity distributions of a vortex to determine the station or stations at which the tip vortices passed nearest the probe.

The data-sampling procedure was restricted only by limitations of the computer. The minimum increment of time at which the data could be sampled was 0.0014 sec, which corresponded approximately to 3 deg blade azimuth for test condition 1 and 2 deg for test conditions 2 and 3.

This required repeated sampling of each data segment in which different initial delays were used, and the overlapping of the results to achieve the degree of definition of the instantaneous velocity characteristics desired. With this procedure, plots of the time-dependent velocity variations in the wake could be obtained at time increments equivalent to $1/2$ deg blade azimuth.

All calibration constants and equations used in the computer program were obtained from the manufacturer of the anemometer with the exception of the equations for calculating the standard deviations of velocity magnitude and direction. These latter equations were based on the normal definition of "standard deviation" and are presented along with the important velocity relationships in Reference 1.

DISCUSSION OF RESULTS

ROTOR INFLOW MEASUREMENTS

Velocity surveys of the flow above the rotor were made at four vertical stations as shown in Figure 5. Radial measurement stations were spaced $0.1R$ apart from $x/R = 0$ to $x/R = 1.5$. The mean inflow velocity data are presented in tabular form in Appendix I for each rotor test condition and for four blade azimuth angles. Direction of the velocity components is shown in Figure 6 and examples of the plotted inflow velocity distributions are illustrated in Figures 7 through 13.

Inspection of the inflow data shows the spanwise velocity distributions to be functions of time, blade pitch, and rotor rpm. In general, the inflow distributions near the blade are characterized by strong spanwise flow just above the blade tips. At $z/R = 0.1$, the magnitude of the spanwise velocity components are of the same order of magnitude as the axial, or vertical components. While the spanwise components of the inflow peak near the blade tips, the axial components are largest further inboard. The swirl components vary across the span and are highly time-dependent. These characteristics of the inflow near the rotor are exhibited by the velocity distributions of Figures 7, 8, 9 and 13.

As distance above the rotor is increased, the spanwise distribution of the velocity tends to become uniform very quickly. The data indicate that both the in-plane and axial components of the flow are essentially constant in the spanwise direction above $z/R = 0.4$. The rapid acceleration of the inflow into the rotor disk near the blade tips between $z/R = 0.4$ to $z/R = 0.1$ may be seen by comparing the velocity distributions of Figures 8, 10, 11, and 12.

The effects of varying blade pitch and angular velocity on the inflow distributions were found by comparisons of the non-dimensionalized velocity data obtained for the three rotor test conditions. Increasing rotor thrust by changing blade pitch at constant rpm produced the most significant changes on the spanwise inflow distributions. In general, increasing rotor thrust by changing either pitch or blade angular velocity reduces the swirl components of the inflow and shifts the axial flow distribution inboard. This latter effect appears significant because of its effect on the spanwise angle of attack distribution of the blade.

The effects of blade pitch on the time-dependent characteristics of the inflow were quite pronounced. Figures 14 and 15 show the effect of blade position on the flow at two fixed locations above the rotor. Near the tip, the flow is highly impulsive in that rapid changes of the velocity components occur as the blade passes beneath. Inboard, the blade impulses are less distinct, although the same general trends of the data are evident. The effect of increasing blade pitch was to increase the amplitude of the velocity impulses due to blade passage with

respect a fixed location in the flow. Thus, operation of the rotor at high angles of collective pitch and low rpm resulted in an amplification of the time-dependent velocity fluctuations of the rotor inflow.

The standard deviation parameters presented in Appendix I were examined to determine the repeatability of the data with respect to time. The deviation of the magnitude of the resultant velocity vector was approximately $\pm 8\%$ for all measurements. Average angular deviation of the velocity vector was computed to be ± 6 degrees.

NEAR WAKE VELOCITY MEASUREMENTS

Figures 16 through 19 show typical spanwise velocity distributions across the near wake. Similar data are presented in Appendix II for the three test conditions of the rotor at seven vertical stations in the wake as shown in Figure 5. Inspection of the data clearly indicates the changes in wake structure due to blade rotation and the relative magnitude of the velocity components of the vortex sheet and flow region beyond the blade tips. Also, an assessment of the effects of blade pitch and rpm can be obtained by comparisons of the velocity distributions for the three test conditions of the rotor.

The spanwise distributions of the velocity components show that the inplane components \bar{V}_x and \bar{V}_y of the inboard vortex sheet are relatively small and do not change significantly with time. However, the magnitude of these components at the outboard edge of the vortex sheet becomes quite large due to the induced velocities of the tip vortices. For example, Figures 16 and 19 illustrate the time-dependent changes in the spanwise flow due the rotor tip vortices. In Figure 16, at $\psi = 45$ deg, the vertical location of the trailing tip vortex corresponds closely to the vertical measurement station, whereas in Figure 19 at $\psi = 0$ degrees, the vortex is above the measurement station. It will be observed that in the immediate vicinity of the radial station corresponding to the radial coordinate of the tip vortex path that all three of the velocity components of the wake undergo large periodic changes of magnitude due to passage of the vortex across the measurement station. Inspection of the velocity distributions at stations lower in the wake (Figures 17 and 18) shows the shift in the velocity distributions due to the changing radial position of the tip vortices. In the near wake, only small variations of the inplane and axial velocity components of the inner wake were noted.

The effects of changing rotor operating variables on the spanwise velocity distributions of the near wake are manifested as radial shifts of the velocity distribution curves and as variations of the peak velocity amplitudes at the wake boundaries. These effects are due to the changes of the radial path coordinates and strength of the rotor tip vortices with changes of the rotor operating variables. The data of Appendix II clearly exhibit the above effects for the three test conditions of angular velocity and rpm.

HELICAL VORTEX MEASUREMENTS

The primary objective of the near wake tests was the acquisition of detailed velocity data in the region of the helical vortex trails from which the characteristics of the vortices could be defined. It was intended to position the probe at closely-spaced radial stations across the paths of the tip vortices, so that the chances of obtaining velocity distributions across the vortex cores would be much higher than those of the previous measurements of Reference 1 in which the spacing of the radial stations was much wider. For this purpose, the radial stations were spaced 1.26 inches apart from $x/R = 0.7$ to 1.0. Inspection of the data obtained with this spacing indicated that even smaller spacing would have been desirable in that the data did not reflect the expected number of captured vortices in some instances. However, the data were sufficient to provide good definition of the mean vortex characteristics at each vertical station in the wake.

The velocity data at each vertical station were first analyzed to determine the radial locations of the vortices. Figure 20 shows the extreme inboard and outboard locations at which vortices were found during 25 revolutions of the rotor at each vertical measurement station. This figure shows the scatter of the vortices with respect to a faired path computed from the generalized vortex coordinate equations of Reference 2. The scatter of the vortices was attributed to three possible causes - wind effects, vortex instability, and blade dissimilarities. Of these, wind effects appear to have been most prominent. Comparisons of the vortex positions in the wake with recorded wind data show a general correlation between the extent of vortex scatter and the variations of wind direction and magnitude which prevailed during the measurements. Since the exact wind conditions which occurred during the measurement of each individual vortex could not be determined, a precise evaluation of the effect of the wind to shift the wake boundaries could not be made.

Examination of the data at each measurement station revealed that small dissimilarities of the paths of the vortices shed from the two blades were exhibited by the data in every instance. For example, the instantaneous velocity distributions of Figure 21 and 22 show that the vortex shed from blade 1 passed closer to the probe sensors than did the vortex from blade 2 as indicated by the magnitude of the various velocity components. This trend was observed at all vertical levels in the wake, indicating that the path coordinates of the vortices shed from the two blades were slightly mismatched due to factors which could not be determined. In order to investigate the stability characteristics of tip vortices in a free environment in future investigations, a means of flow visualization will have to be utilized to determine the unsteady path variations of the vortices shed from each blade.

Figure 21 and 22 show the fluctuations of the velocity components that occurred as the trailing vortices passed near the probe. Similar plots were obtained by sampling the data at a time increment equivalent to 5 deg blade azimuth - a sampling rate sufficient to indicate instances in which the

vortex cores passed directly across the probe sensors. These instances were revealed by "holes" in the peaks of the resultant velocity plots and by peak values of the in plane velocity component v_y . These conditions are exhibited by the second vortex shed from blade 1 in Figures 21 and 22.

Those portions of the velocity data exhibiting the characteristics noted above were further analyzed to determine the characteristics of the helical vortices. For this purpose, the velocity data were sampled at a rate equivalent to 1/2 deg blade azimuth and plotted as shown in Figures 23 through 26. A number of plots similar to these were analyzed at each vertical station in the wake for each of the three test conditions of the rotor to determine the mean values of vortex core radius, maximum tangential velocity at the edge of the core, axial velocity at the center of the vortex, and circulation strength. The trajectory of each vortex across the probe was determined from the ratios of the maximum tangential velocity components of the vortex and the assumption of maximum axial velocity at the core center. The path velocity components of each vortex were calculated from the mean vortex path coordinates plotted in Figures 27 through 29 and used to compute the diameter of the vortex core.

Definition of the vortex velocity distributions was sufficient in most instances to exhibit reasonable structural characteristics of the vortices. However, in some cases the data indicated that the "edge" of the vortex core was not sharply defined by a peak value of tangential velocity. In other cases, the velocity characteristics indicated a lack of axial symmetry of the vortices. Examination of these inconsistencies exhibited by the data resulted in the conclusion that vortex distortion occurred due to the interference effects of the measurement probe entering the high velocity region of the vortex core. The measured characteristics mentioned above may be observed in Figures 23 through 26.

The results of the vortex analysis indicated that the vortex cores increased in size with downstream distance along the helix with a simultaneous decrease in the magnitude of the tangential velocities at the edge of the cores. Because of these conditions, the calculated values of circulation strength of the vortices were nearly constant downstream, except in the case of test condition 2 in which an increase in the circulation strength downstream was noted. This condition is believed to have resulted from a lack of precise definition of the tangential velocities at the edge of the vortex cores due to the sampling procedure used in reducing the data to digital form or because of limitations of the anemometer system in measuring the high peak velocities at the core. Mean values of the vortex core radii and tangential velocities at the edge of the cores are plotted in Figures 30 and 31.

Outside the core region, the vortices exhibited characteristics that were almost two-dimensional, in that the axial or downstream flow components were small in comparison to the tangential components. At the edge of the core, the measured axial components were essentially zero, and were of reversed direction inside the core. Maximum values

of axial velocity were measured in the direction of blade rotation at the center of the cores. The maximum measured values of axial velocity within the vortex cores are shown in Figure 32. Since the magnitude of the axial velocity components was less than the tip speed of the retreating blade, these measurements actually represent the momentum deficiency that exists within the vortex cores. Definition of the axial velocity distribution across the vortex cores could not be established from the present measurements although a linear distribution was indicated. The data show that the axial velocity at the center of the core reaches a maximum value about 100 to 150 tip chord lengths downstream from the tip and thereafter decreases as the vortex core continues to expand.

BOUNDARY LAYER SUBLIMATION STUDY

Photographs of each test section of the blade were made after each sublimation test for later analysis of the boundary layer flow characteristics. The photographs were used to study the boundary layer transition and radial flow characteristics. Each test section consisted of a spanwise portion of the blade equal in length to 0.1 R.

Transition of the boundary layer could easily be determined from the photographs. On the upper surface of the blade, a seam at the juncture of the leading edge cap and the fiber glass overlay of the blade evidently contributed toward the transition from laminar to turbulent flow just behind the chordwise position of the seam at low section angles of attack. This condition is illustrated in Figure 33 with the tip operating at 1.5 deg geometric angle of attack ($\theta_{75} = 2.5$ deg, $\Omega R = 429$ ft/sec). With the blade operating in this condition, transition occurred just behind the seam across the entire blade span, even though the inboard blade sections were operating at higher geometric pitch angles due to the negative 4 deg twist of the blade. The effects of twist, however, were essentially cancelled by the increased induced and rotational components of velocity toward the tip. Calculations made from the measured velocity data of the blade revealed that the section absolute angles of attack were approximately the same across the blade span. This fact indicated that the constant spanwise location of transition behind the blade seam at low section angles of attack was probably due to the effect of the seam to trigger transition of the boundary layer across the span since transition on the blade was expected to exhibit the effects of the spanwise variation of Reynolds number.

Tests at a higher blade pitch angle did reveal a spanwise variation of the chordwise location of transition. Figures 34a and 34b show transition on the 70-80 percent test section of the blade for $\theta_{75} = 6.5$ deg. With the increase of blade pitch, transition on the upper surface moved toward the leading edge and lay ahead of the blade seam as shown in Figure 34a. It is important to notice, however, that the seam on the underside of the blade appeared to have little effect on the chordwise position of transition as shown in Figure 34b. This would indicate that the effect of the blade seam to trigger transition of the boundary

layer was not pronounced when the chordwise pressure gradient was favorable over a large extent of the blade surface.

The measured chordwise locations of transition from laminar to turbulent flow across the blade span are shown in Figure 35 for two rotor speeds at $\theta_{75} = 6.5$ deg. The figure shows the large expanse of laminar flow on the lower surface of the blade and the movement of transition toward the leading edge of the blade on the upper surface as the tip is approached. For the two tip speeds of 604 and 429 ft/sec indicated, the corresponding Reynolds numbers at the tip are approximately 3.2×10^6 and 2.3×10^6 , respectively. The effect of Reynolds number on the chordwise locations of transition near the tip are evident on the lower surface as shown by the data points for the two tip speeds of the rotor. On the upper surface, however, the effects of Reynolds number appear insignificant near the tip where transition occurs close to the leading edge. These results show that the effect of Reynolds number on the chordwise location of transition decreases as the adverse pressure gradient becomes stronger.

The spanwise variation of the chordwise position of transition shown in Figure 35 was attributed to be the result of increasing Reynolds number toward the tip of the blade since the spanwise section angles of attack were again computed to be essentially constant. The results indicate that Reynolds number effects on transition can be significant on full-scale blades, although transition is probably dominated by adverse pressure gradient as previously reported by McCroskey in Reference 4. Also, transition characteristics measured on the outboard 10 percent of the blade indicate that transition in the vicinity of the tip is significantly influenced by the trailing tip vortex and that the effect of the tip vortex is to slightly delay transition near the tip. This can be observed from the data points near the tip in Figure 35. While the present data are insufficient to explain this phenomena, it is believed that the effects of radial flow due to the tip vortex play an important role in determining transition characteristics at the tip.

In an effort to examine the radial flow components of the blade boundary layer, small rivets were glued to the blade surface such that the streamlines of flow could be visualized from the turbulent wake of the rivets. The rivets were attached at the 5, 40, and 75 percent chord stations on the upper and lower surfaces of each test section. The turbulent wedges of these rivets are visible in Figures 34a and 34b. The direction of the flow streamlines was assumed to coincide with a line which bisected the turbulent wedge of each rivet. In addition to the turbulent wedges of the rivets, numerous traces were obtained due to insect collisions with the blade, some of which are visible in the photographs of Figures 33 and 34.

Two test cases were analyzed to determine the directions of the streamlines of flow on the blade at three chordwise stations on each test section. The deflection of the flow streamlines at each chordwise

station were measured relative to a circular arc representing the streamline of two-dimensional flow. The blade streamlines were found to be circular arcs which, in general, coincided closely with the assumed two-dimensional streamlines. In the two test cases, however, a consistent deviation of the measured streamlines with respect to the circular arc streamlines was noted. On the upper surface of the blade, radial flow components were directed outboard near the blade root and inboard at the tip. Maximum deflection of the streamlines was measured at the lowest rotor speed ($\Omega R = 429$ ft/sec, $\theta_{75} = 6.5$ deg). For this test condition, the streamlines at the 0.25 span station on the upper surface lay outside the circular arc streamlines by approximately 7.5 deg at the 0.75 chord station. Corresponding angles at the 0.95 span station of approximately 9 deg were obtained with the flow streamlines lying inboard of the circular arcs. On the outer 5 percent of the blade, the radial flow components become more significant due to the stronger influence of the tip vortex. Maximum deflection angles of 12 to 15 deg were measured in this vicinity. The effect of increasing tip speed to 604 ft/sec was to reduce the flow deflection angles across the span by approximately 3 deg at the 0.75 chord station.

In general, the radial flow components on the upper surface of the test blade were found to be directed outboard near the root of the blade, and inboard near the tip. The spanwise components of the boundary layer were largest at the tip and were observed to increase in magnitude across the span as tip speed was reduced. The flow characteristics on the underside of the blade were similar to those on the upper surface except at the tip where the inboard deflection angles of the streamlines were smaller. The results show that the spanwise flow components of the boundary layer on the test blade were small and became most significant only in the immediate vicinity of the tip. Centrifugal effects of rotation on the boundary layer are obviously heavily outweighed by the effects of the spanwise pressure distribution of the induced flow field about the rotor.

The sublimation tests represented an initial effort by the author in the use of chemical agents on rotating blades. Fluorine was found to produce excellent results, but required that the rotor be operated for excessive time periods before the material on the blade exhibited the desired boundary layer characteristics. As a result, this chemical could be used conveniently only on the outer test sections of the blade where the rotational velocities were high. On the other hand, the rapid sublimation characteristics of naphthalene required that this substance be used only on the test section nearest the root of the blade. On this section, naphthalene produced good results after short test runs, but was not used extensively because of its rapid sublimation rate. Tests with acenaphthene proved this chemical to be most suitable on all blade sections although the running time required varied considerably between the root and tip test sections. The most successful technique utilized was to obtain the blade information during successive operating periods of the rotor in which either acenaphthene or fluorine was used on each spanwise test section of the blade. Temperature, humidity, and appli-

cation rates of each chemical were found to be important factors in determining the proper time period of rotor operation for most definitive results.

RESULTS AND CONCLUSIONS

1. Radial distributions of the inflow velocity components of a hovering rotor were measured at four vertical stations above the rotor disk. The flow exhibited two-per-rev fluctuations of the velocity components which were of largest amplitude in the region immediately above the path of the blade tips. Greatest amplitude of the fluctuations of the velocity components occurred at the largest test value of collective pitch and smallest value of blade rpm.
2. Measurements of the velocity distributions in the near wake of the rotor showed the inplane components of the vortex sheet to be small in comparison to the magnitude of the axial components except in the region bordering the path of the tip vortices. The swirl components of the wake are least affected by the influence of the tip vortex and become large only at the center of the helix.
3. Scatter of the tip vortex locations in the wake was attributed to the variations of wind velocity and direction that occurred during tests rather than to instability of the vortices or to blade variables. The data indicated that the rate of vertical displacement of the tip vortices of the full scale rotor was less than predicted by the generalized equations of Reference 2 derived from model tests.
4. Core radii of the tip vortices were observed to increase with distance below the blade as tangential velocity magnitude at the edge of the cores decreased.
5. Axial velocities were measured within the helical vortices which were maximum at the center of the vortex cores. Peak values of axial velocity at the center of the cores were measured at locations downstream from the blade tip.
6. The effects of Reynolds number on the chordwise location of transition from laminar to turbulent flow on a full-scale blade appear significant although transition is more strongly influenced by adverse pressure gradient.
7. Spanwise flow components of the boundary layer of the rotor blade in the hover condition were small and appeared to be primarily a function of the spanwise pressure distribution due the induced flow field of the rotor.

RECOMMENDATIONS

The current investigation represented a continued effort to define the flow field about a full-scale rotor operating in an open environment. The environmental conditions which existed over the test period prohibited to some extent a definitive analysis of the effects of the rotor operating variables on the flow characteristics of the rotor. It is recommended that instrumentation and test procedures be developed in future investigations to make possible an assessment of the effects of the environmental conditions on the test data, especially the effects of crosswinds.

It is also recommended that an effort be made to improve the anemometer system used in this investigation. It is suggested that reduction of the dimensions of the measurement probe - particularly the dimensions of the stem and sensor array - would provide an instrument more suitable for flow measurements in confined regions where good definition of the flow is required.

A definite lack of comparable three-dimensional data for both large and small rotors suggests a need for continued research in areas related to definition of the flow fields of rotors in hover and forward flight. The results of future experimental studies should be utilized in parallel efforts to formulate realistic mathematical representations of the wakes of rotors of variable geometry and modes of operation.



Figure 1. Whirl Tower Installation and Access Gantry



Figure 2. Mounting Configuration of Total Vector Probe for Inflow Velocity Measurements



Figure 3. Total Vector Anemometer System

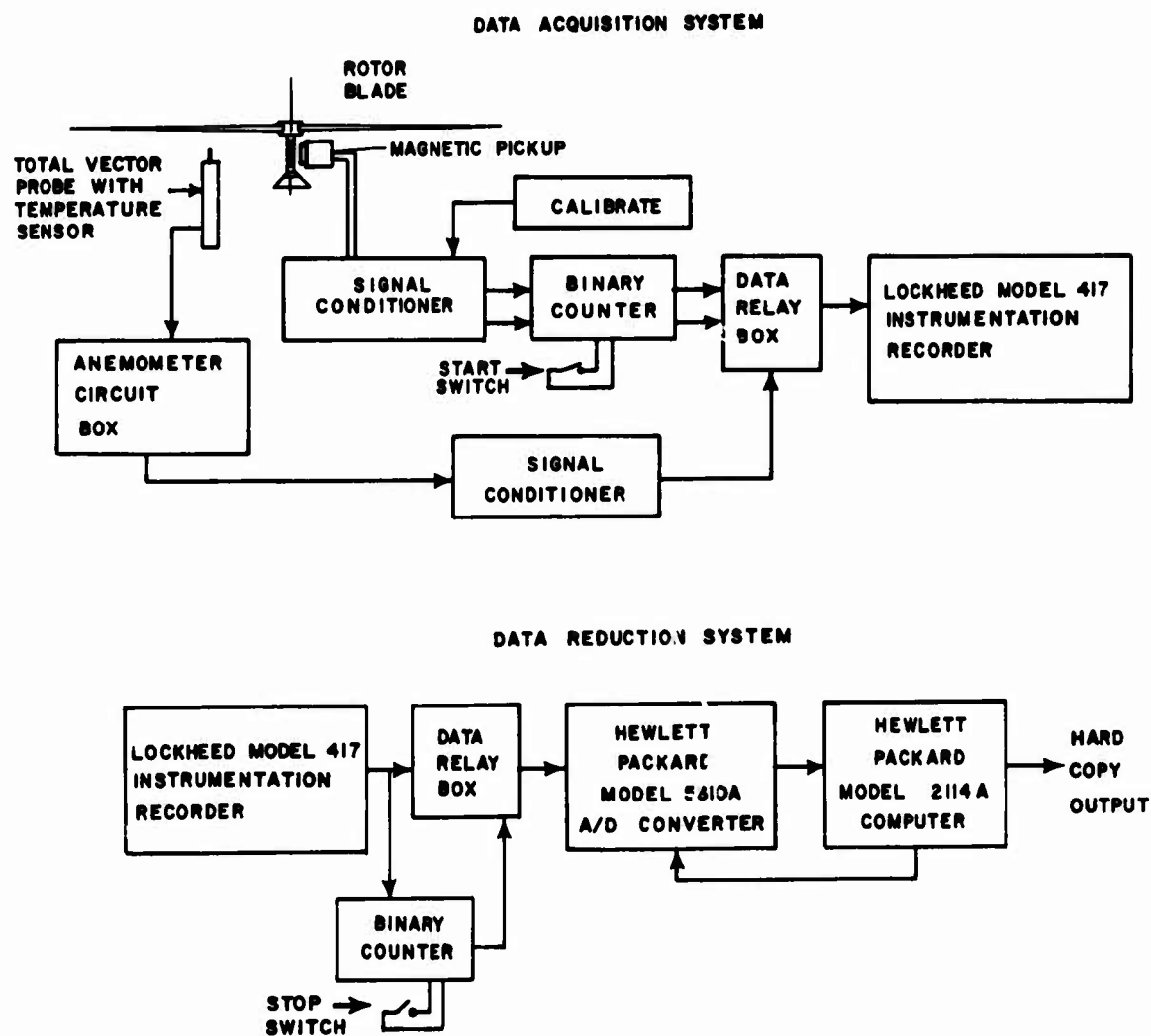


Figure 4. Block Diagram of Data Acquisition and Reduction System

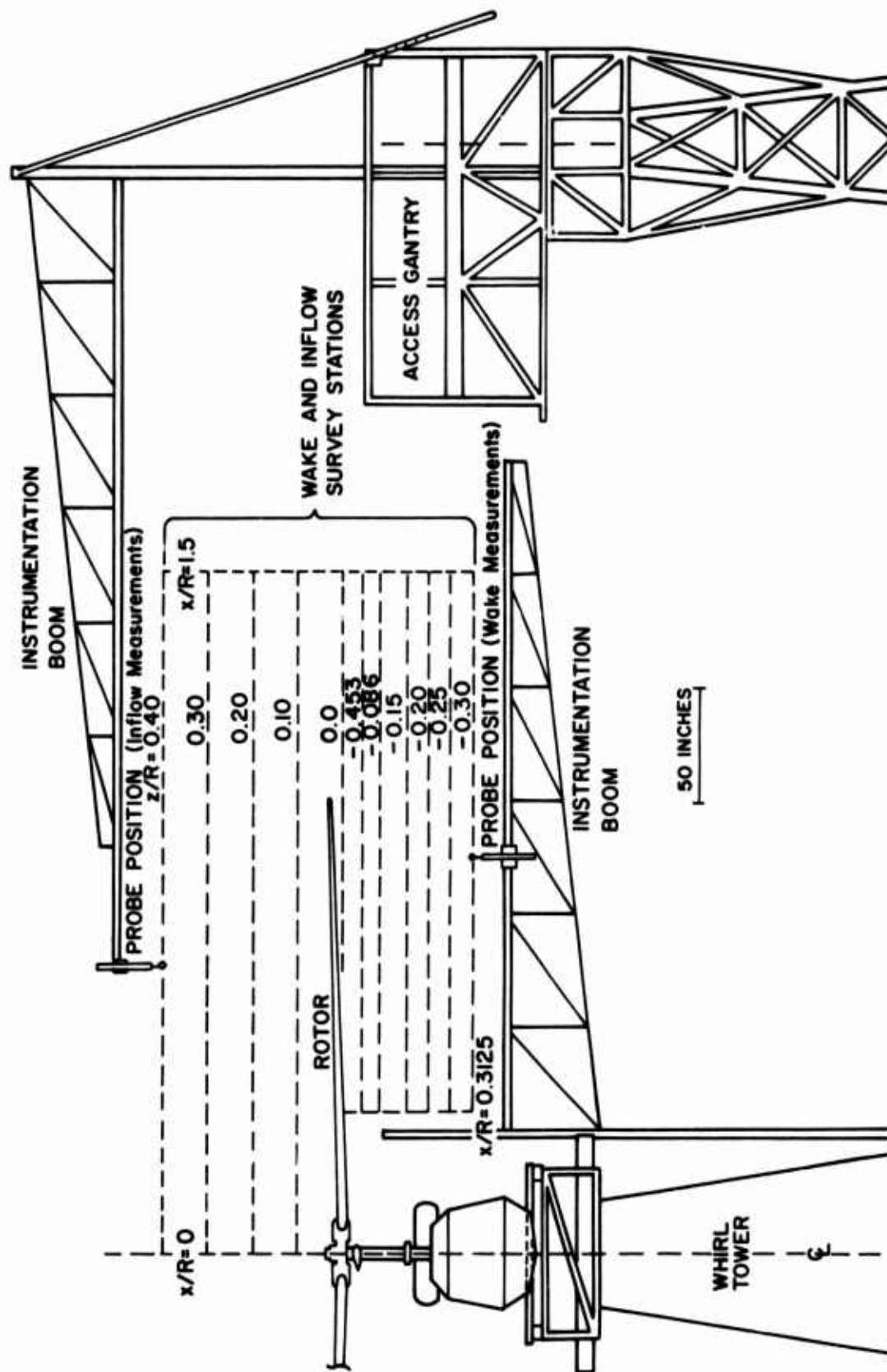


Figure 5. Sketch of the Test Installation Showing Vertical Measurement Stations Above and Below the Rotor

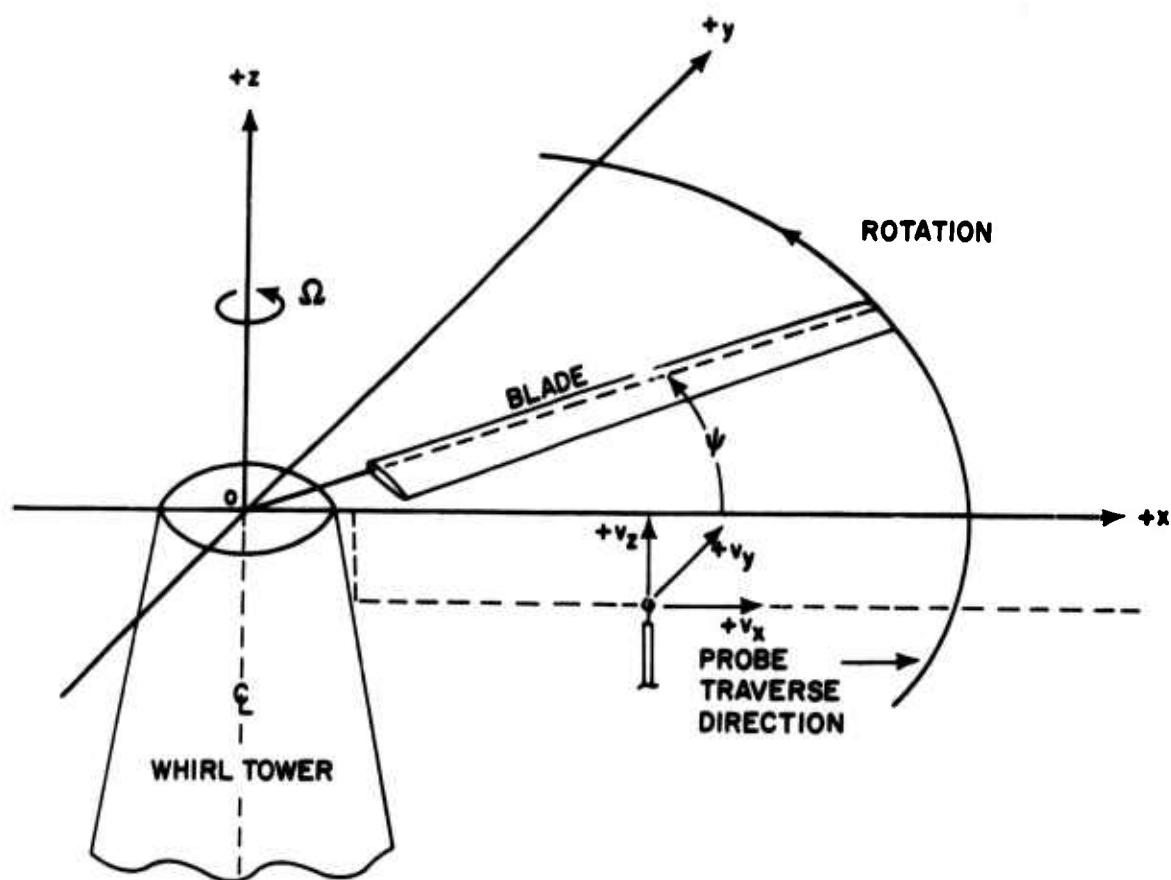


Figure 6. Whirl Tower Fixed Coordinate System

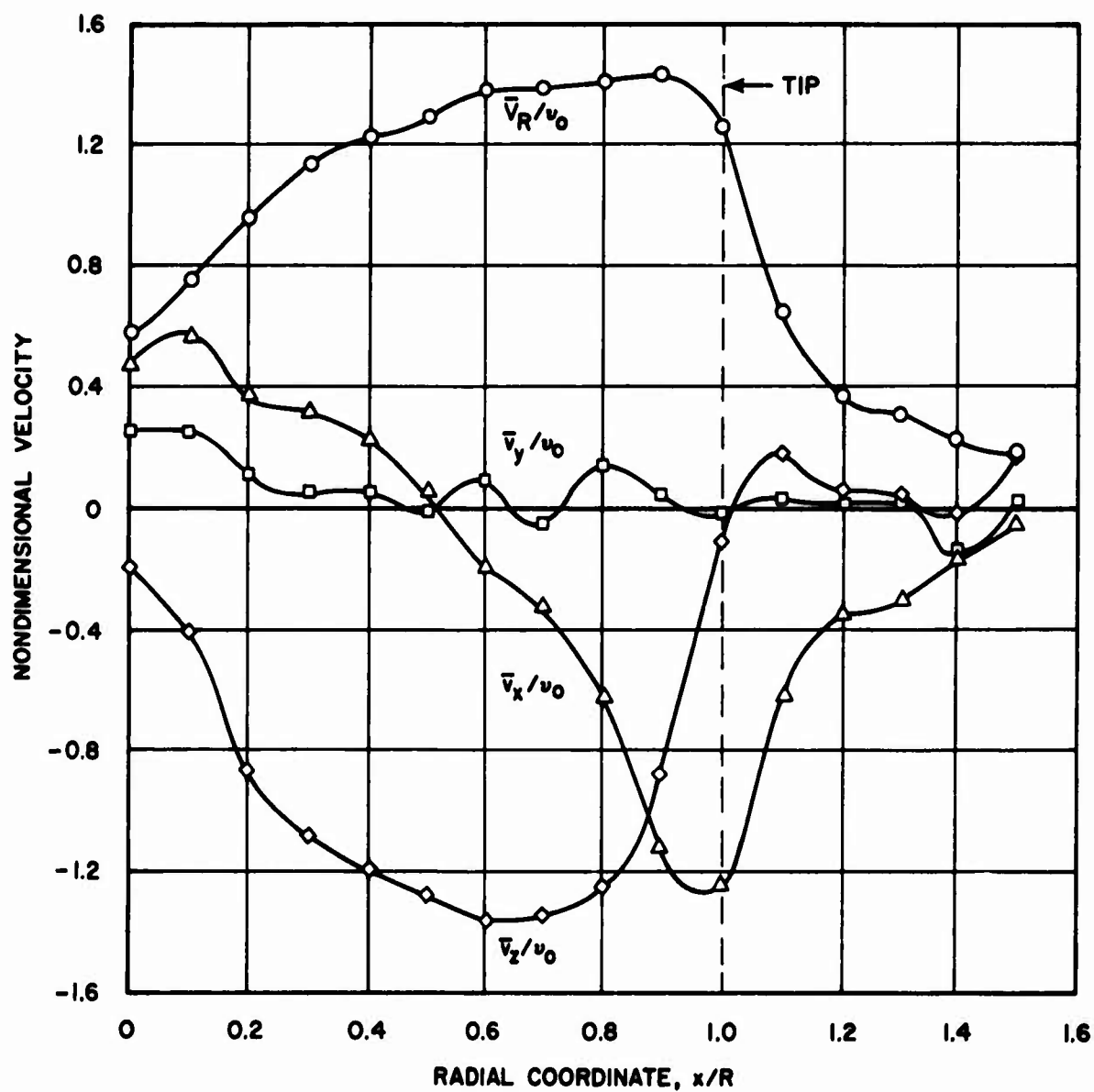


Figure 7. Mean Distribution of Inflow Velocity Components and Total Velocity, Test Condition 1, $z/R = 0.1$, $\psi = 45$ deg

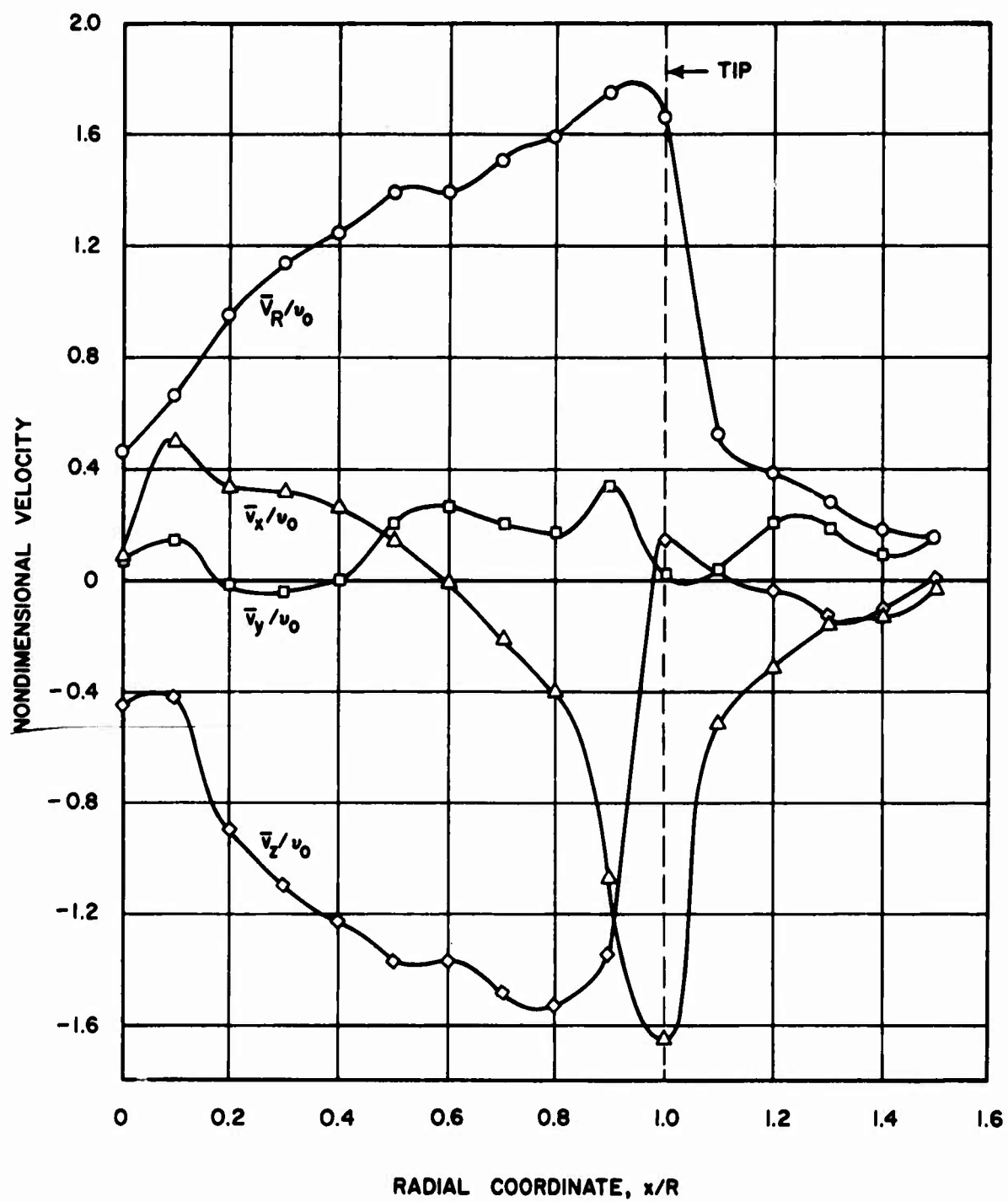


Figure 8. Mean Distribution of Inflow Velocity Components and Total Velocity, Test Condition 2, $z/R = 0.1$, $\psi = 45$ deg

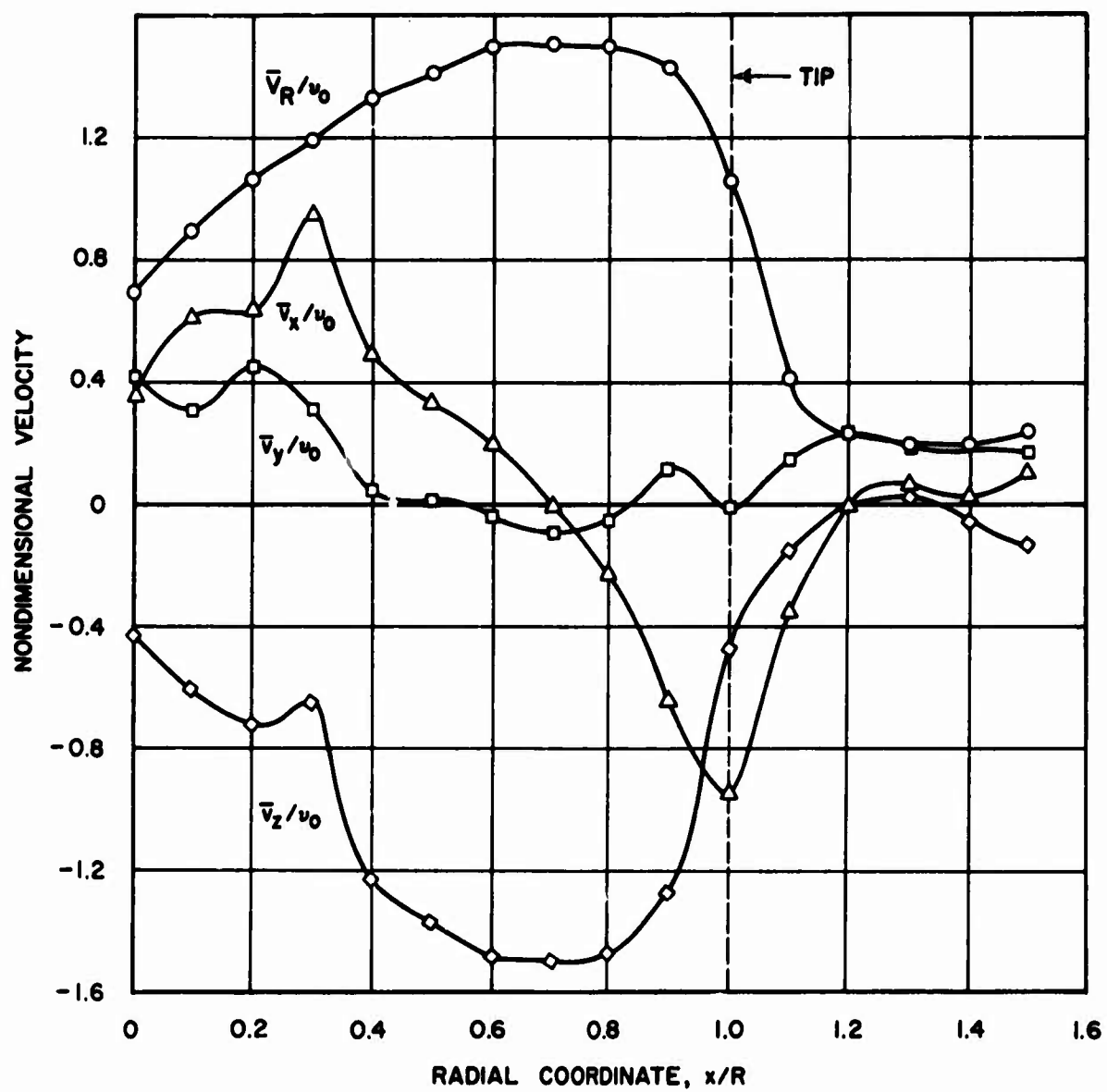


Figure 9. Mean Distribution of Inflow Velocity Components and Total Velocity, Test Condition 3, $z/R = 0.1$, $\psi = 45$ deg

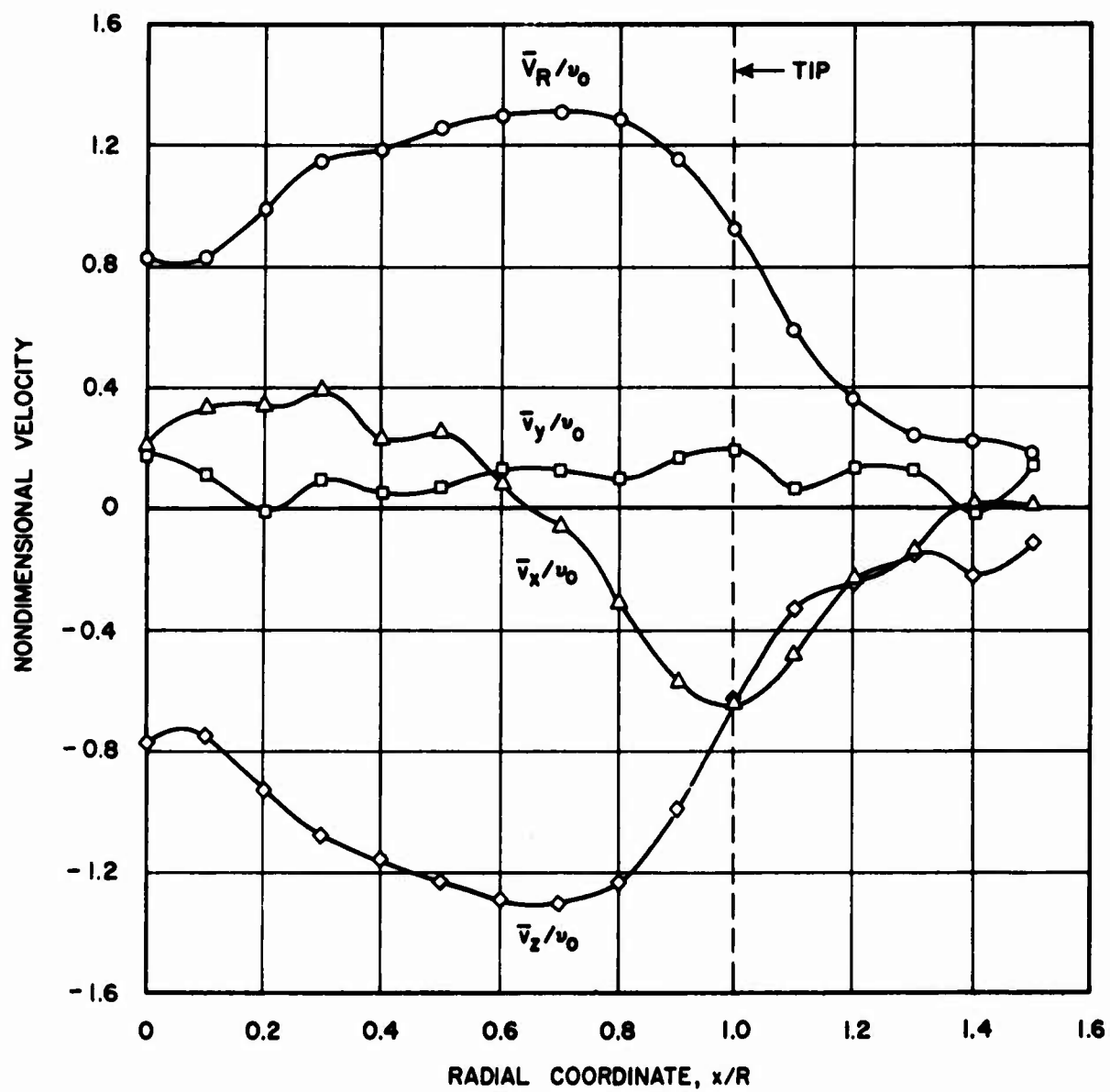


Figure 10. Mean Distribution of Inflow Velocity Components and Total Velocity, Test Condition 2, $z/R = 0.2$, $\psi = 45$ deg

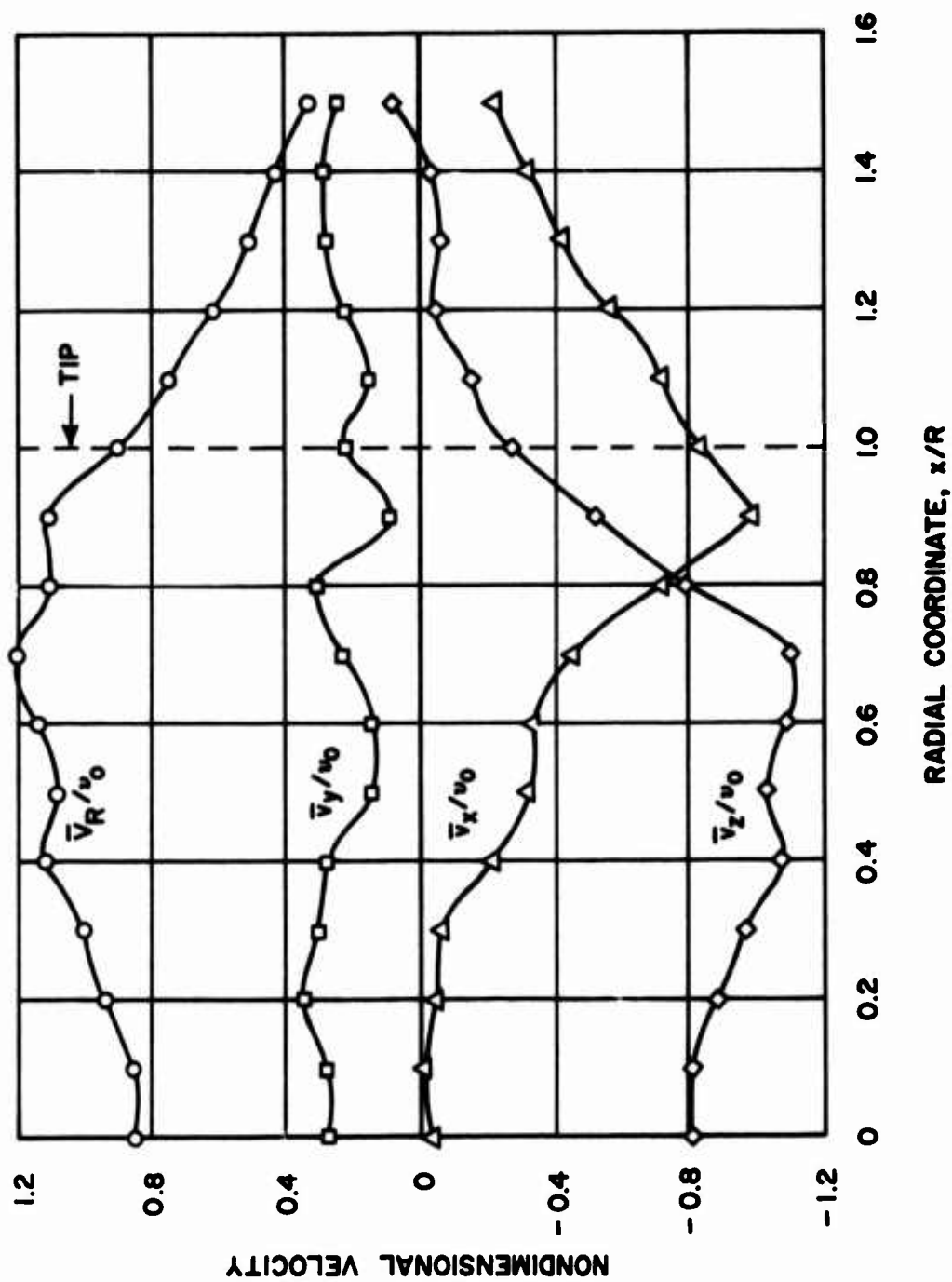


Figure 11. Mean Distribution of Inflow Velocity Components and Total Velocity, Test Condition 2, $z/R = 0.3$, $\psi = 45$ deg

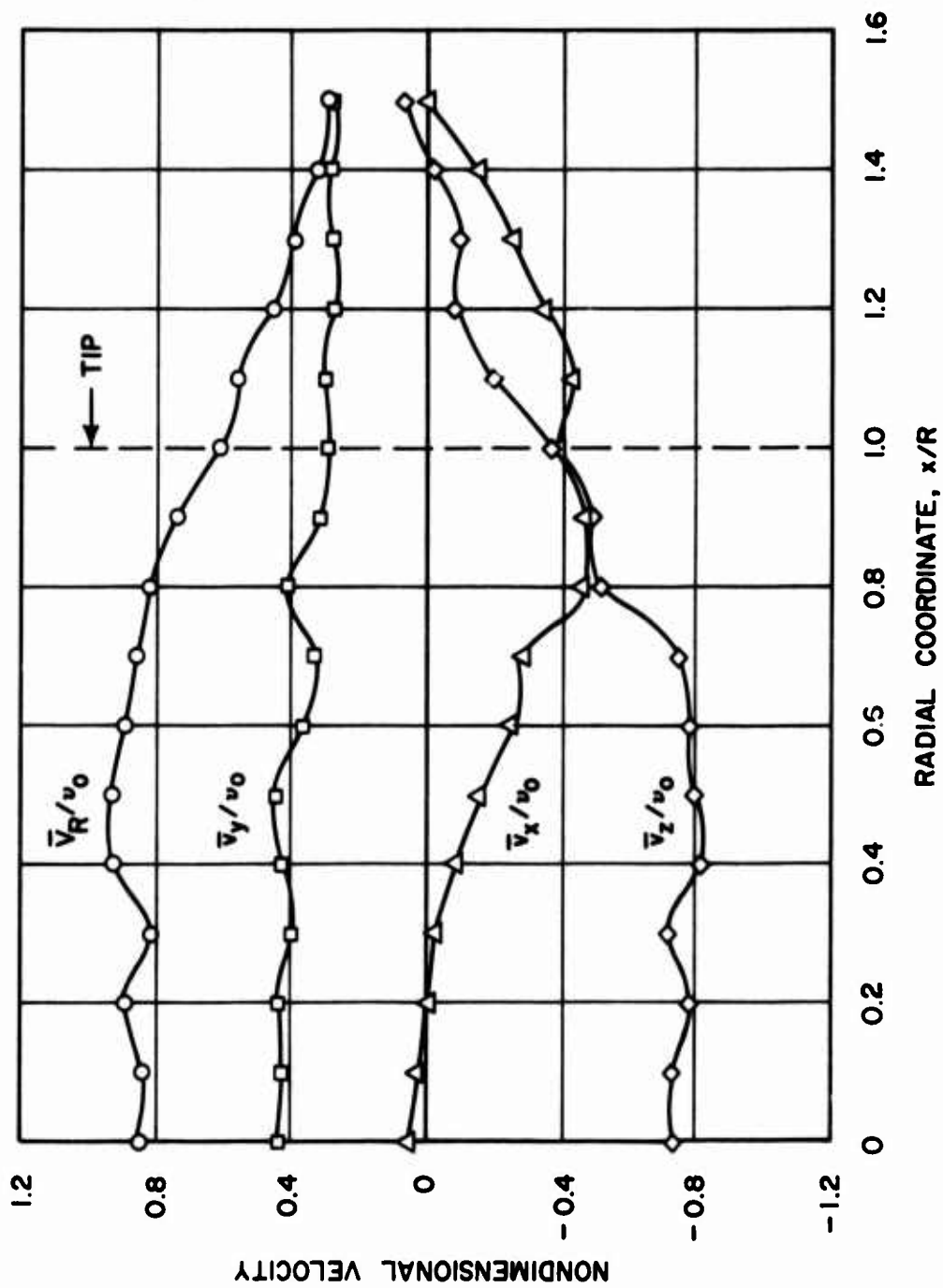


Figure 12. Mean Distribution of Inflow Velocity Components and Total Velocity, Test Condition 2, $z/R = 0.4$, $\psi = 45$ deg

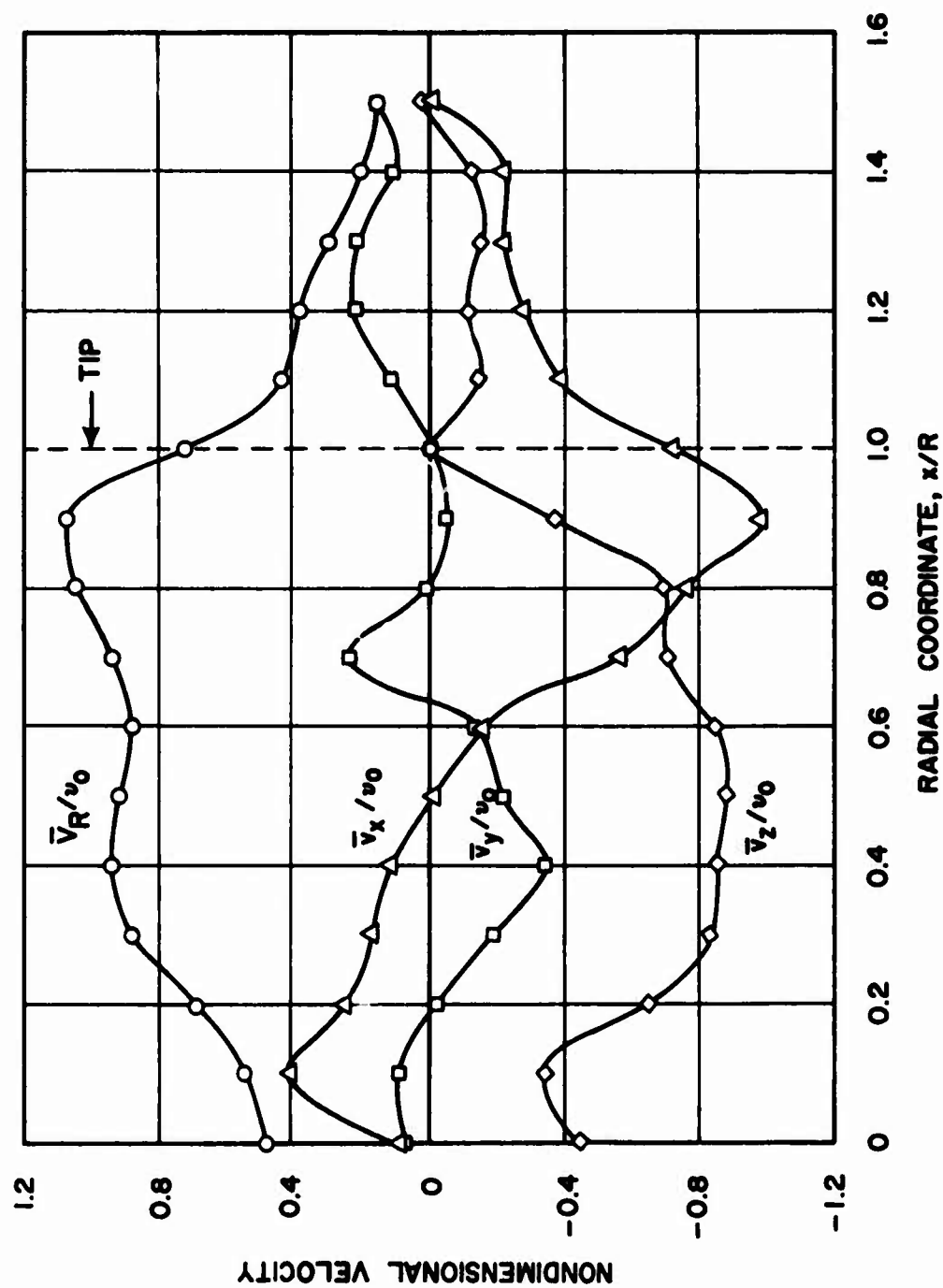


Figure 13. Mean Distribution of Inflow Velocity Components and Total Velocity, Test Condition 2, $z/R = 0.1$, $\psi = 0$ deg

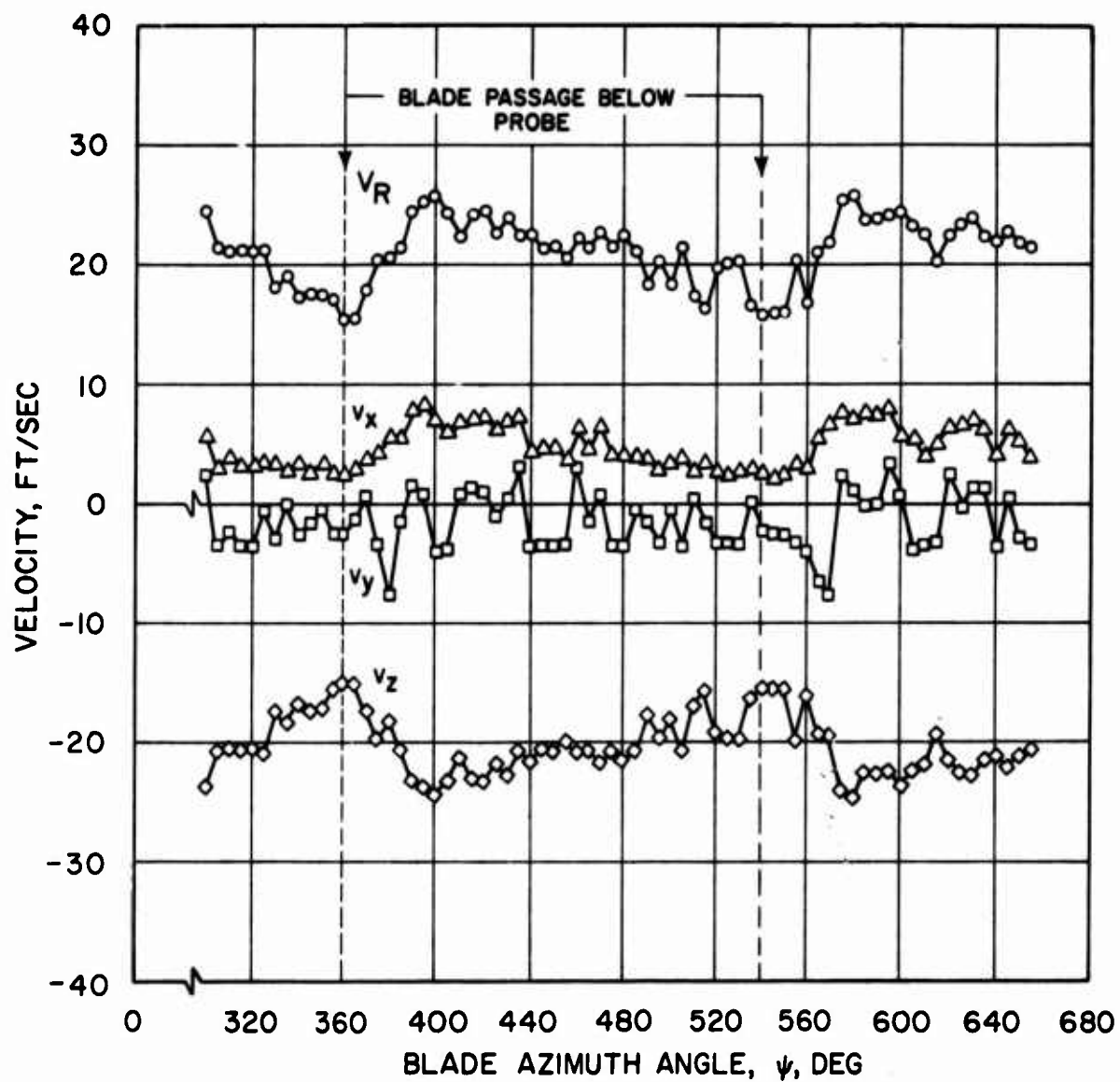


Figure 14. Time-Dependent Inflow Characteristics at $x/R = 0.3$, Test Condition 2, $z/R = 0.1$

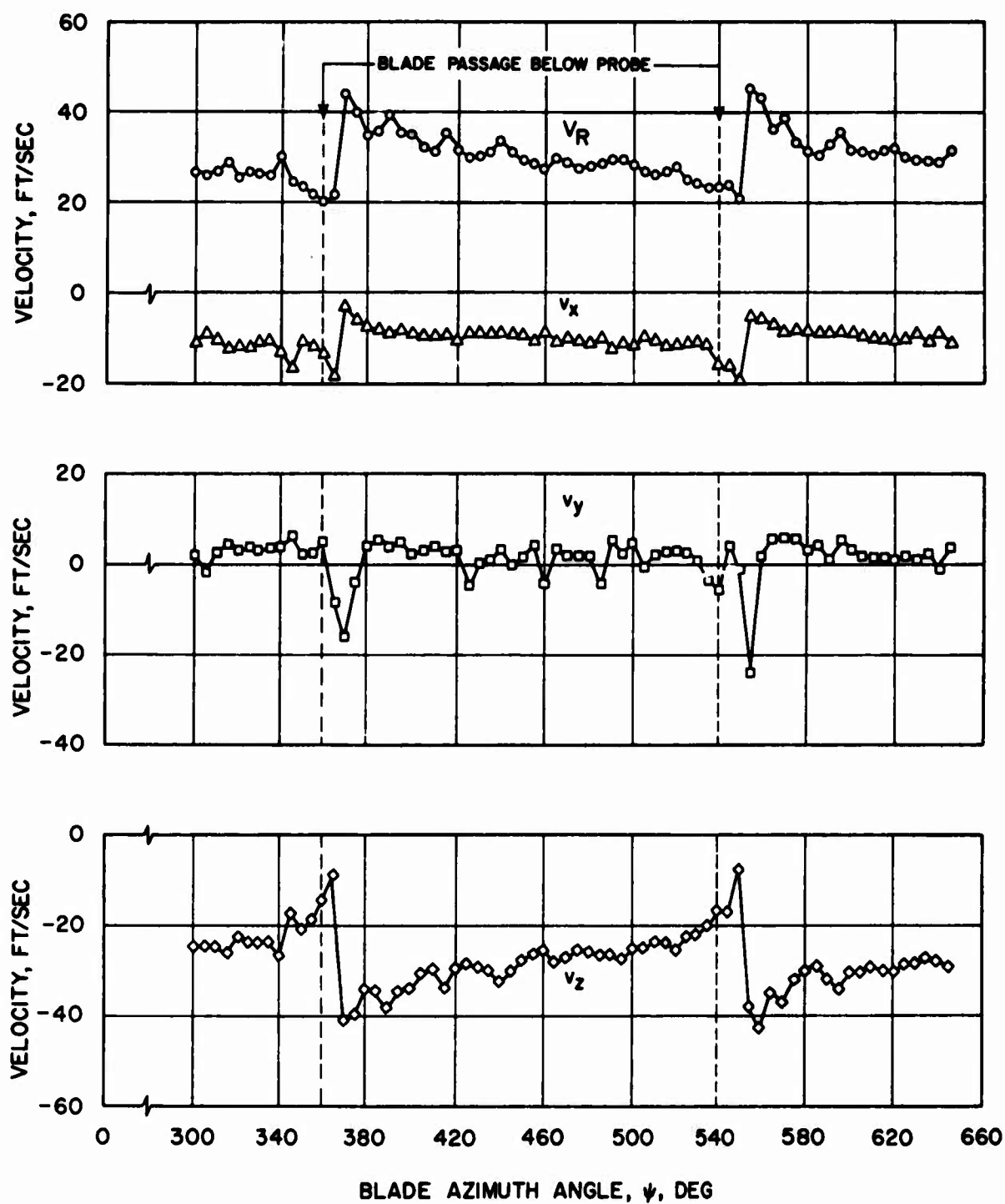


Figure 15. Time-Dependent Inflow Characteristics at $x/R = 0.8$, Test Condition 2, $z/R = 0.1$

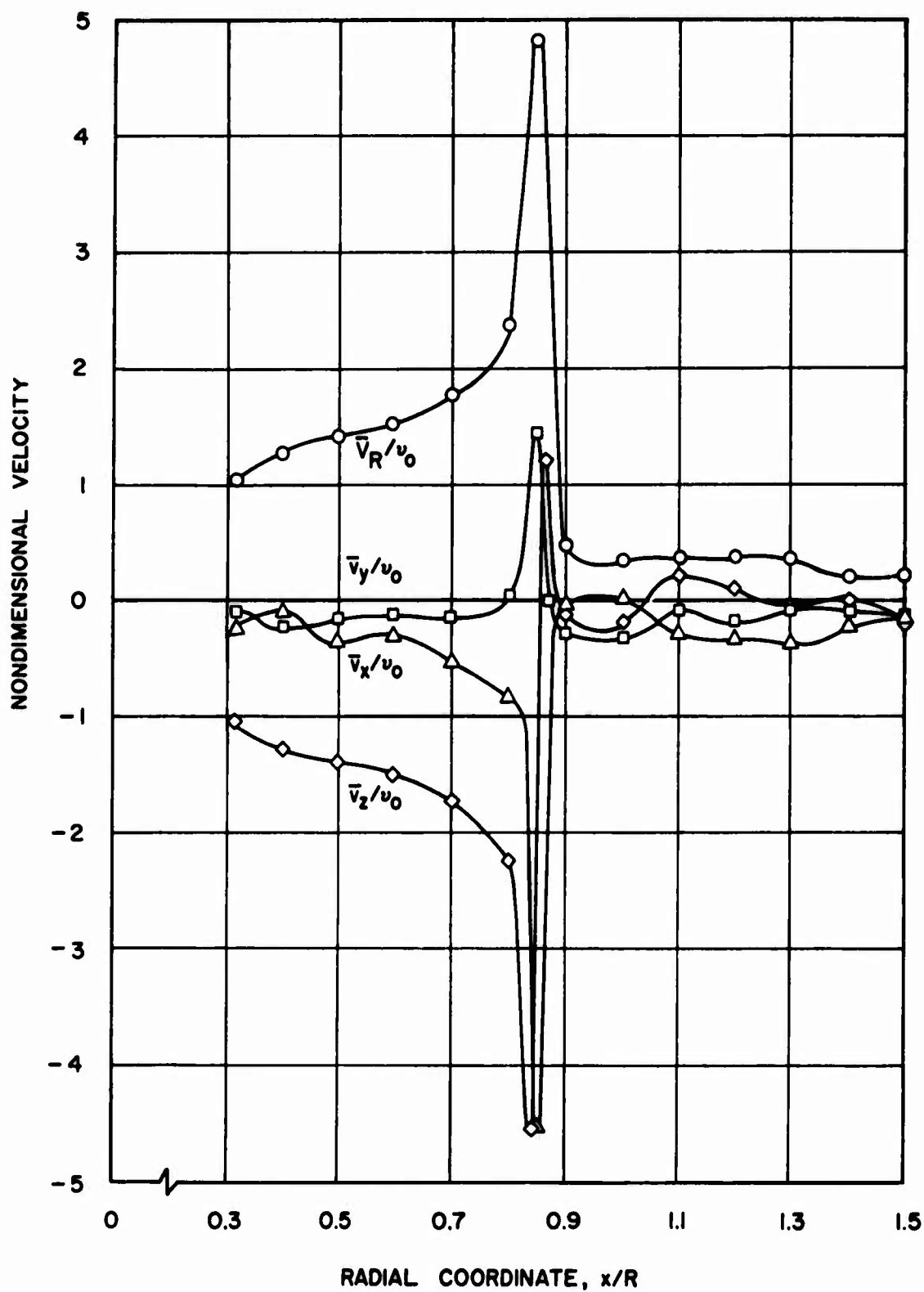


Figure 16. Mean Distribution of Wake Velocity Components and Total Velocity, Test Condition 2, $z/R = -0.045$, $\psi = 45$ deg

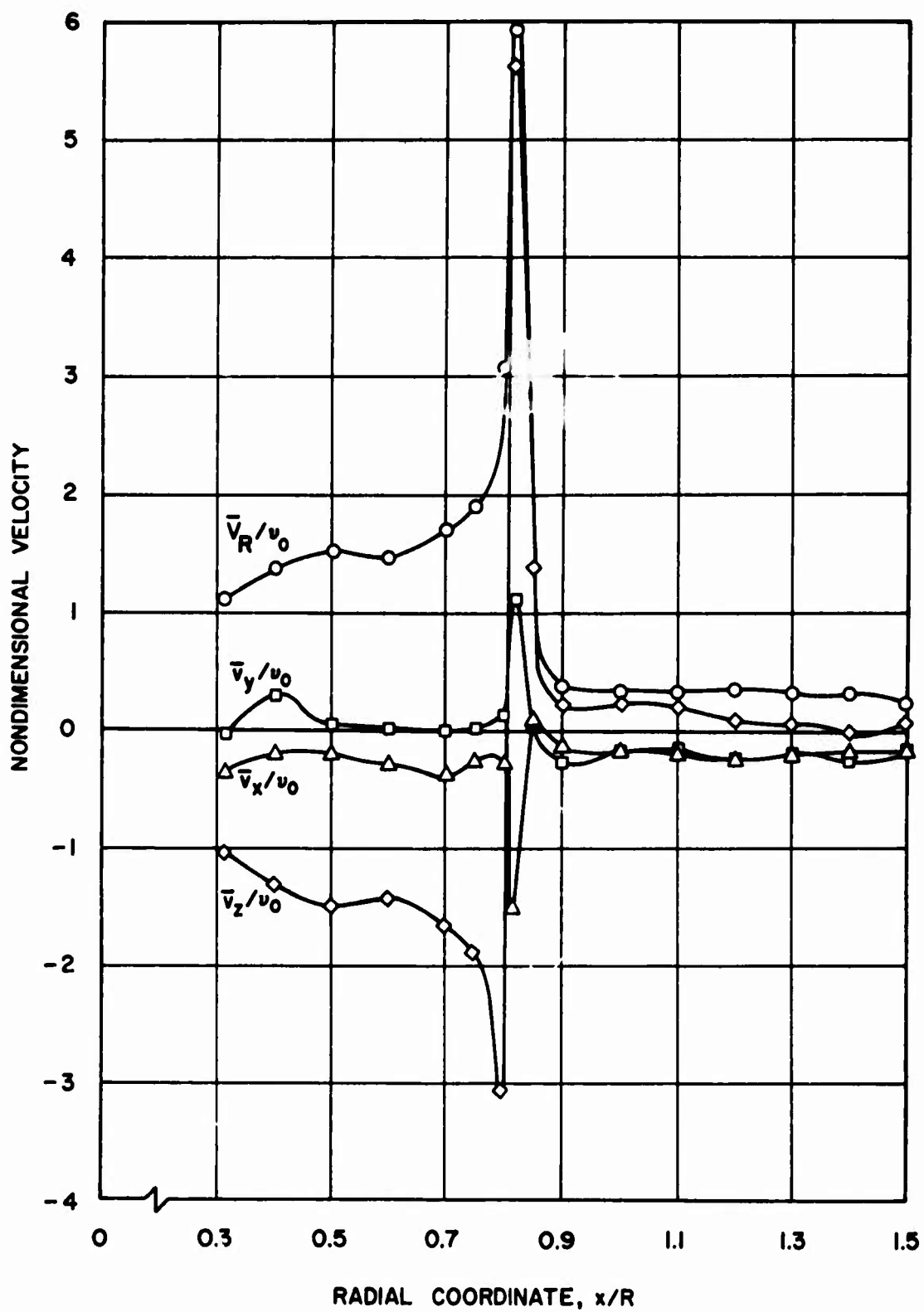


Figure 17. Mean Distribution of Wake Velocity Components and Total Velocity, Test Condition 2, $z/R = -0.15$, $\psi = 0$ deg

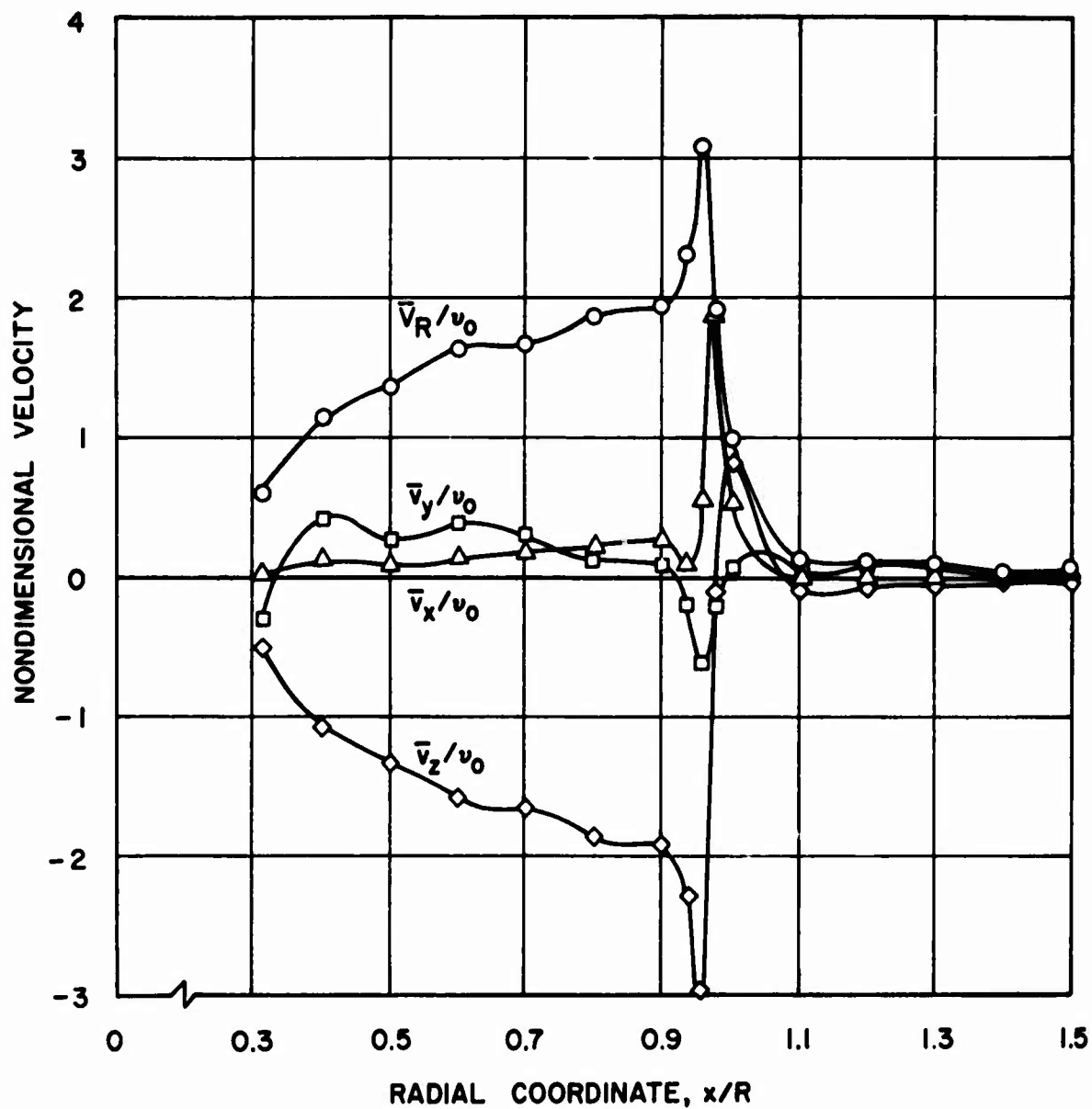


Figure 18. Mean Distribution of Wake Velocity Components and Total Velocity, Test Condition 2, $z/R = -0.30$, $\psi = 90$ deg

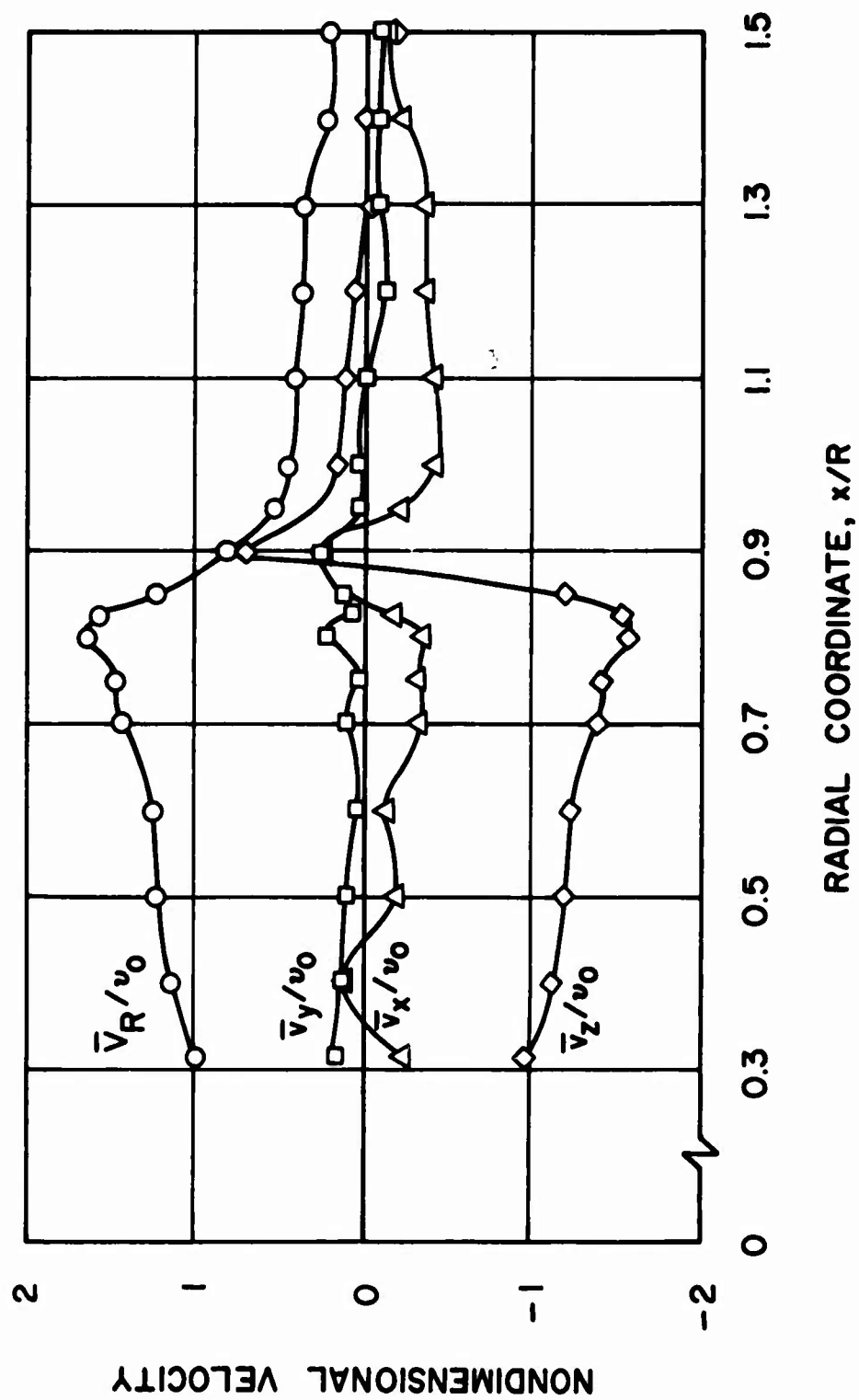


Figure 19. Mean Distribution of Wake Velocity Components and Total Velocity, Test Condition 2, $z/R = -0.045$, $\psi = 0$ deg

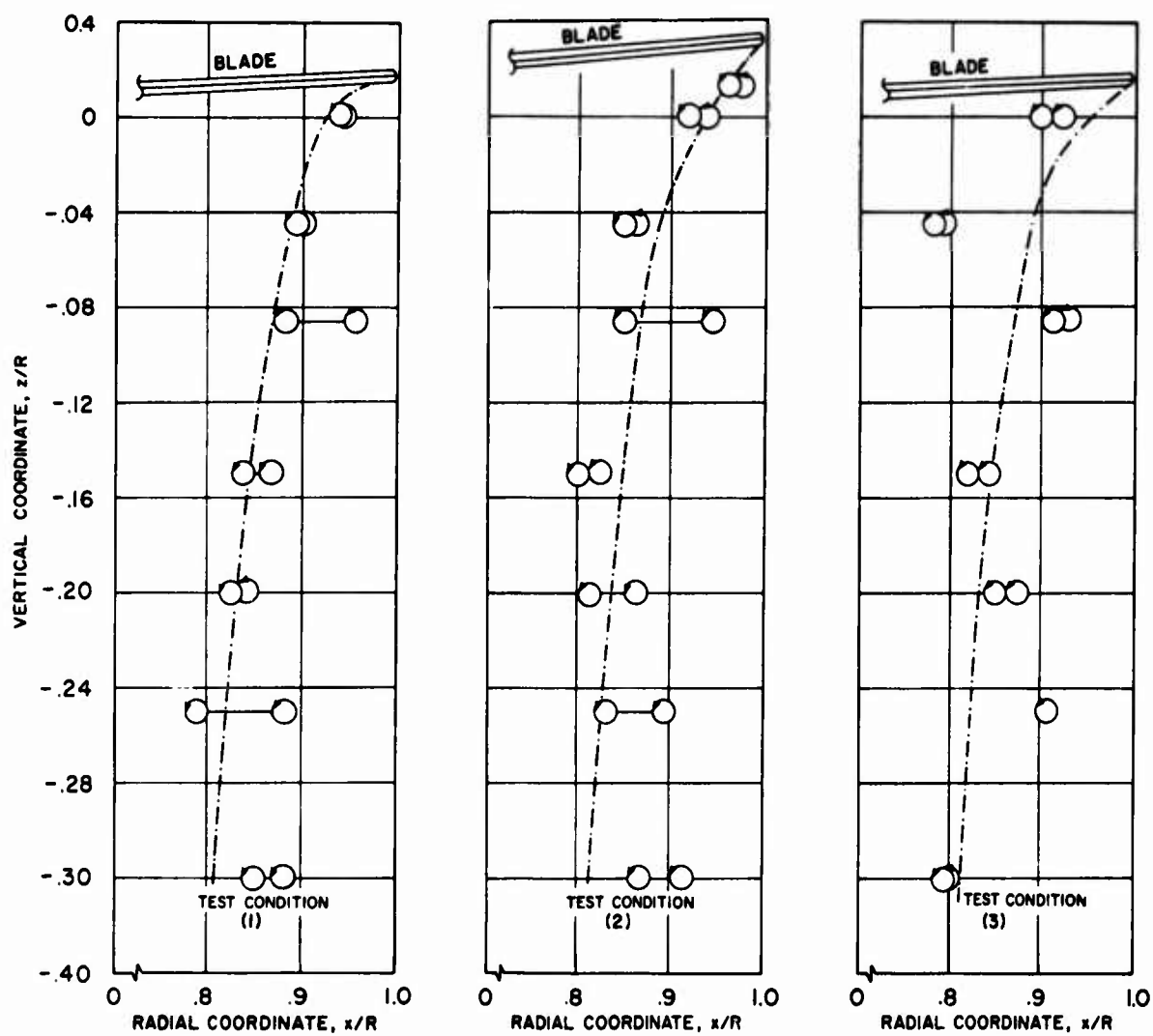


Figure 20. Extent of Vortex Scatter in the Wake Determined from Radial Velocity Surveys with Respect to Predicted Trajectories

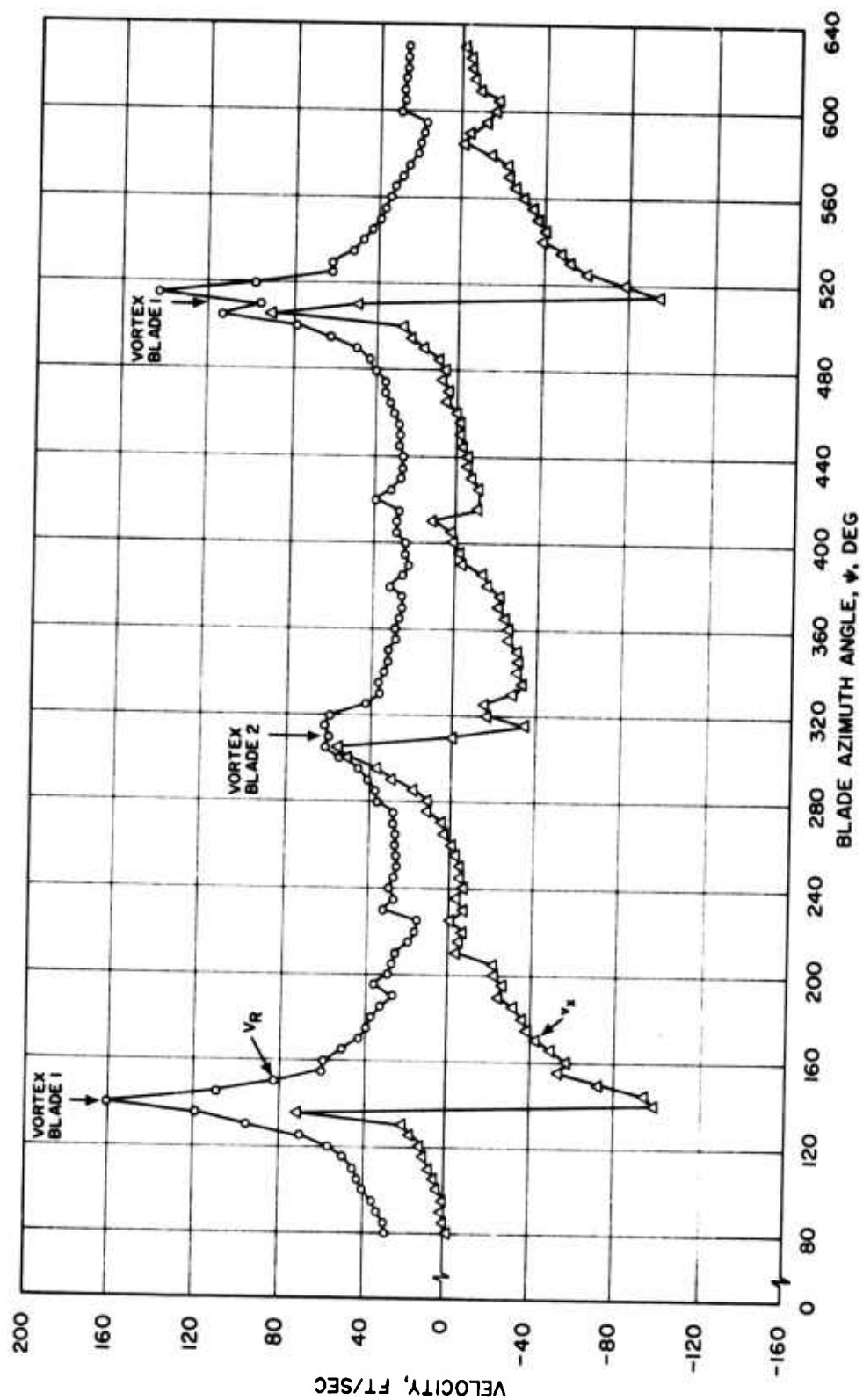


Figure 21. Time-Dependent Total Velocity (V_T) and Radial Velocity Component (V_R) Measured Near the Trailing Vortex, Test Condition 1, $z/R = 0$, $x/R = 0.944$

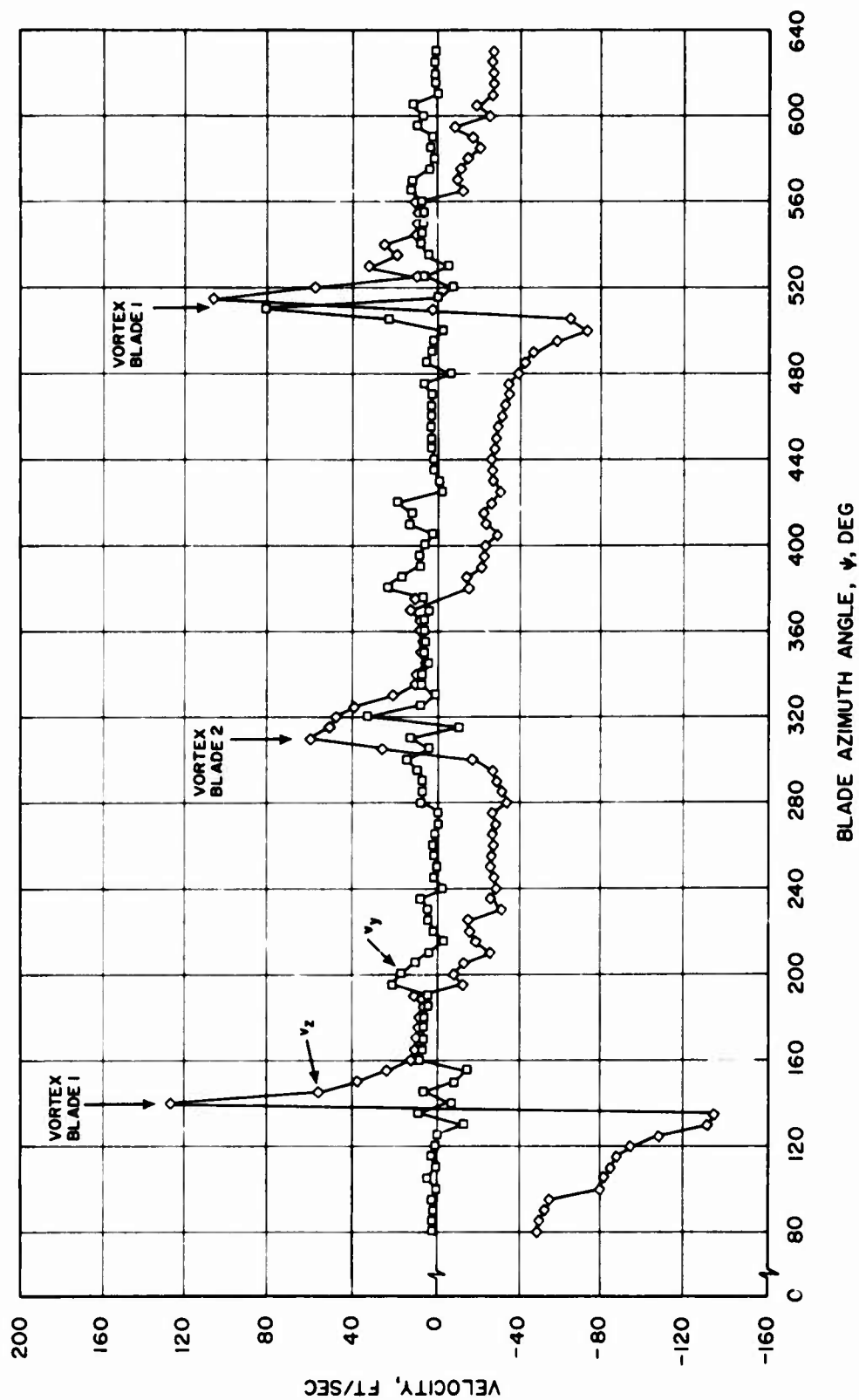


Figure 22. Time-Dependent Velocity Components v_y and v_z Measured Near the Trailing Vortex, Test Condition 1, $z/R = 0$, $x/R = 0.944$

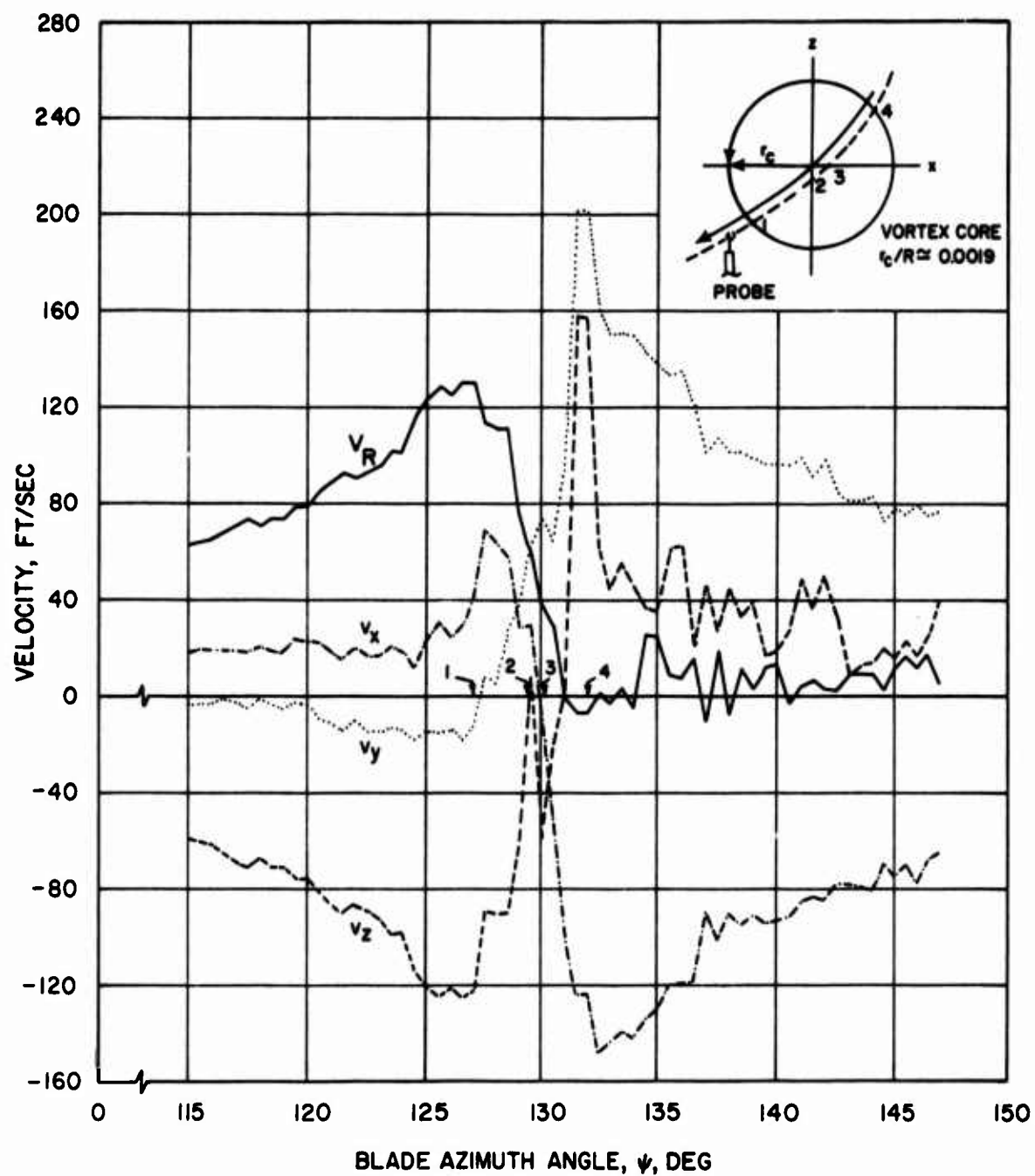


Figure 23. Distribution of the Instantaneous Velocity Components Across a Trailing Vortex, Test Condition 1, $z/R = 0$, $x/R = 0.944$

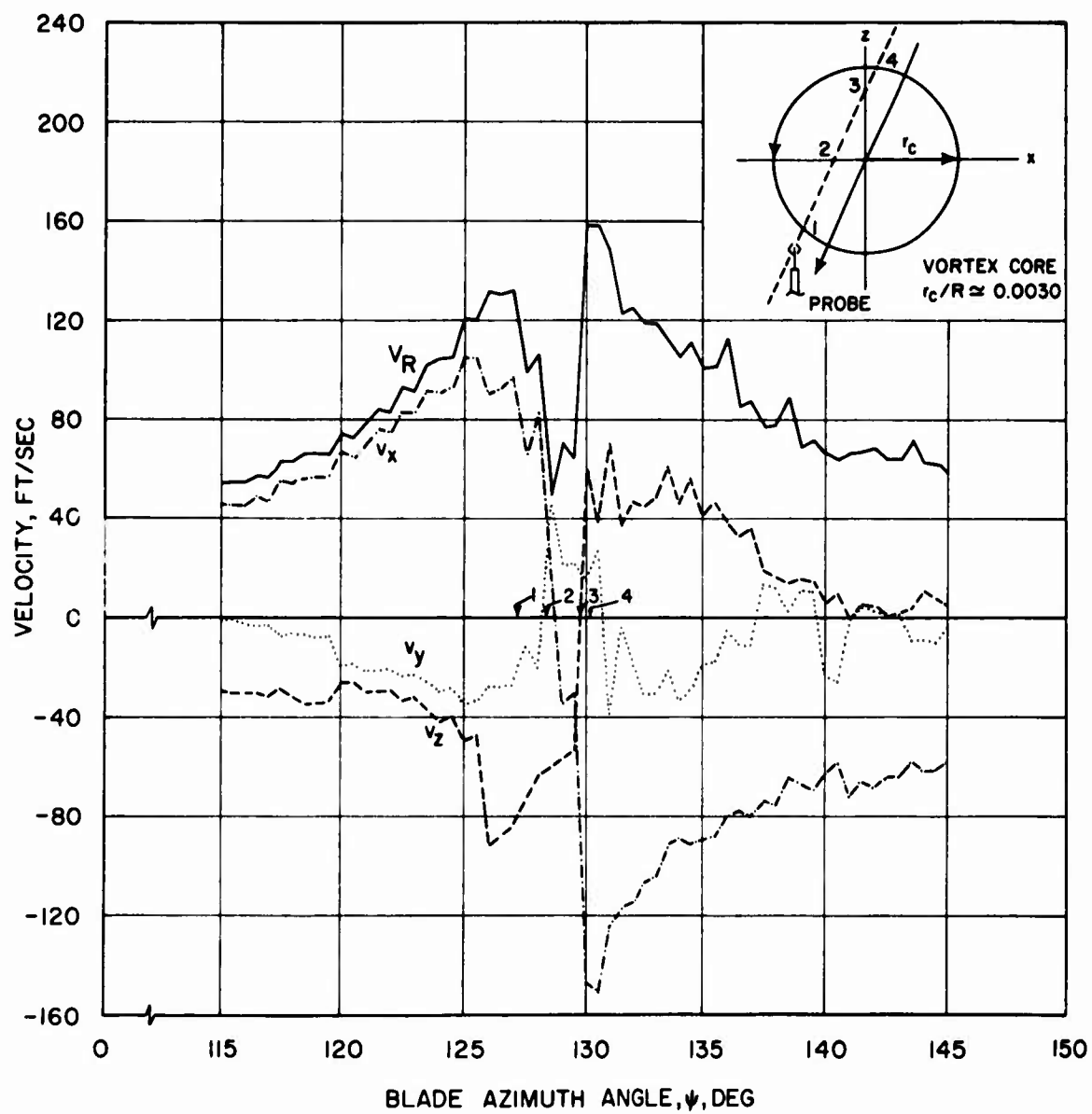


Figure 24. Distribution of the Instantaneous Velocity Components Across a Trailing Vortex, Test Condition 2, $z/R = 0$, $x/R = 0.931$

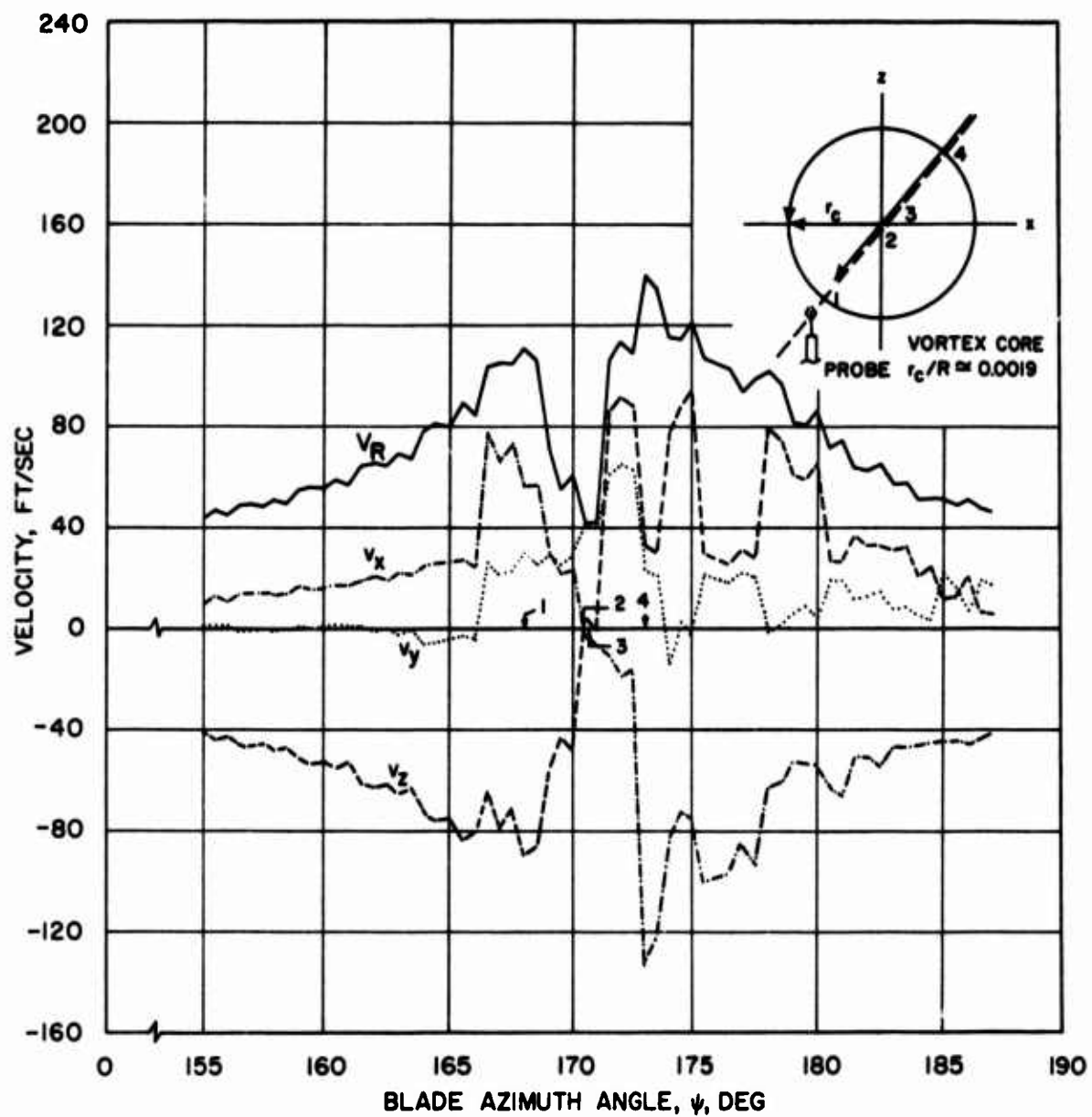


Figure 25. Distribution of the Instantaneous Velocity Components Across a Trailing Vortex, Test Condition 3, $z/R = 0$, $x/R = 0.913$

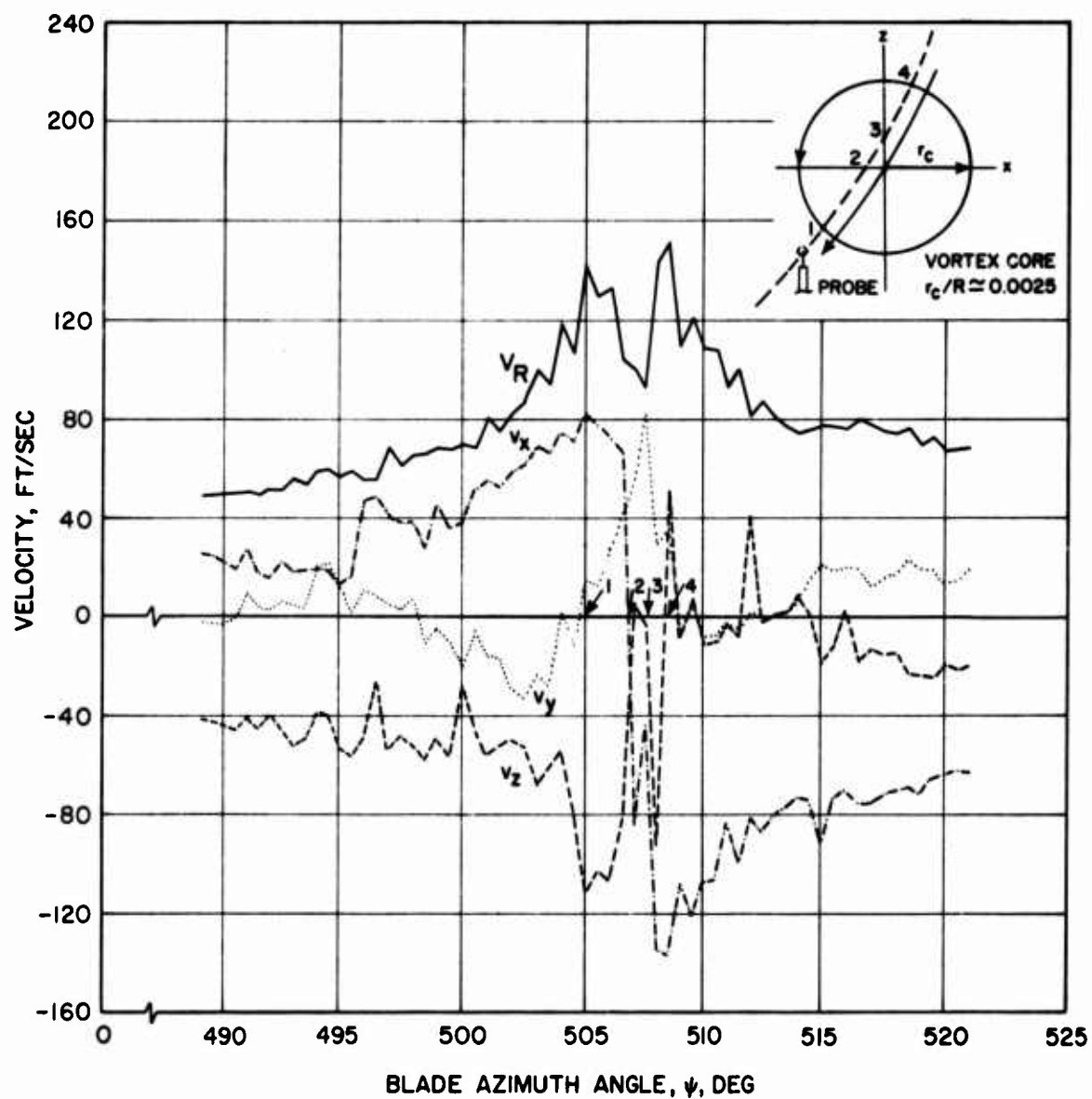


Figure 26. Distribution of the Instantaneous Velocity Components Across a Trailing Vortex, Test Condition 1, $z/R = -0.25$, $x/R = 0.788$

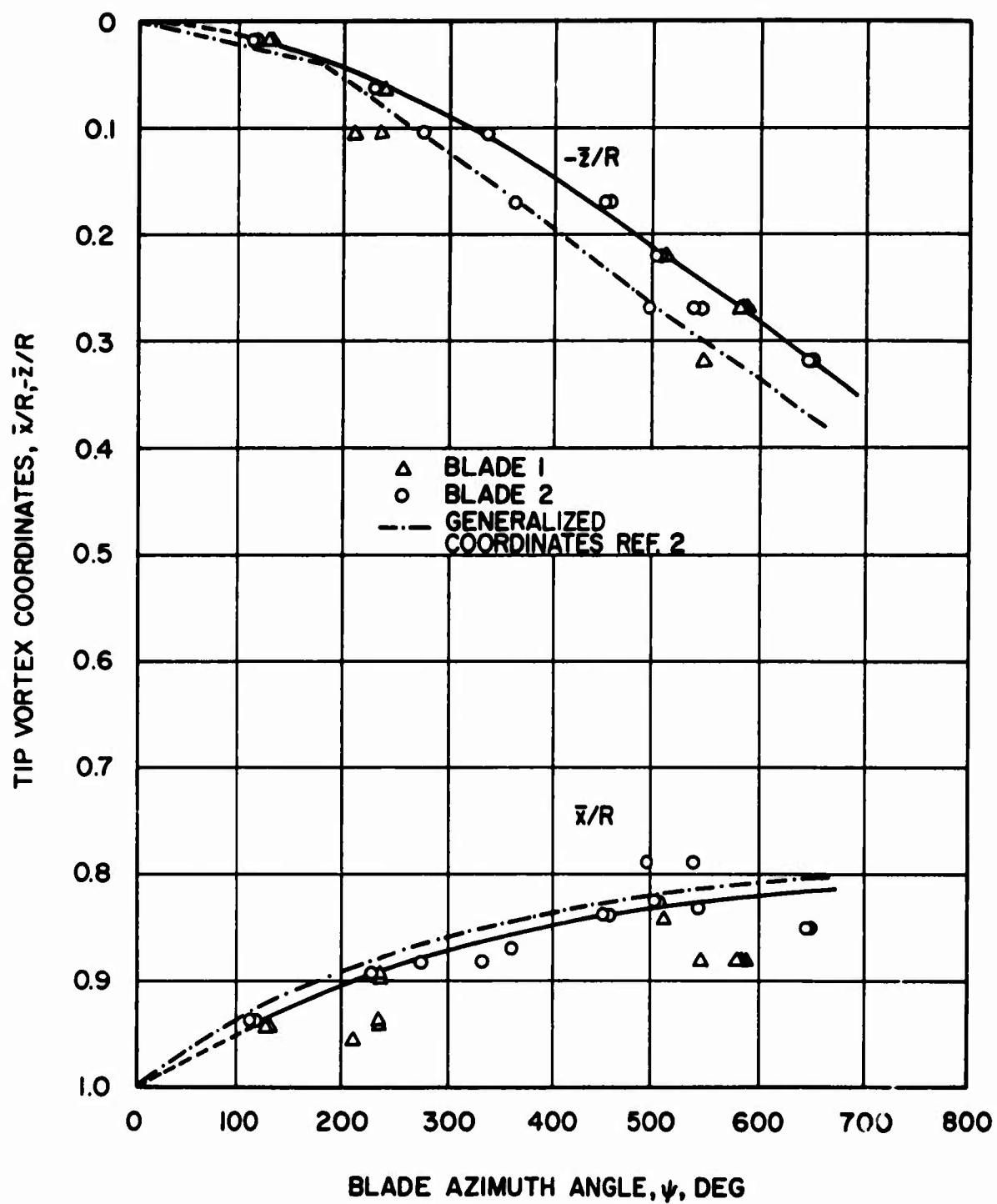


Figure 27. Tip Vortex Coordinates, Test Condition 1

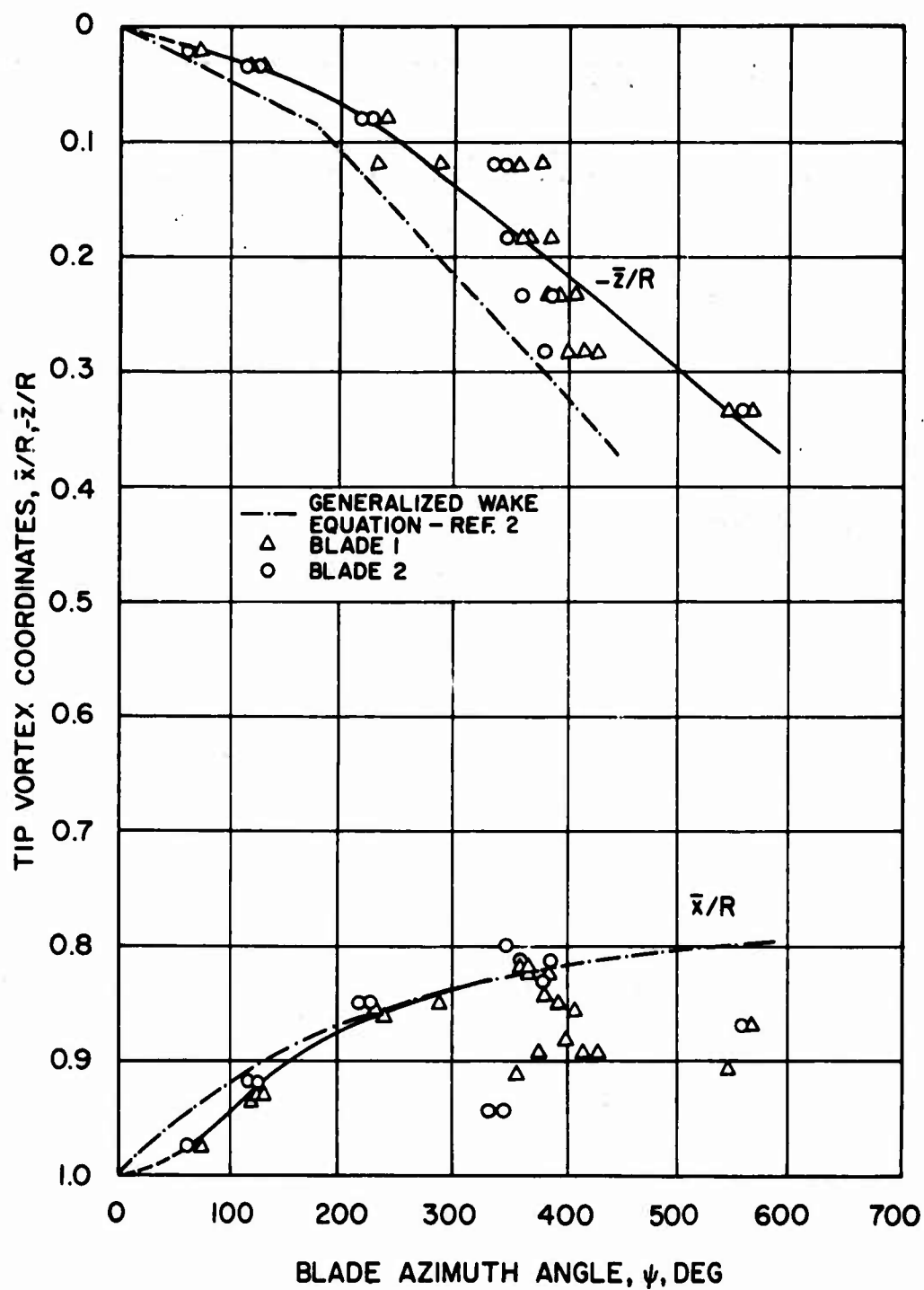


Figure 28. Tip Vortex Coordinates, Test Condition 2

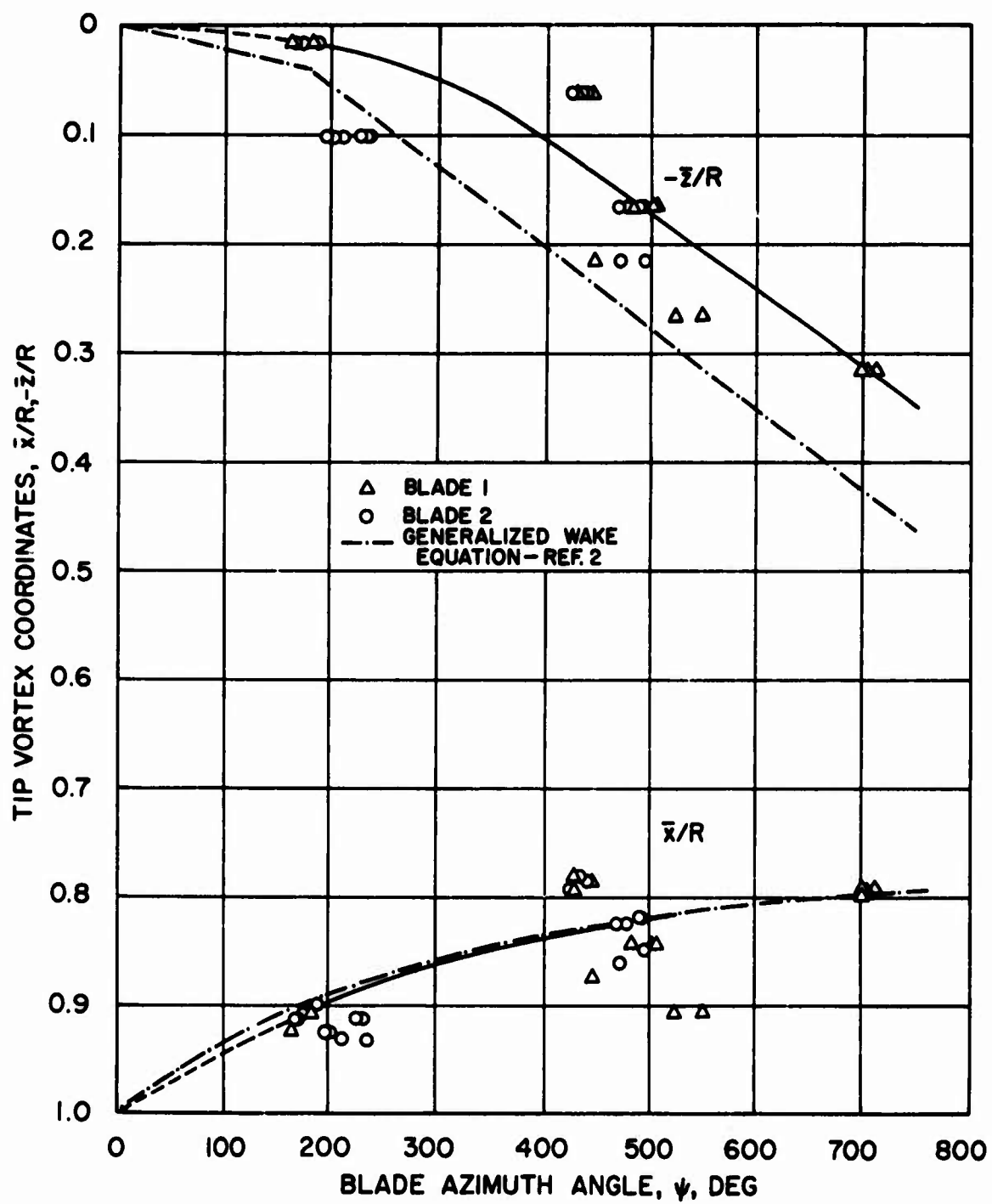


Figure 29. Tip Vortex Coordinates, Test Condition 3

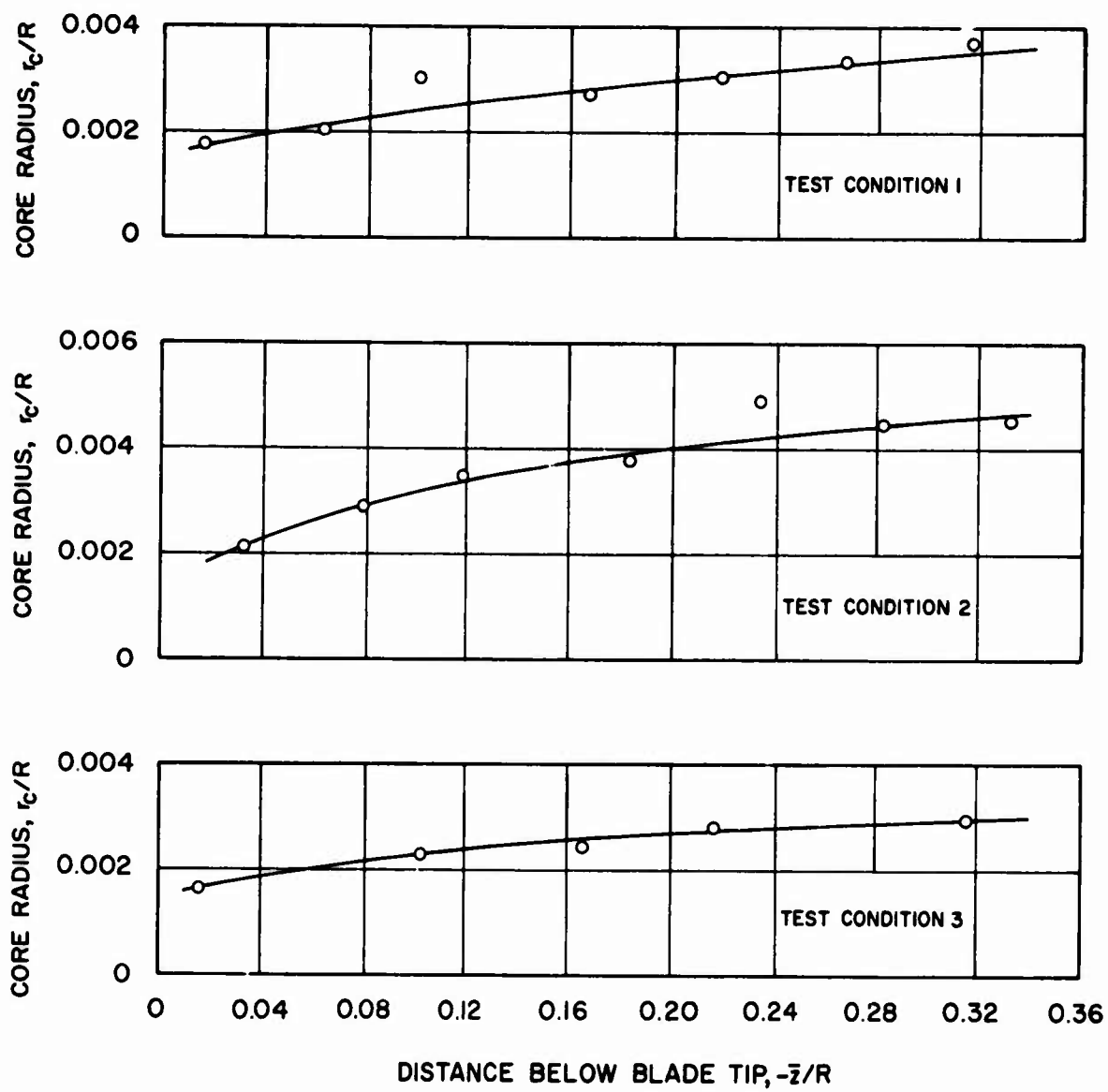


Figure 30. Mean Values of the Vortex Core Radii Determined from Experimental Measurements at Various Distances Below the Rotor

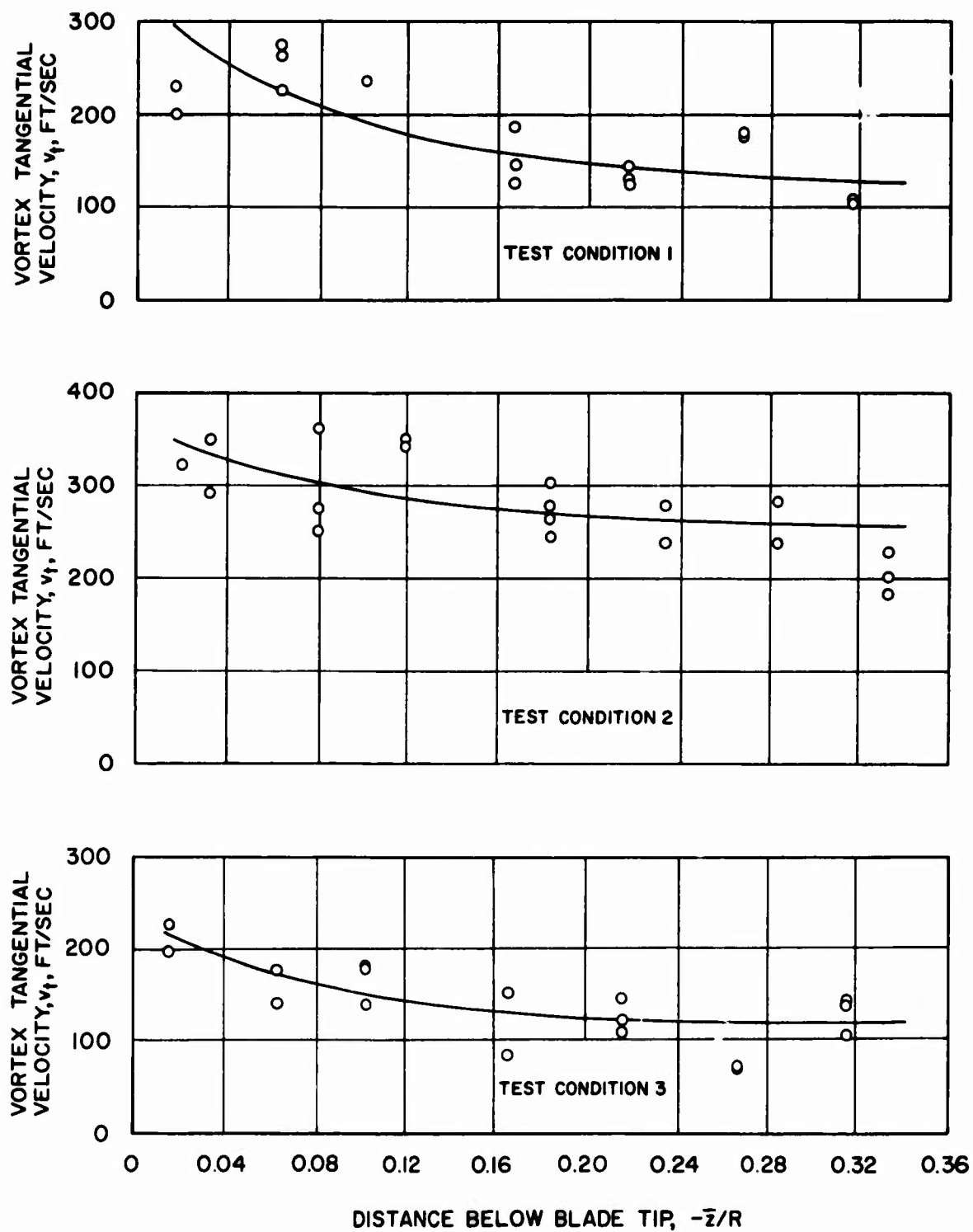


Figure 31. Values of Tangential Velocity Measured at the Edge of the Vortex Cores

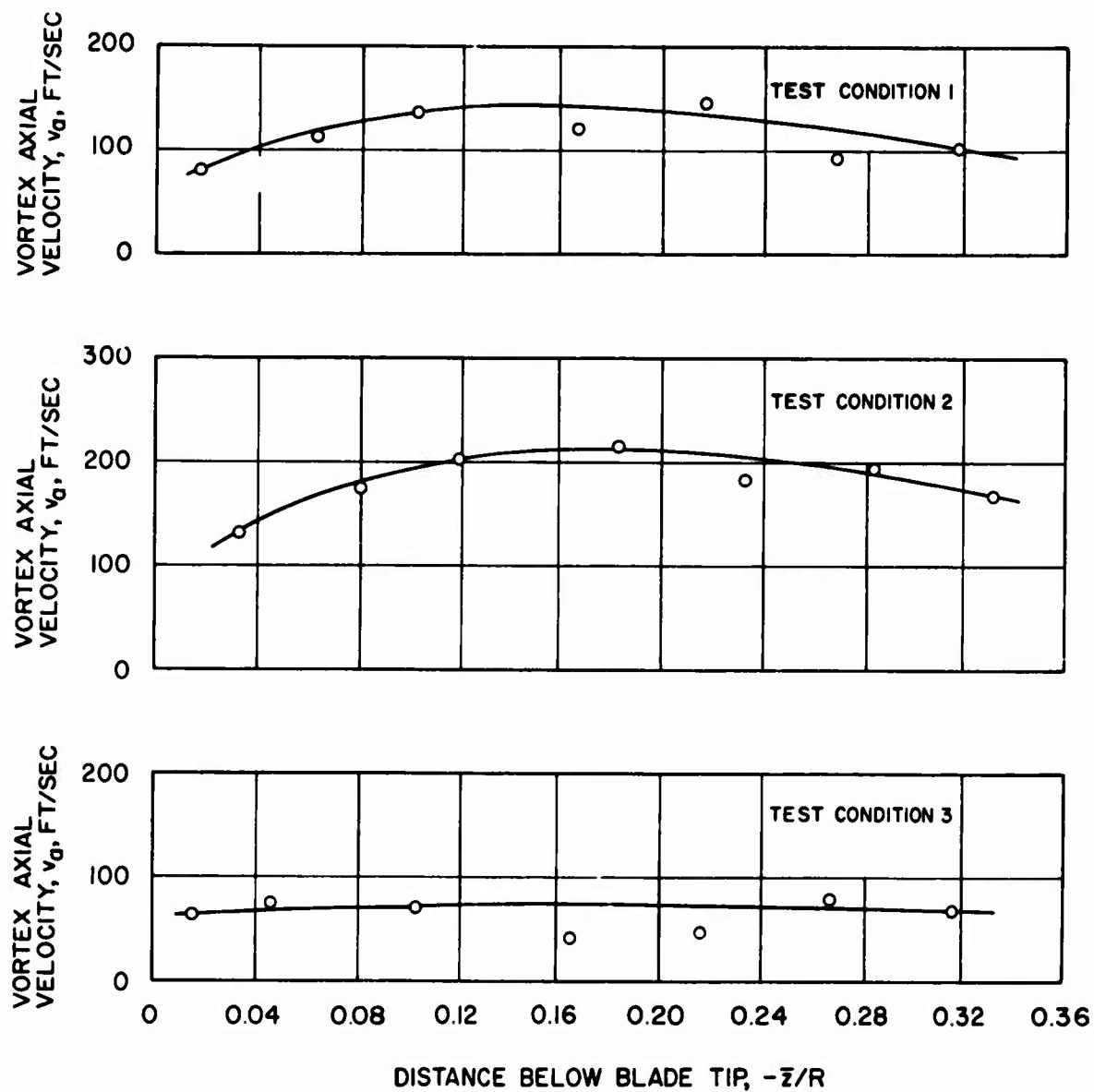
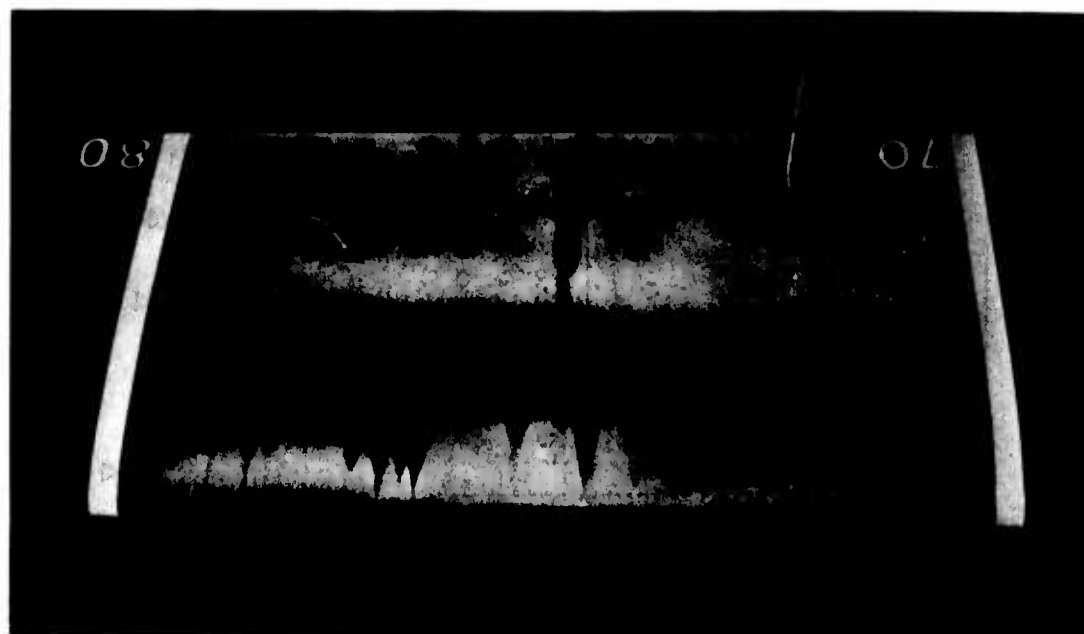


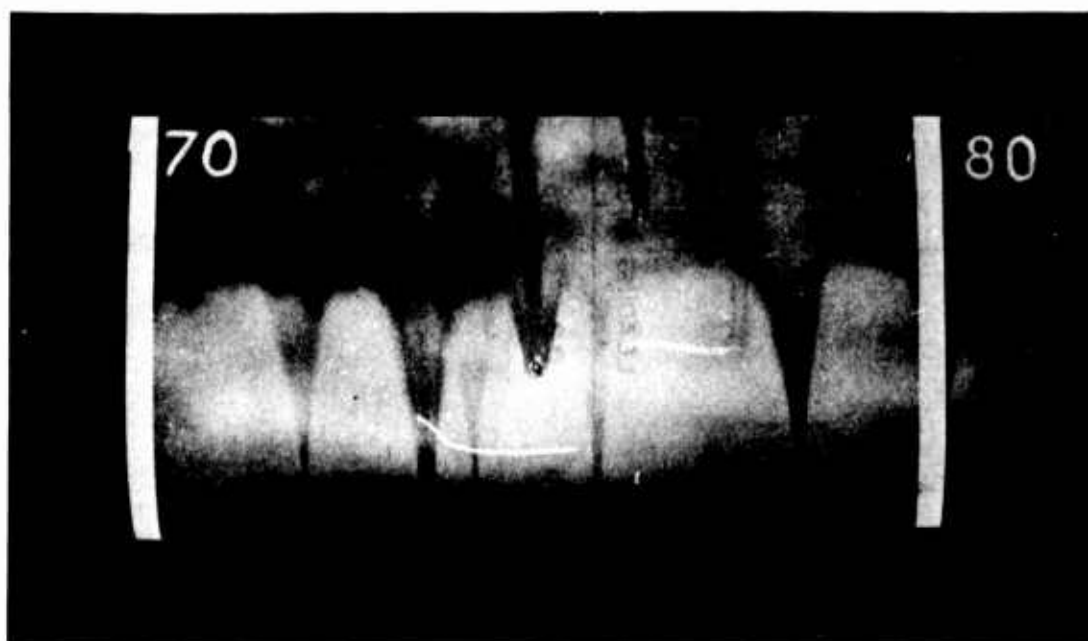
Figure 32. Maximum Values of Axial Velocity Measured Near the Center of the Vortex Cores



Figure 33. Photographs of the Rotor Blade Tip Section Showing Transition and Turbulent Wedges on the Upper Surface, $\theta_{75} = 2.5$ deg, $\Omega R = 429$ ft/sec



(A)



(B)

Figure 34. Results of Sublimation Tests Using Fluorine on the
 (a) Upper and (b) Lower Surfaces of the 70-80 Percent
 Span Test Section, $\theta_{75} = 6.5$ deg, $\Omega R = 604$ ft/sec

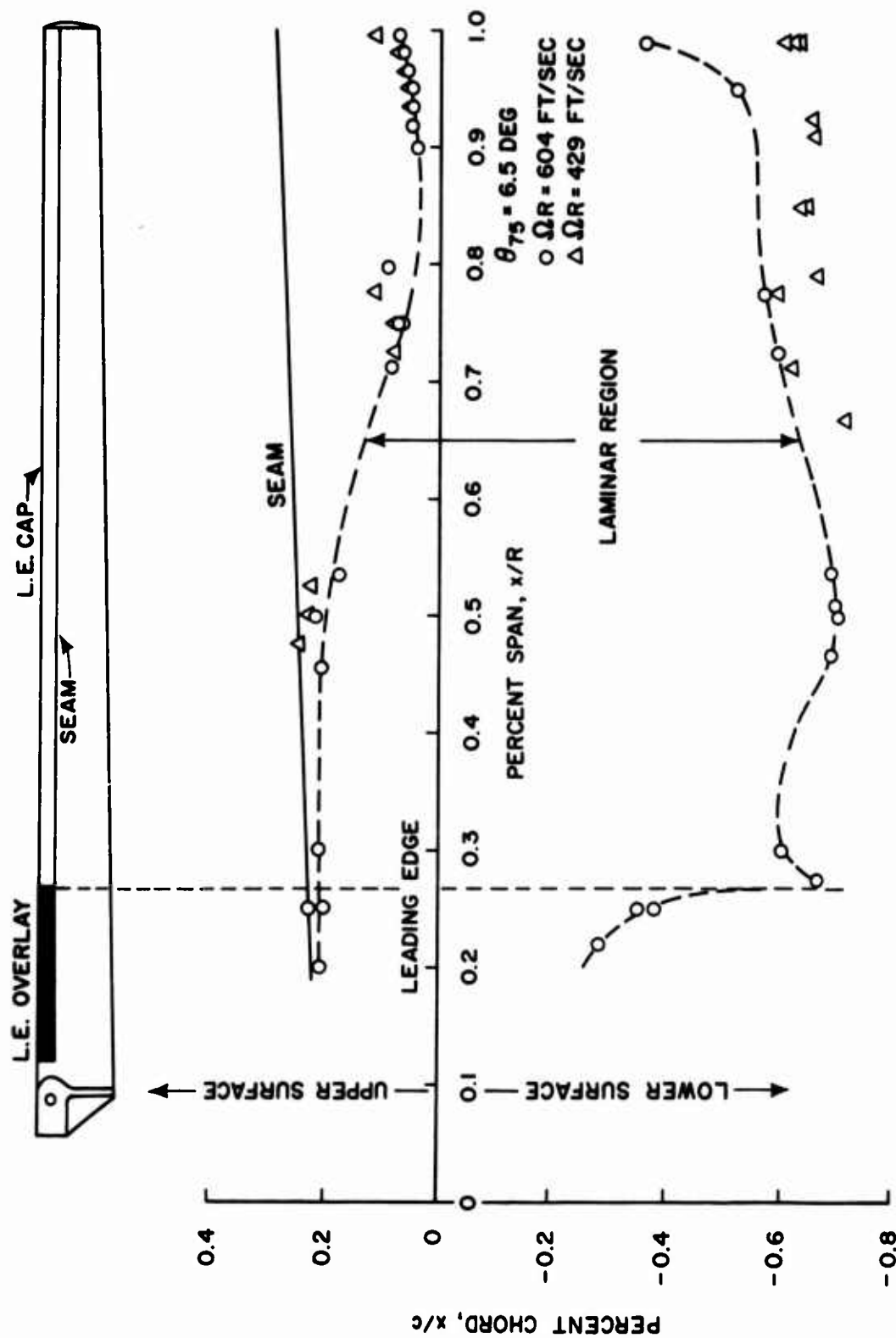


Figure 35. Transition from Laminar to Turbulent Flow on the Test Blade as Determined from Chemical Sublimation Tests

LITERATURE CITED

1. Boatwright, Donald W., MEASUREMENTS OF VELOCITY COMPONENTS IN THE WAKE OF A FULL-SCALE HELICOPTER ROTOR IN HOVER, USAAMRDL Technical Report 72-33, Eustis Directorate, U. S. Army Air Mobility Research and Development Laboratory, Fort Eustis, Virginia, August 1972, AD 754644.
2. Landgrebe, Anton J., AN ANALYTICAL AND EXPERIMENTAL INVESTIGATION OF HELICOPTER ROTOR HOVER PERFORMANCE AND WAKE GEOMETRY CHARACTERISTICS, USAAMRDL Technical Report 71-24, Eustis Directorate, U. S. Army Air Mobility Research and Development Laboratory, Fort Eustis, Virginia, June 1971.
3. Main-Smith, J. D., CHEMICAL SOLIDS AS DIFFUSIBLE COATING FILMS FOR VISUAL INDICATIONS OF BOUNDARY LAYER TRANSITION IN AIR AND WATER, R and M 2755, Aeronautical Research Council Reports and Memoranda, 1954.
4. McCroskey, William J., MEASUREMENTS OF BOUNDARY LAYER TRANSITION, SEPARATION, AND STREAMLINE DIRECTION ON ROTATING BLADES, NASA TN D-6321, National Aeronautics and Space Administration, Washington, DC, April 1971.

APPENDIX I
DISTRIBUTIONS OF MEAN INFLOW VELOCITY COMPONENTS AND STANDARD DEVIATION
PARAMETERS COMPUTED FROM EXPERIMENTAL INFLOW DATA, OH-23B ROTOR, HOVER
CONDITION

TEST CONDITION 1, $z/R = 0.10$

$\Omega R = 624$ ft/sec, $\theta_{75} = 6.18$ deg, $C_T = 0.0020$

x/R	ψ, deg	\bar{v}_R/v_o	\bar{v}_x/v_o	\bar{v}_y/v_o	\bar{v}_z/v_o	σ_{v_R}/v_o	$\sigma_\epsilon, \text{deg}$
0.0	0	.600	.496	.268	-.206	.171	14.0
0.0	45	.571	.474	.251	-.195	.168	15.1
0.0	90	.566	.471	.251	-.190	.168	14.2
0.0	135	.579	.482	.253	-.199	.171	16.2
0.1	0	.761	.489	.153	-.326	.173	10.3
0.1	45	.746	.570	.249	-.412	.191	7.9
0.1	90	.694	.512	.299	-.360	.180	6.9
0.1	135	.622	.484	.256	-.296	.164	6.6
0.2	0	.769	.312	-.016	-.703	.235	7.0
0.2	45	.955	.364	.114	-.875	.314	8.8
0.2	90	.882	.312	.176	-.806	.281	12.1
0.2	135	.810	.255	.129	-.758	.247	8.8
0.3	0	.883	.204	-.137	-.848	.345	15.9
0.3	45	1.124	.309	.048	-1.080	.438	18.5
0.3	90	1.048	.241	.019	-1.020	1.055	32.7
0.3	135	.966	.217	.039	-.940	1.069	33.9
0.4	0	1.012	.134	-.169	-.989	.169	2.6
0.4	45	1.222	.223	.057	-1.200	.204	6.2
0.4	90	1.141	.189	.001	-1.125	.190	7.1
0.4	135	1.084	.133	-.075	-1.073	.180	6.1
0.5	0	1.067	-.034	-.212	-1.045	.346	4.4
0.5	45	1.285	.045	-.003	-1.284	.411	8.0
0.5	90	1.230	.020	-.096	-1.226	.400	6.4
0.5	135	1.165	-.009	-.117	-1.159	.377	4.9
0.6	0	1.058	-.219	-.230	-1.009	.301	6.9
0.6	45	1.371	-.197	.090	-1.354	.375	7.3
0.6	90	1.316	-.207	.061	-1.298	.360	7.0
0.6	135	1.244	-.226	.000	-1.223	.339	6.2
0.7	0	.992	-.487	-.530	-.682	.260	9.1
0.7	45	1.385	-.333	-.050	-1.343	.331	6.0
0.7	90	1.341	-.356	-.022	-1.293	.331	6.1
0.7	135	1.278	-.373	-.045	-1.222	.317	5.2

x/R	ψ, deg	\bar{v}_R/v_o	\bar{v}_x/v_o	\bar{v}_y/v_o	\bar{v}_z/v_o	σ_{V_R}/v_o	$\sigma_\epsilon, \text{deg}$
0.8	0	1.228	-.695	-.187	-.822	.395	10.5
0.8	45	1.404	-.624	.144	-1.250	.495	9.9
0.8	90	1.310	-.594	.083	-1.165	.476	10.3
0.8	135	1.240	-.648	.111	-1.051	1.024	25.5
0.9	0	1.154	-1.078	-.069	-.406	.371	3.2
0.9	45	1.429	-1.123	.042	-.882	.458	7.9
0.9	90	1.386	-1.154	-.057	-.765	.448	7.1
0.9	135	1.299	-1.103	-.087	-.680	.411	6.9
1.0	0	.815	-.815	.005	.028	.283	4.0
1.0	45	1.256	-1.251	-.019	-.106	.470	5.7
1.0	90	1.142	-1.140	-.011	-.065	1.113	24.0
1.0	135	.933	-.927	-.019	-.107	1.016	26.4
1.1	0	.509	-.494	.020	.119	.135	4.9
1.1	45	.646	-.621	.030	.175	.164	4.5
1.1	90	.577	-.559	.024	.142	.155	3.7
1.1	135	.534	-.524	.017	.102	.138	3.6
1.2	0	.323	-.322	.005	.027	.073	3.0
1.2	45	.364	-.359	.011	.062	.086	25.9
1.2	90	.342	-.340	.007	.037	.076	2.9
1.2	135	.337	-.337	.002	.013	.074	2.8
1.3	0	.296	-.293	.033	.016	.024	9.1
1.3	45	.306	-.302	.020	.045	.029	14.6
1.3	90	.303	-.301	.033	.020	.026	8.9
1.3	135	.293	-.291	.035	.005	.025	9.0
1.4	0	.227	-.168	-.151	-.026	.043	10.7
1.4	45	.227	-.174	-.145	-.015	.047	19.2
1.4	90	.227	-.174	-.144	-.025	.045	9.7
1.4	135	.225	-.174	-.140	-.026	.045	9.4
1.5	0	.176	-.064	.028	.162	.025	28.0
1.5	45	.190	-.048	.031	.181	.022	24.0
1.5	90	.186	-.056	.030	.175	.025	27.3
1.5	135	.188	-.044	.031	.180	.025	27.6

TEST CONDITION 2, $z/R = 0.10$
 $\Omega R = 435 \text{ ft/sec}$, $\theta_{75} = 9.96 \text{ deg}$, $C_T = 0.0045$

x/R	ψ, deg	\bar{v}_R/v_o	\bar{v}_x/v_o	\bar{v}_y/v_o	\bar{v}_z/v_o	σ_{V_R}/o	$\sigma_\epsilon, \text{deg}$
0.0	0	.471	.094	.073	-.456	.032	3.9
0.0	45	.464	.090	.076	-.448	.040	4.7
0.0	90	.468	.095	.074	-.452	.043	4.9
0.0	135	.468	.094	.065	-.453	.049	3.7
0.1	0	.542	.410	.092	-.342	.026	9.8
0.1	45	.672	.503	.147	-.420	.045	9.3
0.1	90	.640	.532	.182	-.307	.037	6.3
0.1	135	.540	.448	.136	-.270	.043	11.3
0.2	0	.691	.247	-.024	-.645	.038	6.8
0.2	45	.957	.339	-.017	-.895	.073	7.4
0.2	90	.880	.287	.089	-.827	.108	5.5
0.2	135	.791	.229	.101	-.751	.058	4.4
0.3	0	.881	.173	-.194	-.842	.084	7.4
0.3	45	1.141	.319	-.035	-1.095	.064	6.4
0.3	90	1.051	.233	-.124	-1.018	.057	5.1
0.3	135	.978	.177	-.130	-.953	.069	5.0
0.4	0	.936	.112	-.345	-.863	.109	10.6
0.4	45	1.251	.261	.007	-1.224	.066	5.0
0.4	90	1.153	.206	-.036	-1.134	.061	6.8
0.4	135	1.082	.125	-.148	-1.065	.073	4.2
0.5	0	.918	-.010	-.222	-.891	.071	5.3
0.5	45	1.391	.141	.210	-1.368	.068	3.3
0.5	90	1.271	.123	.132	-1.259	.053	3.4
0.5	135	1.192	.055	.024	-1.191	.072	7.9
0.6	0	.880	-.162	-.138	-.854	.129	3.5
0.6	45	1.395	-.007	.266	-1.369	.236	5.5
0.6	90	1.338	-.064	.261	-1.311	.194	5.3
0.6	135	1.276	-.099	.225	-1.252	.191	5.4
0.7	0	.934	-.567	.231	-.706	.079	6.8
0.7	45	1.513	-.212	.211	-1.483	.070	3.4
0.7	90	1.441	-.273	.184	-1.403	.073	3.3
0.7	135	1.367	-.330	.147	-1.318	.065	3.5
0.8	0	1.035	-.766	.011	-.695	.182	12.0
0.8	45	1.594	-.402	.166	-1.534	.074	4.2
0.8	90	1.467	-.467	.048	-1.389	.055	4.4
0.8	135	1.379	-.520	.105	-1.273	.075	4.0

x/R	ψ, deg	\bar{V}_R/v_o	\bar{v}_x/v_o	\bar{v}_y/v_o	\bar{v}_z/v_o	σ_{V_R}/v_o	$\sigma_\epsilon, \text{deg}$
0.9	0	1.063	-.995	-.050	-.371	.042	4.7
0.9	45	1.754	-1.072	.342	-1.345	.081	7.4
0.9	90	1.598	-1.090	.255	-1.141	.058	4.5
0.9	135	1.389	-1.154	-.010	-.773	.047	6.1
1.0	0	.725	-.723	-.007	-.050	.052	2.9
1.0	45	1.664	-1.657	.025	.147	.073	2.6
1.0	90	1.214	-1.213	-.005	-.028	.056	2.6
1.0	135	.937	-.920	-.009	-.174	.088	4.4
1.1	0	.429	-.386	.113	-.149	.068	7.7
1.1	45	.521	-.519	.042	.028	.097	9.2
1.1	90	.508	-.493	.075	-.095	.095	8.4
1.1	135	.492	-.446	.111	-.176	.083	9.1
1.2	0	.375	-.277	.225	-.113	.048	12.7
1.2	45	.383	-.317	.211	-.036	.053	10.6
1.2	90	.388	-.312	.218	-.076	.054	10.7
1.2	135	.396	-.295	.230	-.130	.054	11.3
1.3	0	.293	-.122	.213	-.160	.022	3.0
1.3	45	.282	-.162	.194	-.127	.023	8.4
1.3	90	.283	-.131	.194	-.158	.027	3.9
1.3	135	.296	-.127	.210	-.165	.023	2.9
1.4	0	.205	-.125	.107	-.122	.039	11.6
1.4	45	.192	-.134	.096	-.099	.041	23.1
1.4	90	.211	-.145	.099	-.116	.043	14.2
1.4	135	.221	-.137	.111	-.133	.045	10.7
1.5	0	.153	-.004	.151	.023	.050	39.0
1.5	45	.157	-.029	.154	.009	.055	38.4
1.5	90	.158	-.015	.156	.019	.059	37.3
1.5	135	.156	-.016	.154	.018	.061	39.3

TEST CONDITION 3, $z/R = 0.10$
 $\Omega R = 447 \text{ ft/sec}$, $\theta_{75} = 6.31 \text{ deg}$, $C_T = 0.0022$

x/R	ψ, deg	\bar{v}_R/v_o	\bar{v}_x/v_o	\bar{v}_y/v_o	\bar{v}_z/v_o	σ_{v_R}/v_o	$\sigma_\epsilon, \text{deg}$
0.0	0	.662	.332	.403	-.406	.043	2.8
0.0	45	.696	.353	.417	-.430	.066	2.7
0.0	90	.692	.344	.426	-.422	.061	2.8
0.0	135	.682	.340	.419	-.417	.057	2.7
0.1	0	.787	.530	.222	-.542	.040	5.7
0.1	45	.911	.609	.307	-.604	.070	6.0
0.1	90	.895	.536	.387	-.603	.100	3.3
0.1	135	.833	.498	.373	-.554	.074	4.2
0.2	0	.879	.570	.245	-.622	.138	3.6
0.2	45	1.066	.633	.462	-.722	.190	2.6
0.2	90	.992	.564	.486	-.656	.173	4.1
0.2	135	.907	.513	.450	-.598	.142	2.6
0.3	0	.904	.606	.134	-.657	.157	9.8
0.3	45	1.175	.940	.323	-.627	.205	8.7
0.3	90	1.095	.903	.297	-.544	.186	7.7
0.3	135	1.037	.870	.252	-.505	.195	8.3
0.4	0	.981	.525	.165	-.812	.068	8.6
0.4	45	1.327	.489	.043	-1.233	.087	9.9
0.4	90	1.220	.408	.041	-1.149	.094	6.3
0.4	135	1.132	.380	.089	-1.062	.090	6.4
0.5	0	1.059	.243	-.157	-1.019	.053	3.7
0.5	45	1.409	.337	.009	-1.368	.099	8.0
0.5	90	1.328	.315	.059	-1.289	.088	6.8
0.5	135	1.208	.265	.151	-1.169	.066	4.3
0.6	0	1.070	.120	-.172	-1.049	.088	3.3
0.6	45	1.496	.196	-.041	-1.483	.105	7.5
0.6	90	1.365	.175	-.094	-1.350	.095	6.0
0.6	135	1.256	.146	.006	-1.248	.086	6.1
0.7	0	1.024	-.060	-.171	-1.008	.140	5.2
0.7	45	1.502	-.005	-.096	-1.499	.078	6.1
0.7	90	1.381	.002	-.125	-1.375	.109	5.8
0.7	135	1.271	-.015	-.077	-1.269	.108	7.4
0.8	0	.900	-.277	-.125	-.847	.038	9.7
0.8	45	1.495	-.233	-.053	-1.476	.083	7.2
0.8	90	1.383	-.214	-.088	-1.363	.078	6.6
0.8	135	1.258	-.218	-.016	-1.239	.082	5.9

x/R	ψ , deg	\bar{v}_R/v_o	\bar{v}_x/v_o	\bar{v}_y/v_o	\bar{v}_z/v_o	σ_{v_R}/v_o	σ_ϵ , deg
0.9	0	.825	-.572	-.051	-.593	.167	14.7
0.9	45	1.432	-.642	.117	-1.274	.067	6.6
0.9	90	1.285	-.586	.106	-1.139	.112	7.3
0.9	135	1.100	-.522	.136	-.958	.079	5.7
1.0	0	.558	-.481	-.017	-.283	.065	7.0
1.0	45	1.056	-.945	-.013	-.473	.065	5.3
1.0	90	.858	-.737	.039	-.437	.077	7.1
1.0	135	.746	-.560	.139	-.472	.055	7.1
1.1	0	.327	-.181	.169	-.213	.025	3.3
1.1	45	.413	-.357	.143	-.150	.042	4.3
1.1	90	.400	-.292	.161	-.220	.031	7.4
1.1	135	.393	-.217	.206	-.255	.035	3.0
1.2	0	.220	.026	.218	-.011	.052	27.6
1.2	45	.232	-.005	.228	-.044	.051	26.1
1.2	90	.237	-.023	.227	-.062	.051	26.3
1.2	135	.239	-.034	.225	-.073	.057	27.7
1.3	0	.211	.129	.164	-.027	.035	21.3
1.3	45	.197	.066	.184	.024	.034	28.2
1.3	90	.221	.132	.176	-.023	.034	20.6
1.3	135	.239	.160	.172	-.045	.023	5.2
1.4	0	.199	.050	.177	-.078	.044	29.3
1.4	45	.190	.028	.179	-.056	.046	30.8
1.4	90	.198	.037	.183	-.065	.046	30.3
1.4	135	.219	.072	.178	-.104	.047	17.7
1.5	0	.241	.108	.165	-.138	.018	3.7
1.5	45	.237	.101	.169	-.132	.022	3.3
1.5	90	.241	.105	.169	-.135	.022	3.5
1.5	135	.250	.110	.174	-.141	.023	3.4

TEST CONDITION 1, $z/R = 0.20$

$\Omega R = 623$ ft/sec, $\theta_{75} = 6.18$ deg, $C_T = 0.0019$

x/R	ψ , deg	\bar{v}_R/v_o	\bar{v}_x/v_o	\bar{v}_y/v_o	\bar{v}_z/v_o	σ_{v_R}/v_o	σ_ϵ , deg
0.0	0	.730	.268	-.010	-.679	.051	6.8
0.0	45	.738	.273	-.017	-.686	.048	5.6
0.0	90	.730	.261	-.031	-.681	.053	7.6
0.0	135	.733	.264	-.028	-.683	.041	6.7

x/R	ψ, deg	\bar{v}_R/v_o	\bar{v}_x/v_o	\bar{v}_y/v_o	\bar{v}_z/v_o	σ_{v_R}/v_o	$\sigma_\epsilon, \text{deg}$
0.1	0	.744	.368	.140	-.631	.059	7.0
0.1	45	.769	.430	.173	-.614	.059	9.0
0.1	90	.772	.361	.101	-.676	.075	8.2
0.1	135	.735	.304	.069	-.666	.070	9.4
0.2	0	.856	.325	.019	-.792	.069	11.0
0.2	45	.919	.387	.065	-.831	.111	10.7
0.2	90	.875	.325	.027	-.812	.073	8.5
0.2	135	.841	.283	.002	-.792	.056	9.3
0.3	0	.908	.439	.160	-.778	.070	10.1
0.3	45	.997	.508	.147	-.845	.098	8.7
0.3	90	.963	.399	.011	-.877	.087	9.3
0.3	135	.882	.352	.034	-.808	.054	8.7
0.4	0	1.006	.214	-.214	-.960	.166	6.1
0.4	45	1.105	.292	-.085	-1.062	.172	6.3
0.4	90	1.056	.234	-.144	-1.020	.154	4.7
0.4	135	.980	.199	-.153	-.948	.168	3.4
0.5	0	1.055	.087	-.193	-1.033	.180	5.4
0.5	45	1.134	.141	-.145	-1.116	.173	4.8
0.5	90	1.097	.115	-.121	-1.085	.191	5.6
0.5	135	.998	.082	-.151	-.983	.167	4.0
0.6	0	1.085	-.088	-.185	-1.066	.164	4.1
0.6	45	1.192	-.077	-.098	-1.186	.178	6.9
0.6	90	1.129	-.071	-.174	-1.113	.173	5.1
0.6	135	1.073	-.075	-.172	-1.056	.166	4.7
0.7	0	1.055	-.091	-.267	-1.016	.062	8.0
0.7	45	1.190	-.091	-.155	-1.176	.063	4.9
0.7	90	1.123	-.089	-.173	-1.107	.074	3.7
0.7	135	1.063	-.081	-.161	-1.047	.062	4.6
0.8	0	.929	-.358	-.403	-.757	.085	6.5
0.8	45	1.106	-.374	-.281	-1.002	.081	10.7
0.8	90	.990	-.327	-.140	-.924	.115	12.4
0.8	135	.869	-.315	-.212	-.782	.068	15.7
0.9	0	.782	-.410	-.251	-.617	.059	8.6
0.9	45	.910	-.562	.019	-.715	.108	15.6
0.9	90	.806	-.527	.034	-.609	.080	16.6
0.9	135	.722	-.473	-.094	-.537	.065	19.8

x/R	Ψ, deg	\bar{v}_R/v_o	\bar{v}_x/v_o	\bar{v}_y/v_o	\bar{v}_z/v_o	σ_{v_R}/v_o	$\sigma_\epsilon, \text{deg}$
1.0	0	.563	-.472	-.054	-.303	.049	20.4
1.0	45	.725	-.606	-.071	-.391	.069	13.2
1.0	90	.665	-.553	-.087	-.360	.043	11.6
1.0	135	.591	-.474	-.085	-.343	.048	12.8
1.1	0	.514	-.358	.186	-.318	.037	16.8
1.1	45	.600	-.429	.236	-.347	.060	11.1
1.1	90	.567	-.370	.221	-.369	.059	13.3
1.1	135	.556	-.329	.219	-.391	.039	15.9
1.2	0	.262	-.152	.011	-.213	.033	22.4
1.2	45	.295	-.183	.090	-.212	.040	9.3
1.2	90	.284	-.165	.074	-.219	.039	15.1
1.2	135	.283	-.148	.049	-.236	.032	14.2
1.3	0	.356	-.004	.030	-.355	.040	8.8
1.3	45	.354	-.019	.038	-.352	.049	6.7
1.3	90	.360	-.011	.040	-.358	.045	7.6
1.3	135	.371	.000	.033	-.369	.042	6.9
1.4	0	.173	-.009	.145	-.093	.073	45.0
1.4	45	.171	-.016	.164	-.043	.081	47.1
1.4	90	.157	.031	.152	-.025	.090	48.9
1.4	135	.162	.045	.145	-.057	.086	46.6
1.5	0	.246	.227	.013	-.094	.059	12.1
1.5	45	.241	.227	.003	-.081	.055	11.5
1.5	90	.249	.231	.016	-.091	.059	10.9
1.5	135	.234	.233	.022	-.010	.056	10.8

TEST CONDITION 2, $z/R = 0.20$

$\Omega R = 447 \text{ ft/sec}$, $\theta_{75} = 9.69 \text{ deg}$, $C_T = 0.0040$

x/R	Ψ, deg	\bar{v}_R/v_o	\bar{v}_x/v_o	\bar{v}_y/v_o	\bar{v}_z/v_o	σ_{v_R}/v_o	$\sigma_\epsilon, \text{deg}$
0.0	0	.822	.209	.162	-.778	.060	4.1
0.0	45	.825	.217	.179	-.776	.046	3.2
0.0	90	.812	.211	.144	-.771	.084	4.1
0.0	135	.823	.219	.154	-.779	.065	3.5
0.1	0	.819	.271	.089	-.768	.070	5.3
0.1	45	.833	.335	.115	-.754	.067	12.9
0.1	90	.817	.325	.73	-.729	.096	14.9
0.1	135	.814	.243	.131	-.765	.067	4.3

x/R	Ψ, deg	\bar{v}_R/v_o	\bar{v}_x/v_o	\bar{v}_y/v_o	\bar{v}_z/v_o	σ_{v_R}/v_o	$\sigma_\epsilon, \text{deg}$
0.2	0	.897	.285	-.037	-.849	.063	6.6
0.2	45	.991	.343	-.006	-.930	.088	8.5
0.2	90	.957	.304	.071	-.904	.080	6.7
0.2	135	.896	.257	.060	-.856	.054	6.9
0.3	0	1.022	.275	-.111	-.978	.059	6.5
0.3	45	1.153	.393	.097	-1.079	.083	6.2
0.3	90	1.081	.314	.087	-1.031	.096	7.2
0.3	135	1.018	.265	.063	-.981	.072	7.7
0.4	0	1.052	.113	-.161	-1.033	.074	5.9
0.4	45	1.182	.230	.056	-1.158	.064	7.5
0.4	90	1.111	.161	-.019	-1.099	.053	8.0
0.4	135	1.028	.108	-.060	-1.021	.086	7.2
0.5	0	1.094	.163	-.148	-1.072	.073	4.3
0.5	45	1.260	.255	.072	-1.232	.086	5.2
0.5	90	1.167	.202	.010	-1.150	.068	7.6
0.5	135	1.087	.147	-.084	-1.074	.072	6.3
0.6	0	1.066	.004	-.176	-1.051	.074	2.6
0.6	45	1.298	.081	.128	-1.290	.077	5.1
0.6	90	1.187	.045	.035	-1.186	.086	8.0
0.6	135	1.100	.007	-.016	-1.100	.087	7.1
0.7	0	1.055	-.085	-.175	-1.037	.076	2.7
0.7	45	1.312	-.055	.127	-1.305	.061	5.1
0.7	90	1.197	-.068	-.009	-1.195	.083	8.2
0.7	135	1.092	-.070	-.064	-1.088	.097	7.3
0.8	0	.901	-.306	-.109	-.841	.115	13.2
0.8	45	1.283	-.314	.100	-1.239	.052	3.1
0.8	90	1.183	-.307	.053	-1.142	.079	5.9
0.8	135	1.043	-.284	-.005	-1.004	.114	8.0
0.9	0	.719	-.448	-.172	-.535	.063	17.7
0.9	45	1.155	-.569	.173	-.990	.067	4.9
0.9	90	1.001	-.532	.176	-.829	.076	10.3
0.9	135	.847	-.379	.095	-.751	.063	7.1
1.0	0	.593	-.415	.075	-.418	.041	14.1
1.0	45	.922	-.643	.197	-.632	.093	9.7
1.0	90	.776	-.510	.216	-.544	.062	8.0
1.0	135	.688	-.413	.208	-.509	.049	7.7

x/R	ψ , deg	\bar{v}_R/v_o	\bar{v}_x/v_o	\bar{v}_y/v_o	\bar{v}_z/v_o	σ_{V_R}/v_o	σ_ϵ , deg
1.1	0	.495	-.336	.138	-.336	.048	10.5
1.1	45	.589	-.485	.067	-.328	.045	12.5
1.1	90	.564	-.396	.139	-.376	.053	12.0
1.1	135	.543	-.348	.209	-.360	.055	10.5
1.2	0	.337	-.194	.146	-.234	.033	7.4
1.2	45	.361	-.230	.138	-.243	.028	11.0
1.2	90	.364	-.210	.170	-.245	.041	7.2
1.2	135	.361	-.199	.161	-.254	.050	10.3
1.3	0	.234	-.138	.102	-.158	.041	13.4
1.3	45	.244	-.135	.131	-.156	.044	8.6
1.3	90	.246	-.137	.121	-.164	.044	9.9
1.3	135	.242	-.136	.108	-.169	.049	15.6
1.4	0	.230	.024	-.030	-.227	.063	32.8
1.4	45	.235	.004	-.032	-.233	.050	25.2
1.4	90	.237	.010	-.023	-.236	.048	18.7
1.4	135	.255	.001	-.038	-.252	.045	19.5
1.5	0	.197	.003	.147	-.130	.092	44.4
1.5	45	.082	.011	.144	-.110	.094	46.3
1.5	90	.189	.047	.148	-.108	.094	45.5
1.5	135	.199	.017	.136	-.145	.089	44.2

TEST CONDITION 3, $z/R = 0.20$
 $\Omega R = 453$ ft/sec, $\theta_{75} = 6.20$ deg, $C_T = 0.0019$

x/R	ψ , deg	\bar{v}_R/v_o	\bar{v}_x/v_o	\bar{v}_y/v_o	\bar{v}_z/v_o	σ_{V_R}/v_o	σ_ϵ , deg
0.0	0	.829	.185	.227	-.775	.058	12.9
0.0	45	.825	.147	.229	-.779	.069	5.9
0.0	90	.836	.182	.239	-.781	.065	12.6
0.0	135	.847	.185	.241	-.790	.075	13.5
0.1	0	.979	.235	.242	-.919	.061	3.5
0.1	45	.884	.335	.275	-.771	.080	18.3
0.1	90	.852	.295	.304	-.739	.060	15.6
0.1	135	.847	.194	.258	-.784	.046	3.4
0.2	0	.928	.124	.222	-.892	.057	3.5
0.2	45	1.045	.176	.292	-.988	.061	4.0
0.2	90	1.082	.151	.391	-.998	.069	3.6
0.2	135	.969	.107	.329	-.905	.082	3.2

x/R	ψ, deg	\bar{v}_R/v_o	\bar{v}_x/v_o	\bar{v}_y/v_o	\bar{v}_z/v_o	σ_{v_R}/v_o	$\sigma_\epsilon, \text{deg}$
0.3	0	1.002	-.027	.213	-.979	.069	4.7
0.3	45	1.111	.035	.341	-1.057	.066	4.3
0.3	90	1.122	-.005	.394	-1.050	.092	4.0
0.3	135	1.069	-.045	.362	-1.005	.077	4.3
0.4	0	1.031	-.082	.163	-1.015	.161	3.8
0.4	45	1.171	-.051	.297	-1.131	.181	3.1
0.4	90	1.137	-.059	.337	-1.084	.177	4.4
0.4	135	1.121	-.111	.343	-1.062	.186	4.7
0.5	0	1.131	-.276	.074	-1.094	.093	6.2
0.5	45	1.309	-.224	.280	-1.259	.100	4.0
0.5	90	1.258	-.256	.305	-1.193	.096	3.7
0.5	135	1.191	-.275	.309	-1.116	.099	4.2
0.6	0	1.193	-.715	.320	-.899	.110	9.6
0.6	45	1.344	-.576	.180	-1.201	.129	10.6
0.6	90	1.349	-.664	.302	-1.135	.152	11.1
0.6	135	1.276	-.688	.339	-1.020	.160	10.6
0.7	0	1.116	-.733	.219	-.812	.083	7.0
0.7	45	1.289	-.657	.228	-1.086	.095	11.8
0.7	90	1.294	-.703	.291	-1.047	.146	11.4
0.7	135	1.326	-.737	.327	-1.053	.139	11.3
0.8	0	1.204	-.920	.045	-.776	.090	10.0
0.8	45	1.399	-.874	.497	-.972	.122	3.2
0.8	90	1.321	-.841	.430	-.923	.123	4.1
0.8	135	1.314	-.838	.418	-.922	.110	4.1
0.9	0	.960	-.809	-.049	-.515	.066	11.3
0.9	45	1.156	-.828	.218	-.776	.124	10.6
0.9	90	1.105	-.786	.217	-.746	.147	10.0
0.9	135	1.009	-.727	.178	-.676	.083	10.4
1.0	0	.687	-.547	.053	-.412	.043	9.1
1.0	45	.860	-.672	.127	-.522	.055	8.0
1.0	90	.803	-.600	.174	-.505	.060	8.2
1.0	135	.744	-.544	.185	-.471	.076	8.5
1.1	0	.525	-.493	.044	-.175	.091	7.8
1.1	45	.619	-.584	.075	-.190	.104	8.8
1.1	90	.592	-.544	.114	-.205	.096	7.9
1.1	135	.546	-.486	.132	-.213	.093	7.5

x/R	ψ , deg	\bar{v}_R/v_o	\bar{v}_x/v_o	\bar{v}_y/v_o	\bar{v}_z/v_o	σ_{v_R}/v_o	σ_ϵ , deg
1.2	0	.422	-.401	.069	-.114	.047	8.2
1.2	45	.458	-.430	.109	-.113	.050	7.0
1.2	90	.439	-.406	.115	-.120	.031	6.6
1.2	135	.427	-.389	.110	-.138	.028	7.7
1.3	0	.318	-.185	.171	-.194	.028	7.8
1.3	45	.335	-.236	.173	-.162	.034	7.8
1.3	90	.341	-.223	.184	-.181	.026	7.8
1.3	135	.338	-.195	.194	-.197	.032	6.4
1.4	0	.257	-.086	.217	-.108	.074	31.7
1.4	45	.257	-.090	.208	-.122	.068	28.5
1.4	90	.259	-.092	.209	-.122	.072	26.2
1.4	135	.270	-.102	.214	-.131	.059	22.4
1.5	0	.236	.071	.222	.033	.045	14.6
1.5	45	.224	.068	.211	.033	.040	14.7
1.5	90	.213	.050	.206	.016	.039	22.7
1.5	135	.216	.056	.207	.022	.039	20.7

TEST CONDITION 1, $z/R = 0.30$

$\Omega R = 624$ ft/sec, $\theta_{75} = 6.23$ deg, $C_T = 0.0021$

x/R	ψ , deg	\bar{v}_R/v_o	\bar{v}_x/v_o	\bar{v}_y/v_o	\bar{v}_z/v_o	σ_{v_R}/v_o	σ_ϵ , deg
0.0	0	.811	-.001	.275	-.763	.045	3.0
0.0	45	.823	-.004	.270	-.777	.049	2.8
0.0	90	.811	-.009	.268	-.766	.070	3.1
0.0	135	.814	-.008	.264	-.770	.059	3.1
0.1	0	.863	-.003	.295	-.810	.058	3.2
0.1	45	.873	-.009	.302	-.819	.059	3.7
0.1	90	.874	-.028	.327	-.810	.069	3.1
0.1	135	.873	-.058	.306	-.815	.049	3.0
0.2	0	.879	-.069	.298	-.824	.043	2.9
0.2	45	.912	-.051	.341	-.845	.058	3.0
0.2	90	.902	-.077	.364	-.821	.057	3.2
0.2	135	.877	-.095	.326	-.809	.038	2.8
0.3	0	.879	-.109	.238	-.839	.147	4.9
0.3	45	.934	-.082	.307	-.879	.155	4.3
0.3	90	.929	-.112	.331	-.861	.164	4.6
0.3	135	.883	-.120	.304	-.820	.141	3.9

x/R	ψ, deg	\bar{v}_R/v_o	\bar{v}_x/v_o	\bar{v}_y/v_o	\bar{v}_z/v_o	σ_{v_R}/v_o	$\sigma_\epsilon, \text{deg}$
0.4	0	.934	-.182	.211	-.891	.060	3.5
0.4	45	1.021	-.160	.270	-.972	.079	4.0
0.4	90	1.002	-.181	.315	-.934	.064	3.2
0.4	135	.944	-.200	.287	-.877	.070	3.1
0.5	0	.925	-.272	.116	-.876	.149	6.5
0.5	45	1.022	-.264	.213	-.964	.181	5.6
0.5	90	1.007	-.293	.290	-.919	.171	4.4
0.5	135	.956	-.308	.265	-.865	.161	4.2
0.6	0	.947	-.355	.110	-.871	.153	5.4
0.6	45	1.044	-.360	.240	-.950	.189	5.9
0.6	90	1.021	-.376	.265	-.911	.177	5.7
0.6	135	.957	-.348	.256	-.854	.165	3.9
0.7	0	.922	-.567	.301	-.662	.151	4.8
0.7	45	1.051	-.529	.311	-.853	.171	7.1
0.7	90	.998	-.549	.351	-.756	.157	7.3
0.7	135	.982	-.587	.394	-.682	.157	5.8
0.8	0	.930	-.815	.065	-.444	.058	8.4
0.8	45	1.030	-.781	.274	-.612	.087	9.4
0.8	90	.991	-.762	.271	-.572	.083	9.5
0.8	135	.937	-.776	.229	-.474	.079	6.6
0.9	0	.882	-.826	-.012	-.307	.078	5.4
0.9	45	.972	-.866	.134	-.420	.079	8.6
0.9	90	.921	-.837	.137	-.360	.076	5.2
0.9	135	.861	-.784	.150	-.323	.051	5.8
1.0	0	.730	-.688	-.017	-.242	.041	5.4
1.0	45	.830	-.777	.006	-.291	.067	6.0
1.0	90	.755	-.705	.019	-.269	.069	7.2
1.0	135	.717	-.670	.035	-.253	.050	6.8
1.1	0	.614	-.592	.117	-.114	.039	6.2
1.1	45	.679	-.646	.161	-.134	.041	5.3
1.1	90	.639	-.596	.179	-.134	.055	3.9
1.1	135	.618	-.580	.173	-.122	.049	4.5
1.2	0	.514	-.154	.015	-.001	.028	4.9
1.2	45	.532	-.531	.020	-.005	.037	5.1
1.2	90	.523	-.522	.028	-.010	.034	5.6
1.2	135	.494	-.492	.037	-.018	.034	6.4

x/R	ψ , deg	\bar{v}_R/v_o	\bar{v}_x/v_o	\bar{v}_y/v_o	\bar{v}_z/v_o	σ_{v_R}/v_o	σ_ϵ , deg
1.3	0	.416	-.389	.148	-.022	.024	6.4
1.3	45	.445	-.414	.161	-.014	.035	7.6
1.3	90	.441	-.403	.178	-.026	.033	4.8
1.3	135	.419	-.382	.169	-.024	.034	5.8
1.4	0	.353	-.329	.120	-.042	.062	5.4
1.4	45	.367	-.344	.122	-.042	.061	5.7
1.4	90	.365	-.338	.132	-.043	.063	6.1
1.4	135	.353	-.324	.131	-.049	.055	4.8
1.5	0	.318	-.297	.111	-.025	.023	4.0
1.5	45	.329	-.305	.120	-.021	.025	4.8
1.5	90	.318	-.295	.114	-.026	.029	5.3
1.5	135	.318	-.293	.120	-.026	.027	3.9

TEST CONDITION 2, $z/R = 0.30$

$\Omega R = 449$ ft/sec, $\theta_{75} = 9.79$ deg, $C_T = 0.0042$

x/R	ψ , deg	\bar{v}_R/v_o	\bar{v}_x/v_o	\bar{v}_y/v_o	\bar{v}_z/v_o	σ_{v_R}/v_o	σ_ϵ , deg
0.0	0	.893	-.036	.290	-.844	.044	2.9
0.0	45	.859	-.030	.278	-.812	.063	3.1
0.0	90	.877	-.026	.283	-.829	.046	3.1
0.0	135	.842	-.027	.257	-.802	.060	3.0
0.1	0	.841	-.038	.252	-.801	.129	5.1
0.1	45	.861	-.010	.281	-.814	.125	4.4
0.1	90	.852	-.014	.303	-.796	.113	5.0
0.1	135	.807	-.039	.260	-.763	.088	5.1
0.2	0	.915	-.092	.319	-.852	.069	3.3
0.2	45	.950	-.043	.350	-.882	.061	3.1
0.2	90	.964	-.076	.399	-.875	.074	3.7
0.2	135	.954	-.099	.393	-.864	.065	3.0
0.3	0	.956	-.137	.257	-.911	.079	4.0
0.3	45	1.015	-.060	.307	-.965	.070	3.6
0.3	90	.992	-.092	.381	-.912	.070	3.8
0.3	135	1.003	-.145	.385	-.915	.096	3.7
0.4	0	1.023	-.252	.148	-.980	.058	5.7
0.4	45	1.122	-.204	.278	-1.068	.070	3.6
0.4	90	1.113	-.218	.328	-1.041	.079	4.2
0.4	135	1.041	-.252	.319	-.958	.081	4.5

x/R	ψ, deg	\bar{V}_R/v_o	\bar{v}_x/v_o	\bar{v}_y/v_o	\bar{v}_z/v_o	σ_{V_R}/v_o	$\sigma_\epsilon, \text{deg}$
0.5	0	1.038	-.383	.298	-.918	.223	5.6
0.5	45	1.083	-.319	.143	-1.025	.245	3.7
0.5	90	1.180	-.314	.306	-1.095	.236	5.0
0.5	135	1.151	-.335	.358	-1.041	.243	4.5
0.6	0	1.025	-.407	.052	-.939	.070	6.3
0.6	45	1.141	-.333	.145	-1.082	.061	5.4
0.6	90	1.103	-.355	.142	-1.034	.057	6.5
0.6	135	1.052	-.355	.100	-.985	.074	7.8
0.7	0	1.005	-.612	.319	-.730	.064	6.8
0.7	45	1.204	-.445	.230	-1.095	.041	4.4
0.7	90	1.148	-.436	.226	-1.038	.048	4.6
0.7	135	1.084	-.491	.289	-.922	.051	6.5
0.8	0	1.051	-.775	.375	-.603	.165	9.2
0.8	45	1.109	-.718	.308	-.787	.187	12.2
0.8	90	1.188	-.746	.394	-.837	.188	12.1
0.8	135	1.154	-.793	.434	-.717	.156	8.9
0.9	0	.896	-.847	-.016	-.292	.071	5.8
0.9	45	1.117	-.986	.092	-.518	.040	5.3
0.9	90	1.060	-.950	.116	-.455	.057	7.3
0.9	135	.950	-.876	.070	-.359	.061	9.1
1.0	0	.709	-.663	.186	-.166	.110	5.9
1.0	45	.906	-.835	.222	-.272	.165	6.0
1.0	90	.839	-.763	.256	-.236	.150	6.7
1.0	135	.778	-.696	.277	-.209	.119	6.5
1.1	0	.614	-.594	.112	-.108	.046	10.0
1.1	45	.750	-.720	.152	-.146	.061	7.9
1.1	90	.699	-.666	.166	-.130	.054	9.0
1.1	135	.642	-.595	.203	-.130	.052	6.8
1.2	0	.539	-.489	.222	-.046	.028	8.1
1.2	45	.606	-.561	.225	-.045	.037	7.6
1.2	90	.577	-.522	.241	-.053	.052	8.5
1.2	135	.540	-.479	.240	-.060	.051	8.9
1.3	0	.472	-.380	.275	-.048	.079	6.6
1.3	45	.504	-.416	.279	-.055	.093	7.2
1.3	90	.486	-.395	.278	-.056	.085	6.8
1.3	135	.483	-.382	.289	-.066	.085	7.4

x/R	ψ, deg	\bar{v}_R/v_o	\bar{v}_x/v_o	\bar{v}_y/v_o	\bar{v}_z/v_o	σ_{V_R}/v_o	$\sigma_\epsilon, \text{deg}$
1.4	0	.411	-.293	.285	-.039	.036	7.8
1.4	45	.422	-.310	.285	-.031	.042	8.6
1.4	90	.431	-.308	.300	-.032	.045	8.2
1.4	135	.426	-.296	.304	-.040	.041	8.9
1.5	0	.327	-.190	.254	.079	.076	23.3
1.5	45	.332	-.207	.247	.078	.079	22.7
1.5	90	.337	-.159	.266	.132	.087	24.8
1.5	135	.325	-.169	.256	.106	.077	25.9

TEST CONDITION 3, $z/R = 0.30$
 $\Omega R = 451 \text{ ft/sec}$, $\theta_{75} = 6.27 \text{ deg}$, $C_T = 0.0021$

x/R	ψ, deg	\bar{v}_R/v_o	\bar{v}_x/v_o	\bar{v}_y/v_o	\bar{v}_z/v_o	σ_{V_R}/v_o	$\sigma_\epsilon, \text{deg}$
0.0	0	.967	.028	.551	-.794	.157	3.2
0.0	45	.965	.036	.546	-.795	.156	3.3
0.0	90	.920	.029	.531	-.751	.156	3.5
0.0	135	.930	.025	.525	-.767	.154	3.5
0.1	0	.957	-.018	.525	-.800	.050	3.1
0.1	45	.977	-.011	.548	-.808	.066	3.1
0.1	90	1.000	-.026	.571	-.820	.069	3.1
0.1	135	.972	-.034	.549	-.801	.078	2.8
0.2	0	.978	-.066	.502	-.836	.053	3.1
0.2	45	.989	-.035	.527	-.836	.047	3.0
0.2	90	.975	-.044	.546	-.806	.037	3.2
0.2	135	.992	-.082	.540	-.828	.068	3.0
0.3	0	1.010	-.134	.495	-.870	.042	3.3
0.3	45	1.071	-.094	.559	-.909	.073	3.1
0.3	90	1.015	-.137	.557	-.838	.074	3.3
0.3	135	.988	-.162	.534	-.815	.060	3.2
0.4	0	.962	-.197	.420	-.843	.142	4.4
0.4	45	1.078	-.193	.539	-.913	.183	4.1
0.4	90	1.050	-.209	.554	-.867	.175	3.8
0.4	135	1.005	-.230	.527	-.824	.167	3.6
0.5	0	1.005	-.292	.411	-.869	.064	3.4
0.5	45	1.160	-.266	.527	-.999	.055	3.1
0.5	90	1.095	-.278	.518	-.924	.063	3.2
0.5	135	1.061	-.323	.510	-.872	.113	3.3

x/R	ψ, deg	\bar{v}_R/v_o	\bar{v}_x/v_o	\bar{v}_y/v_o	\bar{v}_z/v_o	σ_{v_R}/v_o	$\sigma_\epsilon, \text{deg}$
0.6	0	1.001	-.493	.410	-.769	.083	6.9
0.6	45	1.109	-.416	.453	-.923	.079	4.3
0.6	90	1.051	-.440	.491	-.818	.072	6.2
0.6	135	1.045	-.534	.551	-.709	.085	5.0
0.7	0	.972	-.589	.407	-.657	.057	3.9
0.7	45	1.073	-.552	.462	-.796	.062	5.7
0.7	90	1.117	-.615	.551	-.752	.089	3.5
0.7	135	1.007	-.553	.532	-.652	.063	2.8
0.8	0	1.033	-.851	.321	-.489	.055	5.3
0.8	45	1.039	-.718	.453	-.597	.059	6.4
0.8	90	1.008	-.731	.440	-.537	.084	7.5
0.8	135	.985	-.757	.426	-.464	.071	4.5
0.9	0	.918	-.865	.114	-.286	.059	6.6
0.9	45	1.003	-.897	.248	-.376	.066	5.3
0.9	90	.983	-.877	.272	-.352	.057	6.7
0.9	135	.946	-.842	.291	-.319	.062	6.1
1.0	0	.825	-.723	.352	-.183	.038	4.0
1.0	45	.898	-.777	.388	-.229	.058	3.9
1.0	90	.866	-.738	.407	-.198	.037	3.4
1.0	135	.869	-.727	.437	-.188	.050	3.8
1.1	0	.664	-.596	.290	-.038	.098	6.0
1.1	45	.716	-.637	.318	-.070	.120	6.0
1.1	90	.737	-.648	.347	-.059	.131	6.6
1.1	135	.659	-.571	.327	-.043	.115	7.3
1.2	0	.592	-.522	.279	-.006	.051	14.4
1.2	45	.623	-.547	.297	.001	.069	14.8
1.2	90	.622	-.540	.309	-.014	.059	14.2
1.2	135	.636	-.542	.333	-.017	.066	13.6
1.3	0	.491	-.257	.407	.099	.084	4.2
1.3	45	.526	-.311	.418	.072	.090	4.0
1.3	90	.523	-.309	.419	.051	.095	15.9
1.3	135	.505	-.277	.416	.091	.091	13.2
1.4	0	.451	-.217	.391	.063	.081	21.7
1.4	45	.510	-.254	.435	.080	.098	21.2
1.4	90	.466	-.238	.397	.053	.086	22.1
1.4	135	.466	-.206	.410	.084	.087	21.1

x/R	ψ, deg	\bar{v}_R/v_o	\bar{v}_x/v_o	\bar{v}_y/v_o	\bar{v}_z/v_o	σ_{v_R}/v_o	$\sigma_\epsilon, \text{deg}$
1.5	0	.435	-.203	.365	.121	.089	24.1
1.5	45	.453	-.214	.373	.141	.074	24.4
1.5	90	.451	-.221	.370	.131	.086	25.7
1.5	135	.452	-.241	.372	.090	.068	24.9

TEST CONDITION 1, $z/R = 0.40$

$\Omega R = 626 \text{ ft/sec}$, $\theta_{75} = 6.14 \text{ deg}$, $C_T = 0.0019$

x/R	ψ, deg	\bar{v}_R/v_o	\bar{v}_x/v_o	\bar{v}_y/v_o	\bar{v}_z/v_o	σ_{v_R}/v_o	$\sigma_\epsilon, \text{deg}$
0.0	0	.909	-.129	.524	-.732	.042	3.1
0.0	45	.908	-.144	.524	-.728	.055	3.6
0.0	90	.898	-.134	.521	-.719	.039	3.1
0.0	135	.906	-.110	.523	-.731	.046	3.2
0.1	0	.833	-.132	.482	-.666	.214	15.2
0.1	45	.828	-.129	.490	-.655	.211	15.9
0.1	90	.839	-.133	.500	-.661	.201	17.2
0.1	135	.831	-.138	.489	-.658	.193	18.4
0.2	0	.870	-.156	.457	-.724	.241	4.0
0.2	45	.866	-.140	.470	-.714	.256	4.2
0.2	90	.908	-.178	.497	-.739	.253	4.3
0.2	135	.880	-.187	.474	-.718	.247	4.8
0.3	0	.899	-.225	.451	-.744	.069	3.8
0.3	45	.922	-.208	.480	-.759	.063	3.3
0.3	90	.934	-.247	.511	-.742	.078	4.6
0.3	135	.902	-.249	.486	-.718	.049	4.5
0.4	0	.863	-.223	.418	-.721	.217	5.0
0.4	45	.909	-.203	.463	-.755	.226	4.4
0.4	90	.908	-.213	.483	-.739	.226	5.8
0.4	135	.873	-.244	.464	-.698	.225	5.6
0.5	0	.872	-.320	.409	-.700	.191	6.6
0.5	45	.909	-.299	.443	-.735	.213	5.5
0.5	90	.882	-.306	.457	-.689	.207	7.0
0.5	135	.867	-.333	.456	-.658	.191	6.2
0.6	0	.849	-.366	.401	-.653	.138	6.1
0.6	45	.912	-.344	.437	-.723	.152	5.4
0.6	90	.902	-.356	.474	-.680	.148	5.6
0.6	135	.853	-.381	.465	-.606	.131	5.8

x/R	ψ, deg	\bar{v}_R/v_o	\bar{v}_x/v_o	\bar{v}_y/v_o	\bar{v}_z/v_o	σ_{v_R}/v_o	$\sigma_\epsilon, \text{deg}$
0.7	0	.814	-.426	.465	-.515	.276	10.5
0.7	45	.865	-.428	.485	-.574	1.000	22.0
0.7	90	.857	-.428	.525	-.525	1.022	22.4
0.7	135	.839	-.408	.532	-.505	1.026	22.1
0.8	0	.715	-.469	.393	-.370	.155	6.7
0.8	45	.808	-.422	.475	-.499	.179	3.2
0.8	90	.760	-.433	.457	-.425	.170	6.1
0.8	135	.751	-.419	.457	-.424	.157	5.5
0.9	0	.658	-.481	.367	-.258	.105	3.8
0.9	45	.702	-.487	.403	-.306	.121	5.2
0.9	90	.686	-.483	.404	-.270	.103	3.6
0.9	135	.660	-.446	.407	-.266	.108	5.1
1.0	0	.590	-.464	.334	-.144	.108	10.4
1.0	45	.633	-.493	.365	-.159	.107	9.1
1.0	90	.619	-.468	.368	-.168	.108	10.5
1.0	135	.612	-.458	.379	-.145	.116	9.0
1.1	0	.527	-.362	.360	-.128	.086	5.0
1.1	45	.559	-.387	.373	-.154	.100	5.2
1.1	90	.550	-.374	.381	-.132	.097	4.2
1.1	135	.532	-.355	.375	-.128	.091	5.4
1.2	0	.440	-.274	.339	-.057	.130	5.8
1.2	45	.460	-.290	.350	-.071	.132	6.6
1.2	90	.452	-.278	.350	-.068	.132	6.4
1.2	135	.445	-.268	.350	-.064	.135	7.9
1.3	0	.467	-.241	.385	-.109	.079	5.4
1.3	45	.481	-.253	.395	-.106	.084	6.5
1.3	90	.469	-.238	.389	-.114	.078	6.9
1.3	135	.473	-.240	.392	-.112	.083	5.5
1.4	0	.415	-.122	.397	-.013	.101	19.4
1.4	45	.420	-.146	.390	-.055	.101	18.4
1.4	90	.417	-.138	.390	-.053	.102	17.6
1.4	135	.418	-.122	.399	-.028	.099	18.7

TEST CONDITION 2, $z/R = 0.40$
 $\Omega R = 449$ ft/sec, $\theta_{75} = 9.69$ deg, $C_T = 0.0040$

x/R	ψ , deg	\bar{v}_R/v_o	\bar{v}_x/v_o	\bar{v}_y/v_o	\bar{v}_z/v_o	σ_{v_R}/v_o	σ_ϵ , deg
0.0	0	.865	.035	.427	-.751	.053	3.3
0.0	45	.854	.042	.434	-.734	.056	3.2
0.0	90	.847	.043	.416	-.737	.045	3.4
0.0	135	.916	.043	.456	-.793	.086	2.9
0.1	0	.844	.014	.413	-.736	.046	3.2
0.1	45	.842	.020	.421	-.729	.044	3.1
0.1	90	.851	-.000	.435	-.732	.045	3.0
0.1	135	.848	.002	.431	-.731	.061	3.3
0.2	0	.845	-.042	.386	-.751	.046	3.1
0.2	45	.891	-.008	.428	-.782	.052	3.1
0.2	90	.874	-.025	.444	-.753	.048	3.2
0.2	135	.844	-.051	.414	-.734	.059	2.9
0.3	0	.779	-.048	.337	-.700	.174	21.5
0.3	45	.820	-.029	.392	-.720	.165	21.4
0.3	90	.822	-.058	.423	-.702	.153	20.9
0.3	135	.792	-.073	.408	-.675	.133	21.9
0.4	0	.824	-.117	.344	-.740	.142	3.9
0.4	45	.926	-.089	.420	-.821	.149	3.6
0.4	90	.896	-.102	.428	-.781	.138	3.5
0.4	135	.852	-.131	.412	-.734	.136	3.7
0.5	0	.836	-.174	.352	-.738	.109	16.4
0.5	45	.930	-.163	.444	-.800	.098	16.5
0.5	90	.889	-.178	.458	-.741	.095	16.5
0.5	135	.823	-.195	.427	-.677	.067	16.4
0.6	0	.832	-.270	.287	-.733	.056	4.3
0.6	45	.895	-.252	.358	-.781	.070	5.9
0.6	90	.874	-.272	.386	-.736	.074	5.0
0.6	135	.820	-.294	.369	-.671	.060	6.1
0.7	0	.744	-.285	.238	-.695	.112	4.6
0.7	45	.861	-.276	.321	-.750	.136	5.3
0.7	90	.835	-.292	.360	-.694	.127	6.2
0.7	135	.766	-.295	.345	-.617	.110	6.5
0.8	0	.711	-.409	.338	-.473	.056	2.8
0.8	45	.824	-.459	.403	-.552	.048	3.3
0.8	90	.793	-.420	.446	-.503	.049	2.7
0.8	135	.743	-.381	.439	-.462	.045	2.8

x/R	ψ, deg	\bar{v}_R/v_o	\bar{v}_x/v_o	\bar{v}_y/v_o	\bar{v}_z/v_o	σ_{v_R}/v_o	$\sigma_\epsilon, \text{deg}$
0.9	0	.624	-.449	.222	-.371	.041	7.4
0.9	45	.741	-.467	.314	-.482	.053	4.5
0.9	90	.671	-.427	.308	-.416	.040	5.3
0.9	135	.634	-.414	.295	-.378	.041	5.9
1.0	0	.529	-.352	.247	-.308	.043	7.5
1.0	45	.611	-.389	.290	-.371	.041	7.0
1.0	90	.586	-.354	.299	-.359	.052	5.8
1.0	135	.567	-.353	.311	-.316	.040	7.2
1.1	0	.486	-.375	.261	-.167	.034	5.5
1.1	45	.559	-.431	.296	-.199	.048	4.5
1.1	90	.521	-.376	.301	-.199	.033	5.5
1.1	135	.474	-.332	.287	-.179	.055	5.5
1.2	0	.417	-.321	.258	-.067	.034	5.1
1.2	45	.451	-.348	.273	-.089	.040	5.0
1.2	90	.439	-.327	.279	-.090	.035	5.9
1.2	135	.416	-.296	.277	-.091	.039	5.0
1.3	0	.362	-.226	.263	-.104	.030	6.1
1.3	45	.390	-.260	.274	-.098	.032	5.4
1.3	90	.368	-.231	.267	-.106	.033	6.0
1.3	135	.360	-.213	.268	-.111	.025	7.4
1.4	0	.303	-.122	.277	-.008	.051	24.4
1.4	45	.319	-.154	.278	-.023	.046	21.1
1.4	90	.300	-.119	.275	-.013	.041	24.1
1.4	135	.303	-.104	.284	.001	.036	23.6
1.5	0	.273	-.016	.269	.042	.032	21.2
1.5	45	.287	-.006	.280	.063	.040	21.3
1.5	90	.289	-.005	.285	.047	.041	20.7
1.5	135	.286	.003	.282	.049	.073	19.6

TEST CONDITION 3, $z/R = 0.40$

$\Omega R = 449 \text{ ft/sec}$, $\theta_{75} = 6.27 \text{ deg}$, $C_T = 0.0021$

x/R	ψ, deg	\bar{v}_R/v_o	\bar{v}_x/v_o	\bar{v}_y/v_o	\bar{v}_z/v_o	σ_{v_R}/v_o	$\sigma_\epsilon, \text{deg}$
0.0	0	.782	.345	.423	-.560	.078	22.0
0.0	45	.772	.402	.437	-.493	.083	23.2
0.0	90	.772	.352	.427	-.539	.086	22.3
0.0	135	.784	.366	.437	-.538	.092	22.4

x/R	ψ, deg	\bar{v}_R/v_o	\bar{v}_x/v_o	\bar{v}_y/v_o	\bar{v}_z/v_o	σ_{v_R}/v_o	$\sigma_\epsilon, \text{deg}$
0.1	0	.839	.198	.461	-.673	.069	15.2
0.1	45	.825	.205	.452	-.658	.063	13.8
0.1	90	.859	.188	.472	-.692	.054	12.4
0.1	135	.867	.150	.460	-.719	.055	3.3
0.2	0	.871	.058	.437	-.751	.122	3.4
0.2	45	.796	.082	.408	-.679	.130	4.1
0.2	90	.799	.050	.422	-.677	.136	3.9
0.2	135	.785	.055	.416	-.664	.123	3.3
0.3	0	.848	.020	.421	-.736	.052	3.3
0.3	45	.859	.054	.433	-.740	.071	3.4
0.3	90	.863	.023	.470	-.723	.059	3.3
0.3	135	.852	.008	.463	-.715	.048	3.1
0.4	0	.807	-.049	.377	-.712	.126	3.1
0.4	45	.869	-.018	.415	-.763	.145	3.6
0.4	90	.826	-.047	.429	-.704	.133	4.0
0.4	135	.798	-.053	.417	-.679	.121	3.9
0.5	0	.797	-.105	.327	-.719	.048	3.4
0.5	45	.849	-.092	.372	-.757	.043	3.4
0.5	90	.840	-.113	.405	-.727	.063	3.4
0.5	135	.791	-.119	.385	-.680	.054	3.9
0.6	0	.758	-.183	.274	-.683	.064	3.6
0.6	45	.837	-.173	.333	-.748	.060	3.6
0.6	90	.816	-.165	.350	-.718	.067	3.7
0.6	135	.781	-.188	.354	-.671	.058	3.3
0.7	0	.736	-.224	.244	-.657	.057	4.5
0.7	45	.791	-.223	.294	-.700	.048	4.1
0.7	90	.774	-.218	.308	-.676	.051	3.3
0.7	135	.758	-.223	.311	-.655	.055	4.1
0.8	0	.654	-.363	.312	-.446	.048	5.1
0.8	45	.750	-.375	.349	-.547	.057	6.6
0.8	90	.735	-.378	.378	-.504	.044	5.6
0.8	135	.685	-.355	.376	-.450	.050	5.2
0.9	0	.608	-.328	.332	-.390	.031	2.6
0.9	45	.681	-.350	.403	-.424	.041	2.7
0.9	90	.647	-.324	.396	-.397	.052	2.7
0.9	135	.623	-.308	.387	-.379	.051	2.8

x/R	ψ, deg	\bar{v}_R/v_o	\bar{v}_x/v_o	\bar{v}_y/v_o	\bar{v}_z/v_o	σ_{v_R}/v_o	$\sigma_\epsilon, \text{deg}$
1.0	0	.524	-.396	.238	-.246	.045	5.3
1.0	45	.589	-.415	.283	-.307	.047	6.2
1.0	90	.558	-.390	.283	-.281	.055	6.0
1.0	135	.536	-.350	.286	-.288	.044	6.9
1.1	0	.440	-.353	.197	-.174	.066	6.6
1.1	45	.468	-.373	.212	-.188	.072	6.2
1.1	90	.470	-.357	.233	-.197	.076	6.1
1.1	135	.453	-.343	.234	-.180	.077	6.1
1.2	0	.395	-.181	.265	-.230	.025	3.6
1.2	45	.433	-.204	.285	-.254	.030	3.2
1.2	90	.420	-.190	.286	-.242	.037	2.9
1.2	135	.407	-.174	.290	-.227	.037	3.1
1.3	0	.308	-.184	.209	-.132	.025	9.4
1.3	45	.320	-.203	.209	-.134	.031	9.2
1.3	90	.336	-.211	.227	-.129	.036	7.1
1.3	135	.314	-.174	.225	-.134	.036	8.9
1.4	0	.255	-.102	.215	-.091	.036	26.7
1.4	45	.279	-.141	.219	-.098	.034	21.6
1.4	90	.292	-.137	.227	-.123	.033	16.8
1.4	135	.280	-.120	.227	-.112	.034	20.2
1.5	0	.243	-.006	.218	.105	.025	20.8
1.5	45	.252	-.028	.225	.109	.032	25.1
1.5	90	.227	-.035	.211	.076	.039	29.7
1.5	135	.241	.004	.213	.113	.019	13.8

APPENDIX II
DISTRIBUTIONS OF MEAN WAKE VELOCITY COMPONENTS AND STANDARD DEVIATION
PARAMETERS COMPUTED FROM EXPERIMENTAL WAKE SURVEY DATA, OH-23B, HOVER
CONDITION

TEST CONDITION 2, $z/R = 0.125$

$\Omega R = 451 \text{ ft/sec}$, $\theta_{75} = 9.74 \text{ deg}$, $C_T = 0.0041$

x/R	ψ, deg	\bar{v}_R/v_o	\bar{v}_x/v_o	\bar{v}_y/v_o	\bar{v}_z/v_o	σ_{v_R}/v_o	$\sigma_\epsilon, \text{deg}$
0.8500	0	1.110	-.044	.681	-.876	.030	5.2
0.8500	45	1.694	.009	.238	-1.678	.040	2.8
0.8500	90	1.529	-.016	.216	-1.513	.031	2.8
0.8500	135	1.406	-.036	.205	-1.391	.016	2.9
0.9000	0	1.010	-.408	.554	-.739	.114	17.1
0.9000	45	1.818	-.245	.125	-1.797	.043	4.0
0.9000	90	1.761	-.375	.073	-1.719	.057	3.9
0.9000	135	1.427	-.421	.029	-1.363	.044	6.4
0.9125	0	1.000	-.556	.406	-.725	.181	27.2
0.9125	45	1.923	-.246	.089	-1.905	.065	5.5
0.9125	90	1.938	-.547	.029	-1.859	.149	10.3
0.9125	135	1.470	-.657	.038	-1.315	.153	18.7
0.9250	0	1.023	-.630	.564	-.576	.150	20.2
0.9250	45	1.986	-.237	.200	-1.961	.058	3.5
0.9250	90	2.210	-.791	.114	-2.061	.180	8.8
0.9520	135	1.483	-.882	.134	-1.184	.148	18.7
0.9375	0	.962	-.216	.458	-.818	.082	8.3
0.9375	45	2.172	-.153	.129	-2.163	.034	2.8
0.9375	90	1.920	-.585	.060	-1.827	.087	4.4
0.9375	135	1.365	-.391	.045	-1.307	.037	5.8
0.9500	0	.897	-.451	.401	-.664	.287	22.6
0.9500	45	2.509	-.013	.146	-2.504	.194	4.8
0.9500	90	2.429	-1.856	.243	-1.548	.375	15.1
0.9500	135	1.310	-.923	-.011	-.929	.117	21.7
0.9625	0	.769	-.181	.324	-.674	.043	7.4
0.9625	45	3.338	.104	-.000	-3.337	.141	4.0
0.9625	90	2.041	-1.712	.180	-1.096	.107	8.3
0.9625	135	1.238	-.585	-.223	-1.067	.040	8.0
0.9750	0	.744	-.277	.409	-.556	.097	20.1
0.9750	45	3.993	2.490	.009	-3.121	.477	18.4
0.9750	90	1.918	-1.803	.417	-.503	.167	10.6
0.9750	135	1.142	-.893	.177	-.689	.089	18.8

x/R	ψ, deg	\bar{v}_R/v_o	\bar{v}_x/v_o	\bar{v}_y/v_o	\bar{v}_z/v_o	σ_{v_R/v_o}	$\sigma_\epsilon, \text{deg}$
0.9875	0	.587	-.266	.307	-.424	.135	21.6
0.9875	45	1.991	1.458	.263	1.330	.398	27.2
0.9875	90	1.430	-1.411	.230	.015	.091	8.0
0.9875	135	.920	-.839	.098	-.364	.118	8.9
1.0000	0	.541	-.191	.334	-.380	.226	32.3
1.0000	45	1.294	.185	.406	1.215	.176	22.4
1.0000	90	1.050	-1.048	.068	-.004	.145	14.1
1.0000	135	.750	-.568	.065	-.485	.148	29.8
1.1000	0	.362	-.087	.106	-.335	.081	19.7
1.1000	45	.217	-.071	.070	-.193	.075	25.1
1.1000	90	.294	-.133	.050	-.258	.074	23.2
1.1000	135	.363	-.138	.037	-.334	.083	24.0
1.2000	0	.272	-.035	.150	-.225	.053	13.8
1.2000	45	.223	-.023	.132	-.178	.054	26.6
1.2000	90	.241	-.050	.131	-.196	.050	21.8
1.2000	135	.261	-.048	.113	-.230	.050	15.4
1.3000	0	.235	-.019	.136	-.191	.061	24.0
1.3000	45	.214	-.007	.133	-.167	.058	27.9
1.3000	90	.217	-.014	.120	-.181	.056	25.6
1.3000	135	.221	.007	.101	-.197	.049	24.5
1.4000	0	.159	.019	.132	-.086	.072	41.8
1.4000	45	.151	.016	.137	-.061	.079	46.2
1.4000	90	.148	.009	.119	-.088	.077	45.8
1.4000	135	.146	-.004	.110	-.096	.074	44.7
1.5000	0	.230	.022	.163	-.160	.102	32.1
1.5000	45	.226	.013	.160	-.160	.100	33.0
1.5000	90	.213	.023	.145	-.155	.091	34.2
1.5000	135	.205	.019	.123	-.163	.082	32.0

TEST CONDITION 1, $z/R = 0$
 $\Omega R = 626 \text{ ft/sec}$, $\theta_{75} = 6.09 \text{ deg}$, $C_T = 0.0018$

x/R	ψ, deg	\bar{v}_R/v_o	\bar{v}_x/v_o	\bar{v}_y/v_o	\bar{v}_z/v_o	σ_{v_R/v_o}	$\sigma_\epsilon, \text{deg}$
0.8500	0	1.413	-.517	.581	-1.180	.445	18.0
0.8500	45	1.338	-.367	.193	-1.272	.333	9.4
0.8500	90	1.294	-.352	.201	-1.229	.320	7.9
0.8500	135	1.388	-.330	.351	-1.302	.218	14.9

x/R	ψ, deg	\bar{v}_R/v_o	\bar{v}_x/v_o	\bar{v}_y/v_o	\bar{v}_z/v_o	σ_{v_R/v_o}	$\sigma_\epsilon, \text{deg}$
0.8625	0	1.206	-.507	.429	-1.007	.550	24.6
0.8625	45	1.138	-.422	.126	-1.049	.394	26.4
0.8625	90	1.140	-.438	.163	-1.040	.358	22.2
0.8625	135	1.115	-.326	.283	-1.028	.422	14.9
0.8750	0	1.547	-.703	.554	-1.262	.516	17.9
0.8750	45	1.424	-.480	.141	-1.333	.329	9.4
0.8750	90	1.384	-.479	.172	-1.286	.287	9.1
0.8750	135	1.447	-.434	.304	-1.346	.195	14.9
0.8875	0	1.442	-.707	.421	-1.184	.471	24.9
0.8875	45	1.317	-.460	.153	-1.224	.340	9.6
0.8875	90	1.316	-.482	.161	-1.214	.325	8.6
0.8875	135	1.343	-.475	.279	-1.225	.295	16.4
0.9000	0	1.664	-.914	.447	-1.317	.581	21.4
0.9000	45	1.508	-.516	.034	-1.416	.338	5.9
0.9000	90	1.596	-.567	.027	-1.492	.328	4.2
0.9000	135	1.654	-.673	.223	-1.495	.228	18.5
0.9125	0	1.577	-.989	.329	-1.184	.524	24.9
0.9125	45	1.569	-.515	.002	-1.482	.375	4.6
0.9125	90	1.805	-.823	.067	-1.605	.439	13.5
0.9125	135	1.775	-.880	.186	-1.531	.364	24.3
0.9250	0	1.385	-.895	.326	-1.005	.494	31.5
0.9250	45	1.695	-.517	.017	-1.615	.586	8.3
0.9250	90	1.966	-1.301	.074	-1.472	.529	26.8
0.9250	135	1.817	-.919	.171	-1.558	.709	34.0
0.9375	0	1.089	-.689	.459	-.707	.491	41.9
0.9375	45	2.149	-.233	.032	-2.136	1.262	12.1
0.9375	90	1.392	-1.331	.190	-.364	.787	52.8
0.9375	135	2.658	-2.539	.288	-.731	2.353	38.3
0.9500	0	.724	-.408	.284	-.526	.676	54.8
0.9500	45	.716	-.211	.281	.624	1.633	52.4
0.9500	90	.333	-.272	.192	.009	1.325	55.0
0.9500	135	1.056	-.857	.412	.457	1.000	50.7
0.9750	0	.594	.125	.411	.410	.492	53.7
0.9750	45	.532	.048	.237	.474	.510	52.2
0.9750	90	.749	-.470	.132	.568	.412	36.5
0.9750	135	.413	-.079	.235	.330	.522	63.0

x/R	ψ , deg	\bar{v}_R/v_o	\bar{v}_x/v_o	\bar{v}_y/v_o	\bar{v}_z/v_o	σ_{v_R}/v_o	σ_ϵ , deg
1.0000	0	.464	-.141	.265	.354	.190	36.2
1.0000	45	.534	-.143	.233	.459	.214	30.0
1.0000	90	.529	-.383	.186	.314	.172	21.5
1.0000	135	.460	-.247	.188	.340	.214	37.7
1.1000	0	.254	-.194	.145	.078	.240	20.3
1.1000	45	.267	-.171	.161	.126	.252	22.5
1.1000	90	.270	-.221	.138	.072	.262	22.2
1.1000	135	.256	-.159	.156	.125	.293	24.5
1.2000	0	.218	-.129	.173	.031	.070	11.8
1.2000	45	.218	-.130	.173	.027	.071	12.0
1.2000	90	.223	-.119	.187	.021	.071	10.9
1.2000	135	.221	-.125	.180	.030	.075	11.3
1.3000	0	.187	-.114	.111	.099	.274	47.1
1.3000	45	.200	-.169	.089	.059	.312	48.2
1.3000	90	.196	-.093	.128	.115	.333	49.8
1.3000	135	.200	-.127	.107	.112	.369	49.9
1.4000	0	.169	-.050	.124	.103	.363	57.6
1.4000	45	.180	-.167	.062	.022	.390	61.3
1.4000	90	.191	-.126	.141	.021	.427	45.7
1.4000	135	.163	-.119	.083	.076	.459	62.8
1.5000	0	.164	-.001	.158	-.044	.057	28.0
1.5000	45	.172	.014	.168	-.033	.055	23.1
1.5000	90	.174	.015	.170	-.037	.059	21.7
1.5000	135	.174	.015	.170	-.034	.058	21.4

TEST CONDITION 2, $z/R = 0$
 $\Omega R = 450$ ft/sec, $\theta_{75} = 9.74$ deg, $C_T = 0.0041$

x/R	ψ , deg	\bar{v}_R/v_o	\bar{v}_x/v_o	\bar{v}_y/v_o	\bar{v}_z/v_o	σ_{v_R}/v_o	σ_ϵ , deg
0.7500	0	1.412	-.313	.598	-1.240	.039	8.4
0.7500	45	1.576	-.231	.223	-1.543	.044	3.0
0.7500	90	1.527	-.290	.185	-1.487	.035	2.8
0.7500	135	1.423	-.318	.160	-1.378	.021	3.1
0.7750	0	1.436	-.240	.629	-1.268	.027	2.9
0.7750	45	1.619	-.192	.284	-1.582	.030	2.6
0.7750	90	1.518	-.239	.246	-1.478	.030	2.6
0.7750	135	1.418	-.230	.215	-1.382	.021	2.6

x/R	ψ, deg	\bar{v}_R/v_o	\bar{v}_x/v_o	\bar{v}_y/v_o	\bar{v}_z/v_o	σ_{v_R}/v_o	$\sigma_\epsilon, \text{deg}$
0.8000	0	1.485	-.327	.580	-1.327	.138	7.7
0.8000	45	1.685	-.250	.292	-1.640	.096	5.8
0.8000	90	1.526	-.272	.235	-1.483	.116	3.2
0.8000	135	1.438	-.281	.222	-1.392	.106	3.5
0.8500	0	1.743	-1.151	.742	-1.078	.068	8.6
0.8500	45	1.777	-.333	.216	-1.732	.048	2.7
0.8500	90	1.617	-.300	.236	-1.572	.047	2.7
0.8500	135	1.637	-.352	.209	-1.585	.079	5.1
0.8625	0	1.819	-1.308	.720	-1.038	.072	3.9
0.8625	45	1.799	-.377	.196	-1.748	.031	3.1
0.8625	90	1.659	-.289	.213	-1.619	.032	2.8
0.8625	135	1.743	-.386	.152	-1.693	.029	3.0
0.8750	0	1.852	-1.462	.735	-.868	.119	4.9
0.8750	45	1.655	-.395	.191	-1.596	.139	4.1
0.8750	90	1.600	-.344	.171	-1.553	.088	16.1
0.8750	135	1.758	-.476	.096	-1.690	.097	16.6
0.8875	0	1.873	-1.630	.625	-.679	.099	10.8
0.8875	45	1.774	-.451	.113	-1.712	.048	2.8
0.8875	90	1.757	-.269	.197	-1.726	.037	2.6
0.8875	135	2.197	-.595	.024	-2.115	.048	3.8
0.9000	0	1.687	-1.494	.640	-.453	.133	13.8
0.9000	45	1.678	-.367	.135	-1.632	.124	3.0
0.9000	90	1.896	-.211	.197	-1.874	.177	2.9
0.9000	135	2.468	-.866	.119	-2.308	.154	8.7
0.9125	0	1.619	-1.517	.512	.244	.149	16.3
0.9125	45	1.466	-.339	.244	-1.405	.147	17.5
0.9125	90	1.994	.123	.006	-1.990	.256	6.7
0.9125	135	3.852	-1.107	-.613	-3.638	1.009	23.8
0.9250	0	1.411	-1.278	.518	.301	.108	19.4
0.9250	45	1.497	-.178	.197	-1.473	.176	8.4
0.9250	90	2.280	.266	.154	-2.259	.463	16.3
0.9250	135	5.144	-4.923	-.163	-1.484	.902	10.8
0.9375	0	1.230	-1.002	.597	.390	.086	11.3
0.9375	45	1.390	-.036	.216	-1.373	.057	4.4
0.9375	90	2.548	1.688	.125	-1.905	.251	11.5
0.9375	135	3.622	-3.432	.094	1.155	.438	11.6

x/R	ψ, deg	\bar{v}_R/v_o	\bar{v}_x/v_o	\bar{v}_y/v_o	\bar{v}_z/v_o	σ_{v_R}/v_o	$\sigma_\epsilon, \text{deg}$
0.9500	0	1.070	-.733	.653	.426	.111	14.8
0.9500	45	1.242	.285	.383	-1.146	.290	23.0
0.9500	90	1.748	1.732	.195	.140	.320	20.9
0.9500	135	1.640	-.598	.407	1.472	.288	19.1
0.9625	0	.957	-.607	.669	.316	.145	17.2
0.9625	45	1.122	.889	.658	-.193	.321	30.5
0.9625	90	1.385	.538	.652	1.097	.129	21.9
0.9625	135	1.252	-.595	.448	1.006	.151	20.5
0.9750	0	.895	-.522	.681	.254	.128	18.4
0.9750	45	.995	.903	.300	.293	.097	18.9
0.9750	90	1.050	.313	.386	.925	.128	13.9
0.9750	135	1.037	-.491	.407	.818	.136	22.1
1.0000	0	.736	-.406	.563	.243	.080	14.3
1.0000	45	.728	.369	.274	.565	.118	13.4
1.0000	90	.764	-.063	.288	.705	.110	13.4
1.0000	135	.671	-.356	.262	.505	.089	20.8
1.1000	0	.522	-.169	.428	.248	.048	5.2
1.1000	45	.496	-.133	.285	.383	.042	9.2
1.1000	90	.439	-.178	.291	.277	.039	11.9
1.1000	135	.462	-.196	.351	.227	.034	9.0
1.2000	0	.488	-.107	.432	.200	.023	4.4
1.2000	45	.498	-.102	.418	.251	.030	4.8
1.2000	90	.468	-.111	.398	.220	.029	4.6
1.2000	135	.442	-.118	.385	.183	.027	4.3
1.3000	0	.465	-.061	.443	.126	.019	3.3
1.3000	45	.456	-.064	.427	.145	.017	3.1
1.3000	90	.419	-.073	.393	.124	.022	4.1
1.3000	135	.383	-.066	.363	.103	.021	3.5
1.4000	0	.415	-.029	.400	.108	.068	3.4
1.4000	45	.412	-.031	.393	.119	.066	3.8
1.4000	90	.390	-.037	.373	.108	.061	3.4
1.4000	135	.353	-.034	.337	.098	.053	3.5
1.5000	0	.430	.003	.423	.075	.052	3.6
1.5000	45	.438	.012	.430	.081	.056	3.6
1.5000	90	.414	.002	.407	.071	.052	4.2
1.5000	135	.391	-.002	.386	.063	.046	3.9

TEST CONDITION 3, $z/R = 0$
 $\Omega R = 451 \text{ ft/sec}$, $\theta_{75} = 6.24 \text{ deg}$, $C_T = 0.0020$

x/R	ψ, deg	\bar{v}_R/v_o	\bar{v}_x/v_o	\bar{v}_y/v_o	\bar{v}_z/v_o	σ_{v_R}/v_o	$\sigma_\epsilon, \text{deg}$
0.8500	0	1.920	-.295	.929	-1.654	.085	6.0
0.8500	45	1.866	-.303	.461	-1.782	.058	3.8
0.8500	90	1.832	-.389	.424	-1.739	.040	3.5
0.8500	135	1.715	-.414	.462	-1.598	.049	5.0
0.8750	0	2.124	-.445	.632	-1.978	.125	9.0
0.8750	45	2.065	-.578	.114	-1.979	.059	5.0
0.8750	90	1.797	-.536	.125	-1.710	.045	4.8
0.8750	135	1.717	-.516	.268	-1.615	.062	6.1
0.8875	0	2.758	-.722	.962	-2.481	.223	10.0
0.8875	45	2.029	-.659	.262	-1.901	.072	13.4
0.8875	90	1.842	-.450	.226	-1.772	.051	4.4
0.8875	135	1.908	-.402	.225	-1.851	.053	3.1
0.9000	0	4.043	-1.244	.654	-3.791	.649	20.1
0.9000	45	2.066	-1.404	1.086	-1.057	.220	12.8
0.9000	90	1.643	-.582	.191	-1.536	.102	6.6
0.9000	135	1.915	-.258	.220	-1.885	.056	3.7
0.9125	0	3.608	-2.510	.890	2.434	1.597	37.4
0.9125	45	1.777	-.771	.695	-1.442	.231	24.0
0.9125	90	1.679	-.427	.354	-1.585	.070	6.6
0.9125	135	2.138	-.159	.218	-2.121	.085	6.3
0.9250	0	1.982	-.502	1.141	1.542	.161	19.3
0.9250	45	1.787	-.655	1.321	-1.010	.212	20.7
0.9250	90	1.463	-.238	.370	-1.395	.098	6.4
0.9250	135	2.300	.838	-.097	-2.140	.271	8.9
0.9375	0	1.536	-.527	1.073	.963	.261	18.2
0.9375	45	1.411	-.260	.968	-.993	.448	21.5
0.9375	90	1.235	.272	.366	-1.148	.154	7.1
0.9375	135	1.879	1.849	.271	.193	.283	14.8
0.9500	0	1.201	-.420	.838	.751	.247	21.6
0.9500	45	.859	.307	.624	-.504	.287	28.2
0.9500	90	.777	.536	.385	-.410	.234	20.6
0.9500	135	1.169	.505	.440	.958	.253	20.8
0.9625	0	1.274	-.338	1.005	.706	.196	14.0
0.9625	45	.821	.572	.588	-.027	.143	18.4
0.9625	90	.908	.673	.461	.399	.265	29.5
0.9625	135	1.084	.102	.370	1.014	.240	15.8

x/R	ψ, deg	\bar{V}_R/v_o	\bar{v}_x/v_o	\bar{v}_y/v_o	\bar{v}_z/v_o	σ_{V_R}/v_o	$\sigma_\epsilon, \text{deg}$
0.9750	0	1.290	-.340	1.082	.615	.129	11.3
0.9750	45	1.026	.650	.779	.156	.154	16.4
0.9750	90	1.216	.439	.714	.881	.224	21.2
0.9750	135	1.223	-.124	.708	.990	.167	16.9
1.0000	0	1.010	-.224	.787	.592	.061	6.3
1.0000	45	1.022	.270	.573	.802	.087	12.1
1.0000	90	1.025	-.081	.590	.834	.098	5.0
1.0000	135	.892	-.283	.460	.710	.076	10.7
1.1000	0	.714	-.162	.606	.341	.096	7.3
1.1000	45	.718	-.160	.551	.432	.097	7.1
1.1000	90	.666	-.180	.525	.368	.082	6.7
1.1000	135	.637	-.192	.514	.323	.076	7.4
1.2000	0	.570	-.100	.524	.201	.074	4.0
1.2000	45	.577	-.108	.517	.231	.073	5.3
1.2000	90	.532	-.103	.482	.203	.064	4.4
1.2000	135	.493	-.094	.450	.178	.050	4.2
1.3000	0	.575	-.035	.562	.113	.080	4.9
1.3000	45	.560	-.026	.544	.129	.075	5.2
1.3000	90	.519	-.045	.504	.114	.065	5.0
1.3000	135	.469	-.062	.456	.092	.053	10.5
1.4000	0	.571	.048	.567	.051	.045	5.1
1.4000	45	.567	.036	.563	.054	.042	5.3
1.4000	90	.546	.061	.541	.040	.048	5.0
1.4000	135	.510	.070	.505	.019	.041	6.2
1.5000	0	.600	.120	.586	.051	.076	6.2
1.5000	45	.592	.102	.581	.049	.068	6.3
1.5000	90	.561	.115	.549	.031	.064	7.8
1.5000	135	.518	.117	.504	.018	.064	9.7

TEST CONDITION 1, $z/R = -0.045$

$\Omega R = 634 \text{ ft/sec}$, $\theta_{75} = 6.18 \text{ deg}$, $C_T = 0.0020$

x/R	ψ, deg	\bar{V}_R/v_o	\bar{v}_x/v_o	\bar{v}_y/v_o	\bar{v}_z/v_o	σ_{V_R}/v_o	$\sigma_\epsilon, \text{deg}$
0.3125	0	.926	.188	-.116	-.899	.269	7.6
0.3125	45	.894	.216	-.200	-.844	.293	10.5
0.3125	90	.850	.303	-.157	-.779	.242	14.0
0.3125	135	.893	.261	-.160	-.839	.282	7.6

x/R	ψ, deg	\bar{v}_R/v_0	\bar{v}_x/v_0	\bar{v}_y/v_0	\bar{v}_z/v_0	σ_{v_R}/v_0	$\sigma_\epsilon, \text{deg}$
0.4000	0	1.067	.061	-.114	-1.059	.279	7.2
0.4000	45	1.030	.116	-.190	-1.005	.323	10.6
0.4000	90	1.033	.238	-.182	-.988	.273	9.3
0.4000	135	1.021	.153	-.155	-.997	.311	8.5
0.5000	0	1.216	-.298	-.116	-1.173	.232	7.5
0.5000	45	1.180	-.234	-.079	-1.154	.305	13.1
0.5000	90	1.169	-.122	-.167	-1.150	.292	5.9
0.5000	135	1.167	-.179	-.115	-1.148	.343	6.0
0.6000	0	1.265	-.222	-.135	-1.238	.248	6.8
0.6000	45	1.244	-.196	-.074	-1.226	.322	13.9
0.6000	90	1.234	-.096	-.234	-1.208	.287	7.1
0.6000	135	1.193	-.126	-.165	-1.175	.329	6.3
0.7000	0	1.330	-.347	-.160	-1.274	.254	6.5
0.7000	45	1.324	-.335	-.148	-1.272	.350	10.7
0.7000	90	1.312	-.312	-.265	-1.246	.303	6.2
0.7000	135	1.305	-.331	-.195	-1.247	.358	5.3
0.8000	0	1.443	-.437	-.119	-1.369	.279	7.5
0.8000	45	1.487	-.436	-.089	-1.419	.353	13.7
0.8000	90	1.426	-.467	-.190	-1.334	.319	7.9
0.8000	135	1.468	-.464	-.166	-1.383	.389	7.2
0.8500	0	1.530	-.346	.108	-1.487	.328	9.2
0.8500	45	1.527	-.344	.076	-1.486	.391	13.2
0.8500	90	1.448	-.330	-.038	-1.409	.321	6.6
0.8500	135	1.467	-.329	.012	-1.430	.368	8.1
0.8625	0	1.928	-.569	.008	-1.842	.762	9.8
0.8625	45	2.015	-.686	-.248	-1.878	.602	7.4
0.8625	90	1.622	-.707	-.232	-1.442	.457	7.2
0.8625	135	1.532	-.518	-.243	-1.422	.414	8.0
0.8750	0	2.004	-.674	-.311	-1.862	.737	12.7
0.8750	45	2.130	-.805	-.377	-1.936	.785	8.1
0.8750	90	1.554	-.644	-.334	-1.374	.404	10.5
0.8750	135	1.564	-.401	-.308	-1.480	.468	10.4
0.8875	0	1.750	-.829	-.077	-1.539	1.006	31.3
0.8875	45	2.238	-1.758	-.115	-1.380	1.431	24.6
0.8875	90	1.291	-.636	-.230	-1.099	.284	15.7
0.8875	135	1.475	-.260	-.169	-1.442	.714	14.2

x/R	ψ, deg	\bar{v}_R/v_0	\bar{v}_x/v_0	\bar{v}_y/v_0	\bar{v}_z/v_0	σ_{V_R}/v_0	$\sigma_\epsilon, \text{deg}$
0.9000	0	1.266	-.121	.014	-1.260	.653	46.3
0.9000	45	1.361	-1.268	-.217	-.443	.647	33.9
0.9000	90	1.111	-.459	-.279	-.973	.247	15.5
0.9000	135	1.249	.082	-.146	-1.238	.668	19.7
0.9125	0	1.495	-.052	-.128	-1.488	.721	43.7
0.9125	45	1.344	-.824	-.240	-1.034	.341	23.2
0.9125	90	1.212	-.211	-.117	-1.188	.339	20.2
0.9125	135	1.817	.013	-.118	-1.813	1.175	26.7
0.9250	0	1.389	-.059	-1.285	-.524	3.077	58.9
0.9250	45	1.493	-.209	-1.356	-.589	3.090	46.2
0.9250	90	1.475	-.099	-1.319	-.653	3.083	52.1
0.9250	135	1.226	.162	-1.181	-.284	3.153	60.6
0.9500	0	.167	.090	.062	.126	.304	51.6
0.9500	45	.103	.091	-.043	.023	.259	61.2
0.9500	90	.103	.015	-.067	.076	.256	60.0
0.9500	135	.115	.058	.019	.098	.277	54.7
1.0000	0	.186	-.139	-.067	.104	.143	48.3
1.0000	45	.182	-.083	-.121	.106	.097	38.5
1.0000	90	.263	-.193	-.105	.145	.099	20.0
1.0000	135	.219	-.150	-.086	.136	.109	41.4
1.1000	0	.279	-.200	-.158	.113	.090	17.9
1.1000	45	.284	-.197	-.158	.129	.090	19.5
1.1000	90	.295	-.224	-.166	.096	.088	17.0
1.1000	135	.285	-.212	-.156	.109	.092	22.0
1.2000	0	.276	-.138	-.235	.037	.077	8.4
1.2000	45	.273	-.144	-.228	.044	.070	10.8
1.2000	90	.269	-.148	-.224	.018	.069	9.2
1.2000	135	.271	-.150	-.224	.024	.069	9.6
1.3000	0	.248	-.159	-.178	-.069	.066	4.8
1.3000	45	.257	-.164	-.185	-.070	.070	5.8
1.3000	90	.263	-.171	-.184	-.078	.076	6.4
1.3000	135	.263	-.168	-.189	-.072	.092	7.1
1.4000	0	.228	-.127	-.186	-.032	.079	8.5
1.4000	45	.225	-.128	-.182	-.035	.070	8.4
1.4000	90	.221	-.129	-.176	-.038	.061	7.9
1.4000	135	.213	-.124	-.169	-.037	.054	8.1
1.5000	0	.212	-.132	-.154	-.060	.069	7.4
1.5000	45	.209	-.132	-.151	-.057	.055	5.1
1.5000	90	.210	-.133	-.150	-.061	.053	5.4
1.5000	135	.205	-.132	-.146	-.058	.054	5.0

TEST CONDITION 2, $z/R = -0.045$
 $\Omega R = 454 \text{ ft/sec}$, $\theta_{75} = 9.74 \text{ deg}$, $C_T = 0.0041$

x/R	ψ, deg	\bar{v}_R/v_0	\bar{v}_x/v_0	\bar{v}_y/v_0	\bar{v}_z/v_0	σ_{V_R}/v_0	$\sigma_\epsilon, \text{deg}$
0.3125	0	.989	-.023	.186	-.971	.134	16.0
0.3125	45	1.052	-.243	-.095	-1.020	.148	12.8
0.3125	90	1.019	.162	-.173	-.991	.117	16.9
0.3125	135	.966	.138	-.141	-.946	.131	14.8
0.4000	0	1.138	.117	.113	-1.126	.039	7.9
0.4000	45	1.295	-.098	-.213	-1.273	.044	4.8
0.4000	90	1.259	.331	-.245	-1.190	.051	4.7
0.4000	135	1.218	.290	-.252	-1.156	.041	5.2
0.5000	0	1.229	-.191	.110	-1.209	.052	5.4
0.5000	45	1.425	-.355	-.148	-1.372	.031	5.1
0.5000	90	1.369	-.021	-.179	-1.357	.030	4.2
0.5000	135	1.337	-.067	-.163	-1.325	.037	5.5
0.6000	0	1.251	-.127	.049	-1.244	.111	5.2
0.6000	45	1.528	-.288	-.101	-1.497	.185	3.3
0.6000	90	1.462	-.056	-.165	-1.451	.130	4.6
0.6000	135	1.372	-.064	-.152	-1.363	.138	3.9
0.7000	0	1.429	-.326	.111	-1.387	.039	5.5
0.7000	45	1.783	-.514	-.131	-1.702	.045	4.4
0.7000	90	1.595	-.297	-.118	-1.563	.037	4.2
0.7000	135	1.586	-.356	-.120	-1.541	.055	4.2
0.7500	0	1.451	-.322	.029	-1.414	.022	3.4
0.7500	45	1.887	-.562	-.200	-1.790	.054	3.1
0.7500	90	1.702	-.310	-.178	-1.664	.044	3.5
0.7500	135	1.602	-.398	-.187	-1.541	.036	3.6
0.8000	0	1.638	-.353	.225	-1.584	.083	7.0
0.8000	45	2.370	-.805	.068	-2.228	.142	10.6
0.8000	90	1.946	-.572	-.059	-1.860	.090	8.7
0.8000	135	1.633	-.517	-.096	-1.546	.087	7.7
0.8125	0	1.672	-.295	-.005	-1.646	.064	4.8
0.8125	45	2.469	-.899	-.355	-2.273	.147	5.6
0.8125	90	1.928	-.545	-.320	-1.822	.090	5.7
0.8125	135	1.633	-.445	-.259	-1.549	.046	5.3
0.8250	0	1.555	-.176	.079	-1.543	.111	5.2
0.8250	45	3.424	-1.221	-.142	-3.196	.157	5.4
0.8250	90	2.062	-.950	-.243	-1.814	.135	10.5
0.8250	135	1.567	-.622	-.267	-1.413	.099	6.6

x/R	ψ, deg	\bar{v}_R/v_0	\bar{v}_x/v_0	\bar{v}_y/v_0	\bar{v}_z/v_0	σ_{v_R}/v_0	$\sigma_\epsilon, \text{deg}$
0.8375	0	1.702	-.076	.141	-1.694	.090	7.3
0.8375	45	3.217	-1.234	-.050	-2.971	.239	6.9
0.8375	90	1.781	-.877	-.144	-1.543	.158	18.8
0.8375	135	1.503	-.467	-.177	-1.417	.048	5.7
0.8500	0	1.218	.142	.127	-1.203	.096	8.8
0.8500	45	4.808	-4.463	1.454	-1.041	4.317	55.9
0.8500	90	1.495	-1.240	-.106	-.829	.130	16.1
0.8500	135	1.258	-.561	-.283	-1.090	.092	11.1
0.8625	0	.862	.311	.086	-.800	.128	9.1
0.8625	45	1.940	-.144	-.247	1.919	.280	12.3
0.8625	90	1.178	-1.035	-.269	-.495	.081	10.8
0.8625	135	1.045	-.478	-.123	-.921	.157	16.4
0.8750	0	.515	.323	.325	-.236	.270	24.7
0.8750	45	.636	-.367	.004	.520	.378	42.3
0.8750	90	.730	-.662	.003	-.306	.234	23.3
0.8750	135	.633	-.215	.239	-.545	.344	23.5
0.8875	0	.475	.115	.234	.397	.169	32.5
0.8875	45	.238	-.215	-.052	.086	.179	37.6
0.8875	90	.264	-.258	-.025	-.053	.130	35.0
0.8875	135	.107	-.053	-.042	-.083	.210	63.8
0.9000	0	.809	.263	.272	.715	.222	23.6
0.9000	45	.478	-.453	-.107	-.108	.230	30.7
0.9000	90	.498	-.165	.016	-.470	.135	21.2
0.9000	135	.495	.196	.003	-.454	.231	31.6
0.9500	0	.538	-.209	.032	.495	.097	24.8
0.9500	45	.316	.111	-.259	.143	.069	26.5
0.9500	90	.391	-.028	-.317	.228	.066	25.5
0.9500	135	.511	-.205	-.279	.376	.068	20.0
1.0000	0	.459	-.424	.036	.172	.030	12.1
1.0000	45	.198	.040	-.130	.143	.062	36.4
1.0000	90	.293	-.169	-.116	.209	.038	21.0
1.0000	135	.402	-.297	-.090	.256	.023	8.9
1.1000	0	.422	-.407	-.008	.114	.026	11.8
1.1000	45	.374	-.298	-.071	.214	.026	9.4
1.1000	90	.418	-.372	-.075	.177	.021	8.7
1.1000	135	.435	-.414	-.031	.132	.031	9.8

x/R	ψ , deg	\bar{v}_R/v_o	\bar{v}_x/v_o	\bar{v}_y/v_o	\bar{v}_z/v_o	σ_{v_R}/v_o	σ_ϵ , deg
1.2000	0	.388	-.364	-.122	.057	.046	6.9
1.2000	45	.378	-.318	-.174	.108	.050	7.8
1.2000	90	.404	-.358	-.164	.087	.054	6.9
1.2000	135	.401	-.373	-.136	.059	.048	6.9
1.3000	0	.369	-.358	-.083	-.024	.032	7.0
1.3000	45	.371	-.346	-.133	.013	.034	5.3
1.3000	90	.383	-.359	-.135	-.002	.027	5.1
1.3000	135	.378	-.368	-.078	-.038	.029	7.0
1.4000	0	.226	-.211	-.081	.007	.027	15.2
1.4000	45	.286	-.208	-.193	.032	.040	11.2
1.4000	90	.312	-.195	-.243	.006	.048	13.1
1.4000	135	.335	-.202	-.266	-.020	.057	12.4
1.5000	0	.227	-.125	-.096	-.164	.036	24.3
1.5000	45	.236	-.118	-.134	-.155	.039	23.2
1.5000	90	.296	-.129	-.218	-.154	.059	20.5
1.5000	135	.335	-.129	-.273	-.145	.055	16.4

TEST CONDITION 3, $z/R = -0.045$
 $QR = 459$ ft/sec, $\theta_{75} = 6.20$ deg, $C_T = 0.0019$

x/R	ψ , deg	\bar{v}_R/v_o	\bar{v}_x/v_o	\bar{v}_y/v_o	\bar{v}_z/v_o	σ_{v_R}/v_o	σ_ϵ , deg
0.4000	0	1.165	-.282	-.129	-1.123	.054	4.7
0.4000	45	1.163	-.407	-.256	-1.059	.050	4.7
0.4000	90	1.075	-.382	-.038	-1.004	.164	16.0
0.4000	135	1.043	-.177	-.280	-.989	.060	5.5
0.5000	0	1.453	-.527	-.157	-1.345	.070	7.5
0.5000	45	1.485	-.644	-.411	-1.273	.106	6.3
0.5000	90	1.184	-.436	.035	-1.100	.180	19.3
0.5000	135	1.268	-.328	-.400	-1.157	.080	6.8
0.6000	0	1.574	-.553	-.246	-1.453	.198	5.1
0.6000	45	1.645	-.674	-.477	-1.423	.179	3.4
0.6000	90	1.398	-.313	-.375	-1.310	.281	12.0
0.6000	135	1.510	-.403	-.513	-1.362	.172	5.2
0.7000	0	1.591	-.729	-.280	-1.386	.177	5.2
0.7000	45	1.788	-.799	-.519	-1.513	.185	5.4
0.7000	90	1.734	-.635	-.529	-1.524	.195	4.8
0.7000	135	1.680	-.669	-.540	-1.444	.193	4.2

x/R	ψ, deg	\bar{v}_R/v_0	\bar{v}_x/v_0	\bar{v}_y/v_0	\bar{v}_z/v_0	σ_{v_R}/v_0	$\sigma_\epsilon, \text{deg}$
0.7500	0	1.732	-.837	-.322	-1.482	.042	4.5
0.7500	45	1.890	-.854	-.484	-1.615	.046	4.9
0.7500	90	1.836	-.822	-.398	-1.594	.132	11.4
0.7500	135	1.839	-.866	-.535	-1.531	.053	4.1
0.7625	0	1.751	-.828	-.241	-1.524	.066	3.6
0.7625	45	2.000	-.951	-.381	-1.717	.063	4.5
0.7625	90	1.947	-.784	-.198	-1.771	.144	11.7
0.7625	135	1.940	-.934	-.456	-1.632	.075	5.5
0.7750	0	1.767	-.857	-.217	-1.530	.245	11.4
0.7750	45	2.148	-1.052	-.432	-1.822	.322	10.6
0.7750	90	2.027	-1.123	-.349	-1.651	.451	15.8
0.7750	135	1.882	-1.009	-.538	-1.495	.214	8.5
0.7875	0	.996	-.414	.401	-.812	.279	26.9
0.7875	45	1.745	-.279	.622	-1.590	1.006	35.1
0.7875	90	1.612	-1.337	.447	-.781	1.193	44.6
0.7875	135	1.142	-.970	.008	-.602	.560	35.9
0.8000	0	1.130	-.483	-.034	-1.021	.183	14.6
0.8000	45	2.162	-.677	.146	-2.048	.660	19.7
0.8000	90	2.467	-1.541	-.053	-1.925	.598	24.8
0.8000	135	1.654	-1.142	-.287	-1.161	.364	27.7
0.8125	0	1.812	-1.050	-.189	-1.464	.102	12.6
0.8125	45	1.858	-1.016	-.498	-1.474	.079	4.1
0.8125	90	1.712	-.725	-.066	-1.550	.266	14.7
0.8125	135	1.921	-1.074	-.355	-1.554	.176	10.8
0.8250	0	1.402	-.777	.759	-.886	.580	41.2
0.8250	45	1.382	-.998	.052	-.954	.451	32.9
0.8250	90	1.406	-.684	-.009	-1.228	.401	23.2
0.8250	135	1.314	-.613	.340	-1.112	.578	31.1
0.8375	0	.374	.329	.164	-.073	.253	39.5
0.8375	45	.258	-.017	-.252	.050	.215	51.9
0.8375	90	.382	-.268	-.266	-.056	.193	41.4
0.8375	135	.302	-.097	-.280	-.057	.194	41.9
0.8500	0	.354	-.285	.160	-.135	.255	47.4
0.8500	45	.738	-.437	-.138	-.579	.215	23.8
0.8500	90	.627	-.182	-.138	-.584	.228	28.0
0.8500	135	.272	-.133	-.137	-.194	.219	49.3

x/R	ψ, deg	\bar{v}_R/v_0	\bar{v}_x/v_0	\bar{v}_y/v_0	\bar{v}_z/v_0	σ_{v_R}/v_0	$\sigma_\epsilon, \text{deg}$
0.9000	0	.272	.049	.067	.259	.171	39.4
0.9000	45	.289	.024	-.190	-.217	.176	35.3
0.9000	90	.158	.038	-.143	-.058	.179	54.7
0.9000	135	.221	-.051	-.209	.050	.194	48.5
0.9500	0	.591	-.039	-.461	.369	.082	26.8
0.9500	45	.630	.269	-.567	.060	.060	13.7
0.9500	90	.653	.240	-.582	.175	.072	13.9
0.9500	135	.661	.099	-.584	.293	.065	15.3
1.0000	0	.625	-.187	-.492	.337	.131	26.6
1.0000	45	.756	.207	-.597	.414	.233	24.6
1.0000	90	.743	.029	-.597	.441	.206	21.7
1.0000	135	.728	-.177	-.629	.321	.145	20.4
1.1000	0	.558	-.340	-.376	.231	.020	4.4
1.1000	45	.577	-.282	-.404	.300	.025	5.0
1.1000	90	.582	-.332	-.396	.266	.023	4.9
1.1000	135	.577	-.365	-.383	.231	.023	4.8
1.2000	0	.566	-.393	-.400	.074	.032	5.6
1.2000	45	.571	-.380	-.412	.108	.030	4.5
1.2000	90	.554	-.388	-.386	.088	.035	5.8
1.2000	135	.540	-.396	-.362	.064	.037	5.6
1.3000	0	.422	-.322	-.270	-.037	.021	7.8
1.3000	45	.459	-.335	-.312	-.021	.023	7.3
1.3000	90	.472	-.332	-.332	-.042	.021	6.8
1.3000	135	.453	-.329	-.307	-.052	.025	8.2
1.4000	0	.399	-.396	.030	.043	.030	8.4
1.4000	45	.357	-.357	-.001	.004	.026	8.1
1.4000	90	.388	-.380	-.080	.020	.032	12.9
1.4000	135	.384	-.347	-.158	.050	.031	10.4
1.5000	0	.361	-.352	-.040	.073	.045	12.9
1.5000	45	.362	-.347	-.064	.083	.047	12.1
1.5000	90	.372	-.345	-.106	.093	.043	12.6
1.5000	135	.397	-.349	-.165	.093	.037	10.5

TEST CONDITION 1, $z/R = -0.086$
 $\Omega R = 626 \text{ ft/sec}$, $\theta_{75} = 6.18 \text{ deg}$, $C_T = 0.0020$

x/R	ψ, deg	\bar{v}_R/v_o	\bar{v}_x/v_o	\bar{v}_y/v_o	\bar{v}_z/v_o	σ_{v_R}/v_o	$\sigma_\epsilon, \text{deg}$
0.3125	0	.921	.278	-.043	-.877	.314	15.3
0.3125	45	.901	.311	-.132	-.836	.309	16.4
0.3125	90	.882	.328	.069	-.816	.379	26.1
0.3125	135	.910	.283	-.123	-.856	.320	10.1
0.4000	0	1.048	.267	-.084	-1.010	.336	5.4
0.4000	45	1.004	.230	-.103	-.972	.339	6.0
0.4000	90	1.016	.247	-.079	-.983	.384	7.4
0.4000	135	1.000	.210	-.001	-.977	.316	13.1
0.5000	0	1.186	.105	-.060	-1.180	.347	5.7
0.5000	45	1.138	.107	.027	-1.133	.359	12.8
0.5000	90	1.157	.143	-.092	-1.144	.342	6.7
0.5000	135	1.180	.192	-.076	-1.162	.354	6.1
0.6000	0	1.159	-.012	-.103	-1.154	.336	15.8
0.6000	45	1.174	.026	-.178	-1.160	.367	16.1
0.6000	90	1.140	.002	-.122	-1.133	.376	16.0
0.6000	135	1.137	.080	-.115	-1.128	.378	5.5
0.7000	0	1.288	-.022	-.103	-1.284	.343	6.7
0.7000	45	1.285	-.021	-.148	-1.276	.388	5.4
0.7000	90	1.248	-.010	-.108	-1.244	.379	5.2
0.7000	135	1.280	-.008	-.108	-1.275	.369	3.8
0.7500	0	1.353	-.041	.032	-1.352	.347	5.5
0.7500	45	1.343	-.026	-.037	-1.342	.399	4.2
0.7500	90	1.291	-.010	-.004	-1.291	.382	7.0
0.7500	135	1.324	-.025	.013	-1.323	.366	5.0
0.8000	0	1.424	-.138	.053	-1.417	.350	7.0
0.8000	45	1.428	-.127	-.016	-1.422	.386	6.3
0.8000	90	1.330	-.127	.016	-1.324	.373	5.5
0.8000	135	1.388	-.140	.046	-1.380	.380	6.7
0.8500	0	1.449	.148	-.047	-1.440	.388	9.8
0.8500	45	1.462	.115	-.135	-1.451	.416	7.3
0.8500	90	1.425	.102	-.033	-1.421	.445	9.5
0.8500	135	1.435	.092	-.093	-1.429	.420	5.8
0.8625	0	1.549	.057	-.188	-1.537	.379	8.1
0.8625	45	1.551	.049	-.248	-1.530	.424	7.5
0.8625	90	1.468	.031	-.153	-1.460	.417	10.4
0.8625	135	1.530	.045	-.194	-1.517	.388	5.5

x/R	ψ, deg	\bar{v}_R/v_o	\bar{v}_x/v_o	\bar{v}_y/v_o	\bar{v}_z/v_o	σ_{v_R}/v_o	$\sigma_\epsilon, \text{deg}$
0.8750	0	1.612	-.141	.068	-1.604	.429	10.5
0.8750	45	1.585	-.173	.005	-1.576	.447	12.5
0.8750	90	1.516	-.139	.070	-1.508	.462	13.1
0.8750	135	1.591	-.155	-.027	-1.584	.408	10.8
0.8875	0	1.630	-.237	.038	-1.612	.378	13.7
0.8875	45	1.715	-.258	-.037	-1.695	.536	10.0
0.8875	90	1.518	-.203	-.085	-1.502	.408	8.0
0.8875	135	1.602	-.156	-.049	-1.593	.426	6.4
0.9000	0	1.590	.169	-.081	-1.579	.388	6.4
0.9000	45	1.570	.157	-.154	-1.555	.423	4.8
0.9000	90	1.527	.120	-.013	-1.522	.451	11.3
0.9000	135	1.556	.119	-.098	-1.548	.377	5.5
0.9125	0	1.592	-.121	-.095	-1.584	.491	15.1
0.9125	45	1.824	-.476	-.066	-1.760	1.046	16.4
0.9125	90	1.389	-.203	-.170	-1.363	.385	12.9
0.9125	135	1.548	-.032	-.130	-1.542	.523	12.0
0.9250	0	1.480	-.240	-.158	-1.452	.573	25.1
0.9250	45	1.647	.017	-.127	-1.642	.789	21.1
0.9250	90	1.304	-.107	-.185	-1.286	.382	23.2
0.9250	135	1.603	-.037	-.041	-1.602	.627	20.5
0.9375	0	.924	-.287	.199	-.856	.576	46.3
0.9375	45	.771	-.363	-.017	-.680	.870	44.4
0.9375	90	.904	-.137	.042	-.893	.411	34.8
0.9375	135	1.215	.352	.357	-1.106	1.348	42.5
0.9500	0	.907	-.231	-.044	-.876	.824	43.7
0.9500	45	.892	-.153	-.225	-.849	.454	28.7
0.9500	90	.727	.219	-.097	-.686	1.458	33.4
0.9500	135	.960	-.090	-.127	-.947	.761	49.8
1.0000	0	.337	-.083	-.321	-.062	.127	29.1
1.0000	45	.373	-.055	-.363	-.067	.132	20.5
1.0000	90	.359	-.075	-.343	-.071	.132	21.0
1.0000	135	.343	-.014	-.341	-.033	.166	29.3
1.1000	0	.292	-.050	-.259	-.125	.130	26.5
1.1000	45	.314	-.049	-.284	-.125	.134	28.0
1.1000	90	.319	-.068	-.279	-.139	.128	25.8
1.1000	135	.313	-.047	-.279	-.134	.138	25.9

x/R	ψ, deg	\bar{v}_R/v_o	\bar{v}_x/v_o	\bar{v}_y/v_o	\bar{v}_z/v_o	σ_{v_R}/v_o	$\sigma_\epsilon, \text{deg}$
1.2000	0	.189	.021	-.149	-.113	.103	34.4
1.2000	45	.200	.020	-.158	-.120	.102	32.8
1.2000	90	.205	.021	-.153	-.135	.107	31.5
1.2000	135	.196	.017	-.150	-.125	.107	30.2
1.3000	0	.369	.176	-.274	-.173	.163	15.5
1.3000	45	.365	.179	-.261	-.182	.158	16.3
1.3000	90	.367	.163	-.271	-.187	.148	14.0
1.3000	135	.365	.163	-.273	-.179	.145	14.8
1.4000	0	.282	.162	-.159	-.168	.169	23.6
1.4000	45	.289	.169	-.168	-.163	.169	21.6
1.4000	90	.296	.163	-.174	-.176	.182	21.4
1.4000	135	.291	.165	-.182	-.157	.175	21.0
1.5000	0	.250	.135	-.187	-.096	.098	16.1
1.5000	45	.255	.142	-.188	-.098	.096	15.3
1.5000	90	.253	.137	-.188	-.099	.102	16.4
1.5000	135	.254	.142	-.189	-.092	.100	13.9

TEST CONDITION 2, $z/R = -0.086$
 $\Omega R = 449 \text{ ft/sec}$, $\theta_{75} = 9.90 \text{ deg}$, $C_T = 0.0044$

x/R	ψ, deg	\bar{v}_R/v_o	\bar{v}_x/v_o	\bar{v}_y/v_o	\bar{v}_z/v_o	σ_{v_R}/v_o	$\sigma_\epsilon, \text{deg}$
0.3125	0	1.016	.534	.286	-.815	.254	28.6
0.3125	45	1.121	.555	.333	-.915	.226	28.3
0.3125	90	1.033	.643	.000	-.809	.198	25.4
0.3125	135	.968	.753	.111	-.599	.231	26.5
0.4000	0	1.350	.680	-.087	-1.162	.064	15.2
0.4000	45	1.379	.542	-.206	-1.233	.042	5.2
0.4000	90	1.266	.522	-.318	-1.108	.062	8.9
0.4000	135	1.438	.894	-.309	-1.084	.073	11.9
0.5000	0	1.446	.454	-.113	-1.369	.040	8.6
0.5000	45	1.479	.350	-.262	-1.413	.069	7.1
0.5000	90	1.440	.499	-.176	-1.339	.149	13.3
0.5000	135	1.494	.651	-.352	-1.297	.068	8.3
0.6000	0	1.536	.524	-.030	-1.444	.050	4.0
0.6000	45	1.627	.466	-.247	-1.539	.049	3.4
0.6000	90	1.651	.713	-.079	-1.487	.152	12.0
0.6000	135	1.628	.780	-.276	-1.402	.063	4.0

x/R	ψ, deg	\bar{v}_R/v_o	\bar{v}_x/v_o	\bar{v}_y/v_o	\bar{v}_z/v_o	σ_{v_R}/v_o	$\sigma_\epsilon, \text{deg}$
0.7000	0	1.533	.285	-.136	-1.500	.052	8.7
0.7000	45	1.791	.211	-.335	-1.747	.060	8.7
0.7000	90	1.743	.400	-.365	-1.657	.074	7.6
0.7000	135	1.646	.352	-.368	-1.565	.071	8.9
0.7500	0	1.532	.312	.103	-1.497	.050	5.0
0.7500	45	1.744	.312	-.105	-1.713	.049	4.6
0.7500	90	1.675	.388	-.069	-1.628	.079	6.7
0.7500	135	1.587	.370	-.133	-1.537	.054	4.6
0.8000	0	1.538	.098	.087	-1.532	.182	8.2
0.8000	45	1.843	.047	-.132	-1.838	.182	8.6
0.8000	90	1.787	.160	-.195	-1.769	.163	8.3
0.8000	135	1.648	.109	-.183	-1.634	.167	8.2
0.8125	0	1.537	.241	-.035	-1.517	.127	6.5
0.8125	45	1.824	.208	-.235	-1.796	.205	4.2
0.8125	90	1.787	.343	-.223	-1.739	.171	5.0
0.8125	135	1.650	.271	-.233	-1.610	.140	5.1
0.8250	0	1.840	-.146	.096	-1.832	.237	10.8
0.8250	45	2.153	-.351	-.241	-2.110	.329	10.1
0.8250	90	1.879	-.213	-.177	-1.859	.199	7.2
0.8250	135	1.692	-.211	-.163	-1.671	.140	9.0
0.8375	0	1.824	-.087	.014	-1.822	.089	8.0
0.8375	45	2.089	-.228	-.202	-2.066	.112	9.1
0.8375	90	1.855	-.156	-.300	-1.824	.094	7.0
0.8375	135	1.715	-.105	-.268	-1.691	.096	6.8
0.8500	0	1.447	.012	-.001	-1.447	.254	11.7
0.8500	45	3.245	.458	.811	-3.109	.584	27.0
0.8500	90	1.847	-1.250	-.081	-1.357	.304	26.0
0.8500	135	1.396	-.508	-.300	-1.265	.184	11.4
0.8625	0	1.907	-.006	-.105	-1.904	.256	4.7
0.8625	45	2.049	-.166	-.312	-2.018	.240	6.3
0.8625	90	1.828	.005	-.308	-1.801	.179	6.2
0.8625	135	1.728	.038	-.294	-1.702	.160	4.8
0.8750	0	1.835	.051	.019	-1.834	.282	9.8
0.8750	45	1.987	.134	-.287	-1.962	.114	9.9
0.8750	90	1.869	.139	-.313	-1.838	.086	9.3
0.8750	135	1.818	.166	-.277	-1.789	.100	6.6

x/R	ψ, deg	\bar{v}_R/v_o	\bar{v}_x/v_o	\bar{v}_y/v_o	\bar{v}_z/v_o	σ_{v_R}/v_o	$\sigma_\epsilon, \text{deg}$
0.8875	0	2.521	.490	.465	-2.429	1.518	30.1
0.8875	45	1.957	-1.341	-.253	-1.402	.446	25.6
0.8875	90	1.462	-.417	-.176	-1.390	.223	11.5
0.8875	135	1.439	-.051	-.155	-1.430	.184	8.7
0.9000	0	1.655	.363	.285	-1.589	.838	35.8
0.9000	45	1.884	-.785	.332	-1.680	1.469	41.6
0.9000	90	1.660	-.076	-.165	-1.650	.256	16.0
0.9000	135	1.626	.122	-.165	-1.613	.289	16.4
0.9500	0	.738	-.414	-.377	.480	.326	32.6
0.9500	45	.764	-.384	-.392	-.532	.252	23.9
0.9500	90	.870	.155	-.309	-.798	.249	21.6
0.9500	135	.980	.678	-.341	-.621	.393	27.0
1.0000	0	.493	-.366	-.329	.027	.098	22.0
1.0000	45	.514	-.007	-.406	-.316	.101	22.6
1.0000	90	.540	.285	-.380	-.257	.205	20.9
1.0000	135	.573	.287	-.487	.096	.185	19.4
1.1000	0	.478	-.166	-.448	.018	.065	12.9
1.1000	45	.527	-.048	-.522	.054	.058	12.2
1.1000	90	.517	-.118	-.501	.037	.064	13.3
1.1000	135	.511	-.172	-.481	.009	.071	11.2
1.2000	0	.441	-.075	-.434	.023	.101	16.0
1.2000	45	.477	-.051	-.472	.050	.086	15.8
1.2000	90	.462	-.082	-.453	.040	.091	14.5
1.2000	135	.426	-.123	-.408	.009	.083	16.3
1.3000	0	.482	.030	-.480	.032	.165	24.0
1.3000	45	.539	.064	-.531	.064	.180	22.5
1.3000	90	.511	.038	-.507	.047	.165	20.6
1.3000	135	.463	.028	-.462	.023	.152	21.2
1.4000	0	.650	.307	-.489	-.298	.113	11.1
1.4000	45	.664	.301	-.519	-.283	.125	11.3
1.4000	90	.661	.303	-.511	-.290	.119	10.9
1.4000	135	.621	.286	-.460	-.304	.109	11.4
1.5000	0	.499	.173	-.437	-.167	.210	30.8
1.5000	45	.589	.207	-.541	-.109	.233	28.0
1.5000	90	.599	.143	-.552	-.183	.266	25.0
1.5000	135	.524	.182	-.473	-.134	.324	23.7

TEST CONDITION 3, $z/R = -0.086$
 $\Omega R = 453 \text{ ft/sec}$, $\theta_{75} = 6.31 \text{ deg}$, $C_T = 0.0022$

x/R	ψ, deg	\bar{v}_R/v_0	\bar{v}_x/v_0	\bar{v}_y/v_0	\bar{v}_z/v_0	σ_{V_R/v_0}	$\sigma_\epsilon, \text{deg}$
0.3125	0	1.001	.195	.099	-.977	.095	12.0
0.3125	45	1.094	.111	-.194	-1.071	.048	4.7
0.3125	90	1.069	.060	-.254	-1.037	.046	4.8
0.3125	135	.997	.007	-.229	-.971	.064	5.5
0.4000	0	1.261	.157	-.005	-1.252	.041	2.9
0.4000	45	1.306	-.020	-.140	-1.299	.052	2.8
0.4000	90	1.238	-.079	-.182	-1.222	.046	3.5
0.4000	135	1.163	.002	.128	-1.156	.118	11.1
0.5000	0	1.422	-.310	-.175	-1.398	.116	18.0
0.5000	45	1.532	-.448	-.336	-1.426	.115	19.0
0.5000	90	1.378	-.409	-.327	-1.275	.205	7.2
0.5000	135	1.289	-.140	-.269	-1.253	.271	20.8
0.6000	0	1.576	-.296	.098	-1.545	.187	8.6
0.6000	45	1.708	-.361	-.118	-1.665	.180	6.9
0.6000	90	1.672	-.420	-.160	-1.611	.181	6.4
0.6000	135	1.586	-.225	-.172	-1.560	.175	11.0
0.7000	0	1.679	-.401	.008	-1.630	.035	3.3
0.7000	45	1.799	-.469	-.184	-1.726	.041	3.4
0.7000	90	1.747	-.492	-.196	-1.665	.033	3.0
0.7000	135	1.706	-.396	-.231	-1.643	.033	3.2
0.7500	0	1.773	-.427	.242	-1.704	.066	4.9
0.7500	45	1.855	-.467	.065	-1.795	.047	4.4
0.7500	90	1.820	-.483	.017	-1.754	.043	4.2
0.7500	135	1.862	-.521	.018	-1.788	.065	4.1
0.8000	0	1.925	-.362	.627	-1.784	.124	5.5
0.8000	45	1.924	-.372	.364	-1.853	.144	5.2
0.8000	90	1.826	-.264	.327	-1.776	.183	5.6
0.8000	135	2.136	-.459	.371	-2.053	.293	4.7
0.8125	0	2.086	-.461	.517	-1.968	.153	5.4
0.8125	45	1.959	-.508	.250	-1.875	.076	9.3
0.8125	90	1.866	-.154	.588	-1.765	.193	12.6
0.8125	135	2.459	-.622	.476	-2.331	.177	4.7
0.8250	0	2.053	-.418	.524	-1.941	.138	8.9
0.8250	45	2.034	-.359	.200	-1.993	.141	3.0
0.8250	90	2.346	.129	.436	-2.301	.370	16.8
0.8250	135	2.460	-1.070	.370	-2.183	.371	16.2

x/R	ψ, deg	\bar{v}_R/v_0	\bar{v}_x/v_0	\bar{v}_y/v_0	\bar{v}_z/v_0	σ_{v_R}/v_0	$\sigma_\epsilon, \text{deg}$
0.8375	0	1.917	-.590	.482	-1.759	.093	15.6
0.8375	45	1.918	-.243	.310	-1.877	.032	2.7
0.8375	90	3.529	-.239	.642	-3.462	.127	4.0
0.8375	135	2.094	-1.732	.694	-.950	.093	4.2
0.8500	0	1.747	-.955	.496	-1.376	.208	23.1
0.8500	45	1.757	-.185	.238	-1.731	.085	4.6
0.8500	90	3.567	.927	.085	-3.443	.512	7.3
0.8500	135	2.333	-2.152	.550	-.713	.224	7.6
0.8625	0	.718	.056	.706	.120	.410	33.5
0.8625	45	.525	.004	.504	-.149	.364	41.2
0.8625	90	.481	.035	.480	-.018	.308	40.7
0.8625	135	.389	-.056	.379	.065	.286	51.8
0.8750	0	.578	.012	.578	.019	.484	34.4
0.8750	45	.345	.046	.341	-.001	.538	43.9
0.8750	90	.258	-.003	.249	.071	.537	42.3
0.8750	135	.270	.005	.242	.119	.545	50.7
0.8875	0	.968	-.528	.809	-.054	.166	15.3
0.8875	45	.645	-.039	.459	-.452	.167	23.6
0.8875	90	.545	-.152	.497	.165	.173	29.8
0.8875	135	.708	-.437	.551	-.080	.081	20.6
0.9000	0	.670	-.325	.571	-.131	.088	14.2
0.9000	45	.410	.023	.286	-.292	.116	27.0
0.9000	90	.387	-.223	.309	-.065	.129	33.0
0.9000	135	.531	-.297	.399	-.186	.120	20.7
0.9500	0	.676	-.125	.535	.393	.098	9.6
0.9500	45	.435	.006	.354	.253	.068	14.2
0.9500	90	.504	-.053	.359	.350	.088	10.4
0.9500	135	.570	-.131	.355	.425	.087	11.5
1.0000	0	.618	-.231	.465	.334	.098	12.3
1.0000	45	.481	-.084	.321	.349	.091	14.1
1.0000	90	.516	-.166	.324	.365	.098	11.3
1.0000	135	.557	-.267	.348	.343	.117	18.5
1.1000	0	.793	-.361	.599	.374	.038	6.8
1.1000	45	.748	-.281	.521	.457	.042	5.9
1.1000	90	.757	-.334	.546	.403	.042	6.9
1.1000	135	.773	-.414	.572	.314	.043	7.6

x/R	ψ , deg	\bar{v}_R/v_0	\bar{v}_x/v_0	\bar{v}_y/v_0	\bar{v}_z/v_0	σ_{v_R}/v_0	σ_ϵ , deg
1.2000	0	.729	-.427	.550	.216	.027	9.2
1.2000	45	.717	-.385	.543	.265	.038	7.9
1.2000	90	.721	-.438	.535	.205	.031	8.3
1.2000	135	.736	-.439	.551	.214	.031	8.7
1.3000	0	.648	-.580	.271	.104	.063	8.7
1.3000	45	.626	-.559	.256	.118	.070	8.6
1.3000	90	.652	-.580	.278	.109	.074	9.1
1.3000	135	.668	-.596	.286	.099	.070	8.2
1.4000	0	.581	-.570	.099	-.053	.047	5.3
1.4000	45	.562	-.560	-.013	-.043	.052	4.9
1.4000	90	.571	-.569	-.029	-.046	.049	3.7
1.4000	135	.580	-.561	.135	-.064	.048	6.3
1.5000	0	.560	-.513	.210	.079	.076	10.9
1.5000	45	.534	-.527	.060	.068	.073	7.8
1.5000	90	.525	-.525	.005	.004	.082	7.6
1.5000	135	.528	-.528	.012	.009	.082	8.3

TEST CONDITION 1, $z/R = -0.15$
 $\Omega R = 624$ ft/sec, $\theta_{75} = 5.95$ deg, $C_T = 0.0015$

x/R	ψ , deg	\bar{v}_R/v_0	\bar{v}_x/v_0	\bar{v}_y/v_0	\bar{v}_z/v_0	σ_{v_R}/v_0	σ_ϵ , deg
0.3125	0	.963	.056	.009	-.961	.335	8.7
0.3125	45	.913	-.035	-.035	-.912	.305	3.8
0.3125	90	.935	.028	.100	-.929	.330	9.5
0.3125	135	.903	.005	.010	-.903	.281	3.8
0.4000	0	.961	-.145	-.019	-.950	.458	22.9
0.4000	45	1.015	-.178	-.037	-.998	.429	29.8
0.4000	90	.911	-.075	.121	-.900	.498	21.7
0.4000	135	1.015	-.174	-.056	-.998	.482	29.2
0.5000	0	1.028	-.246	-.006	-.998	.575	38.4
0.5000	45	.990	-.212	.018	-.966	.585	39.5
0.5000	90	.958	-.251	-.054	-.923	.582	37.7
0.5000	135	.982	-.288	-.012	-.939	.567	36.6
0.6000	0	1.489	-.188	.042	-1.476	.394	4.8
0.6000	45	1.465	-.185	.134	-1.447	.447	8.6
0.6000	90	1.449	-.224	.016	-1.432	.439	3.3
0.6000	135	1.481	-.187	.076	-1.468	.466	4.3

x/R	ψ, deg	\bar{v}_R/v_0	\bar{v}_x/v_0	\bar{v}_y/v_0	\bar{v}_z/v_0	σ_{v_R}/v_0	$\sigma_\epsilon, \text{deg}$
0.7000	0	1.492	-.257	.188	-1.458	.433	10.0
0.7000	45	1.471	-.238	.207	-1.436	.463	8.9
0.7000	90	1.444	-.223	.081	-1.424	.438	4.9
0.7000	135	1.482	-.271	.166	-1.447	.475	6.7
0.7500	0	1.583	-.421	.033	-1.526	.399	6.7
0.7500	45	1.591	-.422	.249	-1.513	.494	13.9
0.7500	90	1.526	-.417	.001	-1.467	.439	7.9
0.7500	135	1.570	-.423	.009	-1.512	.458	6.6
0.8000	0	1.576	-.308	.034	-1.545	.331	6.2
0.8000	45	1.597	-.282	.061	-1.571	.318	10.9
0.8000	90	1.567	-.337	.003	-1.530	.417	10.9
0.8000	135	1.595	-.295	.048	-1.567	.551	8.1
0.8125	0	1.599	-.319	-.008	-1.566	.288	6.1
0.8125	45	1.609	-.295	.136	-1.575	.315	13.8
0.8125	90	1.542	-.366	.019	-1.497	.417	15.1
0.8125	135	1.605	-.326	.020	-1.571	.597	13.4
0.8250	0	1.609	-.322	-.040	-1.576	.354	11.1
0.8250	45	1.712	-.382	-.105	-1.666	.315	14.5
0.8250	90	1.549	-.391	-.009	-1.499	.562	21.3
0.8250	135	1.673	-.291	-.057	-1.647	.736	15.5
0.8375	0	1.305	-.268	.270	-1.249	.482	23.6
0.8375	45	1.806	-.362	.165	-1.761	.416	19.7
0.8375	90	1.431	-.545	.266	-1.296	.823	31.4
0.8375	135	1.384	-.400	.289	-1.293	.652	26.8
0.8500	0	1.057	-.043	.170	-1.042	.581	37.0
0.8500	45	1.420	-.228	.594	-1.270	1.186	43.0
0.8500	90	1.262	-.289	.189	-1.214	.777	40.9
0.8500	135	1.307	-.349	.263	-1.232	.866	34.6
0.8625	0	1.510	.192	.468	-1.423	1.234	43.6
0.8625	45	1.179	-.426	.354	-1.041	1.038	52.3
0.8625	90	1.878	-.397	.539	-1.755	1.685	33.5
0.8625	135	.932	-.360	.269	-.816	.765	43.9
0.8750	0	.429	.286	.270	-.172	.943	67.7
0.8750	45	.373	-.092	.195	-.304	.933	66.9
0.8750	90	.689	-.392	.255	.506	1.083	59.7
0.8750	135	.551	-.491	.145	-.205	.405	50.4

x/R	ψ, deg	\bar{v}_R/v_0	\bar{v}_x/v_0	\bar{v}_y/v_0	\bar{v}_z/v_0	σ_{V_R}/v_0	$\sigma_\epsilon, \text{deg}$
0.9000	0	.264	.075	.247	-.054	.376	55.8
0.9000	45	.209	.013	.208	.005	.394	59.6
0.9000	90	.246	-.068	.223	-.079	.378	58.3
0.9000	135	.299	-.166	.247	-.033	.246	47.6
1.0000	0	.196	-.162	.055	.096	.078	10.7
1.0000	45	.193	-.171	.036	.081	.066	13.6
1.0000	90	.223	-.198	.052	.089	.073	10.1
1.0000	135	.208	-.184	.048	.084	.073	10.2
1.1000	0	.198	-.184	.042	.060	.075	6.2
1.1000	45	.203	-.193	.035	.050	.071	6.3
1.1000	90	.211	-.202	.035	.049	.069	6.7
1.1000	135	.203	-.193	.037	.053	.076	5.4
1.2000	0	.179	-.176	.018	.025	.062	3.7
1.2000	45	.184	-.180	.020	.029	.063	4.3
1.2000	90	.192	-.189	.020	.028	.065	3.3
1.2000	135	.187	-.184	.019	.027	.065	4.6
1.3000	0	.156	-.155	.011	.015	.049	4.8
1.3000	45	.155	-.154	.013	.019	.051	6.0
1.3000	90	.167	-.166	.010	.014	.054	3.9
1.3000	135	.164	-.163	.010	.014	.060	4.4
1.4000	0	.134	-.133	.009	.013	.038	9.0
1.4000	45	.132	-.131	.008	.012	.038	17.0
1.4000	90	.136	-.135	.009	.013	.040	11.7
1.4000	135	.145	-.143	.014	.019	.054	8.4
1.5000	0	.125	-.111	.050	.029	.044	13.8
1.5000	45	.120	-.112	.029	.032	.043	11.7
1.5000	90	.121	-.113	.034	.028	.038	10.3
1.5000	135	.121	-.113	.025	.033	.044	14.5

TEST CONDITION 2, $z/R = -0.15$

$\Omega R = 445 \text{ ft/sec}$, $\theta_{75} = 9.59 \text{ deg}$, $C_T = 0.0038$

x/R	ψ, deg	\bar{v}_R/v_0	\bar{v}_x/v_0	\bar{v}_y/v_0	\bar{v}_z/v_0	σ_{V_R}/v_0	$\sigma_\epsilon, \text{deg}$
0.3125	0	1.106	-.372	-.049	-1.041	.057	5.0
0.3125	45	1.192	-.077	.064	-1.188	.097	6.8
0.3125	90	1.212	-.073	-.143	-1.201	.050	3.9
0.3125	135	1.139	-.184	-.138	-1.115	.055	4.2

x/R	ψ, deg	\bar{v}_R/v_o	\bar{v}_x/v_o	\bar{v}_y/v_o	\bar{v}_z/v_o	σ_{v_R}/v_o	$\sigma_\epsilon, \text{deg}$
0.4000	0	1.371	-.218	.293	-1.322	.082	8.1
0.4000	45	1.451	-.134	-.025	-1.445	.027	2.6
0.4000	90	1.392	-.229	-.091	-1.370	.027	2.8
0.4000	135	1.317	-.345	-.142	-1.263	.025	2.7
0.5000	0	1.514	-.209	.042	-1.499	.017	2.7
0.5000	45	1.590	-.328	-.066	-1.555	.040	2.7
0.5000	90	1.553	-.359	-.108	-1.507	.030	2.6
0.5000	135	1.531	-.406	-.117	-1.471	.024	2.7
0.6000	0	1.472	-.289	.019	-1.443	.245	4.9
0.6000	45	1.556	-.357	-.058	-1.513	.279	4.6
0.6000	90	1.528	-.387	-.060	-1.476	.276	5.9
0.6000	135	1.513	-.388	-.050	-1.462	.286	5.3
0.7000	0	1.706	-.387	.009	-1.661	.051	2.7
0.7000	45	1.872	-.465	-.106	-1.810	.034	2.6
0.7000	90	1.805	-.480	-.127	-1.735	.025	2.6
0.7000	135	1.778	-.436	-.080	-1.722	.038	2.8
0.7500	0	1.903	-.268	.037	-1.884	.066	2.6
0.7500	45	2.103	-.526	-.154	-2.031	.062	2.6
0.7500	90	1.895	-.553	-.160	-1.806	.057	3.8
0.7500	135	2.030	-.158	.145	-2.019	.205	6.8
0.7750	0	2.147	-.232	.054	-2.134	.183	4.1
0.7750	45	2.148	-.696	-.186	-2.024	.135	5.2
0.7750	90	1.824	-.579	-.187	-1.720	.180	4.8
0.7750	135	2.335	.231	.109	-2.321	.354	9.3
0.7875	0	2.467	-.234	.117	-2.453	.164	5.2
0.7875	45	2.241	-.783	-.140	-2.095	.228	8.9
0.7875	90	1.793	-.643	-.184	-1.664	.195	11.3
0.7875	135	2.539	.530	-.104	-2.481	.231	9.6
0.8000	0	3.089	-.276	.133	-3.074	.220	4.5
0.8000	45	2.151	-1.058	-.220	-1.860	.151	9.3
0.8000	90	1.670	-.432	-.181	-1.604	.089	8.1
0.8000	135	2.740	1.349	.001	-2.385	.214	6.6
0.8125	0	2.741	-1.210	-.347	-2.435	2.694	48.6
0.8125	45	1.935	-1.741	-.672	-.513	2.293	40.9
0.8125	90	1.276	-1.032	-.636	-.400	2.492	50.1
0.8125	135	.602	-.134	-.586	-.035	3.000	71.4

x/R	ψ, deg	\bar{V}_R/v_o	\bar{v}_x/v_o	\bar{v}_y/v_o	\bar{v}_z/v_o	σ_{V_R}/v_o	$\sigma_\epsilon, \text{deg}$
0.8250	0	3.061	2.425	1.426	1.207	2.470	51.8
0.8250	45	1.751	-1.631	-.341	-.538	.478	18.0
0.8250	90	.966	-.332	-.216	-.881	.296	24.3
0.8250	135	.932	.901	-.145	.187	.305	36.9
0.8375	0	1.185	.741	.224	.897	1.461	56.8
0.8375	45	1.055	-.997	-.311	-.156	.565	39.1
0.8375	90	.750	-.270	-.339	-.612	.433	33.6
0.8375	135	.550	.509	-.139	.156	.524	53.1
0.8500	0	1.391	.125	.066	1.383	.159	15.0
0.8500	45	.902	-.823	-.367	.017	.242	30.1
0.8500	90	.520	-.161	-.385	-.310	.266	36.6
0.8500	135	.479	.110	-.441	.150	.260	42.6
0.8625	0	.711	-.142	-.216	.663	.288	41.5
0.8625	45	.586	-.483	-.330	-.039	.160	28.9
0.8625	90	.327	-.115	-.286	-.110	.119	32.4
0.8625	135	.422	-.153	-.323	.224	.159	28.2
0.8750	0	.424	-.148	-.179	.355	.184	41.4
0.8750	45	.366	-.252	-.266	-.001	.137	31.6
0.8750	90	.298	-.094	-.274	-.071	.166	34.6
0.8750	135	.383	-.172	-.300	.164	.111	28.8
0.9000	0	.377	-.149	-.270	.216	.073	25.8
0.9000	45	.382	-.175	-.335	.055	.056	16.2
0.9000	90	.402	-.155	-.361	.084	.065	17.8
0.9000	135	.476	-.220	-.348	.239	.081	9.8
1.0000	0	.341	-.176	-.184	.226	.012	5.2
1.0000	45	.328	-.130	-.297	.050	.014	3.2
1.0000	90	.374	-.131	-.316	.153	.017	7.2
1.0000	135	.402	-.207	-.271	.214	.017	3.6
1.1000	0	.327	-.204	-.163	.196	.046	16.0
1.1000	45	.308	-.142	-.214	.171	.050	15.5
1.1000	90	.331	-.176	-.202	.194	.053	16.8
1.1000	135	.354	-.219	-.190	.203	.050	14.9
1.2000	0	.355	-.249	-.237	.089	.017	7.1
1.2000	45	.343	-.209	-.254	.100	.017	8.6
1.2000	90	.359	-.228	-.261	.094	.023	7.8
1.2000	135	.364	-.251	-.249	.085	.020	5.8

x/R	ψ, deg	\bar{v}_R/v_o	\bar{v}_x/v_o	\bar{v}_y/v_o	\bar{v}_z/v_o	σ_{v_R}/v_o	$\sigma_\epsilon, \text{deg}$
1.3000	0	.326	-.220	-.235	.053	.039	4.9
1.3000	45	.333	-.188	-.270	.047	.042	6.8
1.3000	90	.337	-.205	-.264	.045	.041	5.5
1.3000	135	.331	-.222	-.241	.048	.040	4.8
1.4000	0	.324	-.192	-.260	-.020	.025	8.0
1.4000	45	.319	-.187	-.258	-.010	.029	8.0
1.4000	90	.325	-.196	-.259	-.014	.028	7.9
1.4000	135	.321	-.200	-.250	-.017	.027	7.9
1.5000	0	.247	-.164	-.162	.088	.060	22.6
1.5000	45	.240	-.155	-.158	.093	.064	26.1
1.5000	90	.253	-.173	-.164	.085	.070	22.1
1.5000	135	.245	-.173	-.151	.086	.074	23.4

TEST CONDITION 3, $z/R = -0.15$

$\Omega R = 458 \text{ ft/sec}$, $\Theta_{75} = 6.04 \text{ deg}$, $C_T = 0.0015$

x/R	ψ, deg	\bar{v}_R/v_o	\bar{v}_x/v_o	\bar{v}_y/v_o	\bar{v}_z/v_o	σ_{v_R}/v_o	$\sigma_\epsilon, \text{deg}$
0.3125	0	1.313	-.196	-.354	-1.249	.039	2.9
0.3125	45	1.355	-.336	-.408	-1.247	.046	2.9
0.3125	90	1.283	-.389	-.481	-1.124	.031	5.5
0.3125	135	1.203	-.136	-.097	-1.192	.089	9.2
0.4000	0	1.599	-.364	-.409	-1.502	.070	3.6
0.4000	45	1.668	-.604	-.244	-1.535	.138	9.2
0.4000	90	1.698	-.231	-.399	-1.634	.066	3.2
0.4000	135	1.560	-.301	-.302	-1.501	.087	3.1
0.5000	0	1.865	-.466	-.333	-1.775	.032	2.6
0.5000	45	1.902	-.454	-.159	-1.840	.120	5.8
0.5000	90	1.862	-.561	-.358	-1.739	.045	2.6
0.5000	135	1.798	-.581	-.337	-1.667	.078	2.7
0.6000	0	1.886	-.521	-.326	-1.783	.035	3.0
0.6000	45	1.824	-.510	.115	-1.747	.140	10.7
0.6000	90	1.942	-.663	-.397	-1.781	.040	2.6
0.6000	135	1.933	-.640	-.392	-1.781	.053	2.7
0.7000	0	1.971	-.616	-.328	-1.843	.037	2.6
0.7000	45	2.107	-.575	-.309	-2.003	.059	5.2
0.7000	90	2.056	-.681	-.443	-1.888	.047	2.7
0.7000	135	1.998	-.683	-.432	-1.827	.043	2.7

x/R	ψ, deg	\bar{v}_R/v_0	\bar{v}_x/v_0	\bar{v}_y/v_0	\bar{v}_z/v_0	σ_{v_R}/v_0	$\sigma_\epsilon, \text{deg}$
0.7125	0	1.919	-.601	-.327	-1.793	.216	3.0
0.7125	45	1.992	-.579	.058	-1.905	.251	7.8
0.7125	90	1.959	-.699	-.361	-1.794	.206	3.1
0.7125	135	1.908	-.666	-.375	-1.748	.219	3.3
0.7250	0	2.112	-.521	-.067	-2.046	.178	10.7
0.7250	45	2.175	-.645	.091	-2.075	.142	10.3
0.7250	90	2.067	-.648	-.246	-1.947	.080	7.5
0.7250	135	1.973	-.669	-.226	-1.843	.067	6.3
0.7375	0	1.989	-.599	-.339	-1.866	.045	2.6
0.7375	45	1.996	-.498	.053	-1.932	.165	8.4
0.7375	90	2.029	-.706	-.405	-1.858	.053	2.9
0.7375	135	2.003	-.672	-.406	-1.842	.044	2.8
0.7500	0	1.970	-.584	-.318	-1.854	.237	3.0
0.7500	45	1.918	-.588	.148	-1.820	.234	10.1
0.7500	90	1.978	-.692	-.363	-1.817	.218	4.3
0.7500	135	1.939	-.654	-.366	-1.788	.205	3.1
0.7625	0	1.928	-.641	-.245	-1.802	.208	5.3
0.7625	45	1.820	-.549	-.117	-1.732	.254	10.2
0.7625	90	1.928	-.659	-.192	-1.801	.252	6.6
0.7625	135	1.912	-.641	-.259	-1.782	.207	5.1
0.7750	0	2.107	-.521	.394	-2.003	.436	22.8
0.7750	45	1.989	-.621	.038	-1.890	.286	17.8
0.7750	90	1.925	-.834	-.329	-1.704	.207	16.4
0.7750	135	1.889	-.671	-.413	-1.717	.252	17.8
0.7875	0	2.026	-.660	.014	-1.915	.164	10.3
0.7875	45	1.816	-.613	.117	-1.705	.205	13.9
0.7875	90	1.890	-.539	.104	-1.808	.124	9.3
0.7875	135	1.983	-.578	-.008	-1.897	.117	6.4
0.8000	0	1.832	-.890	.253	-1.581	.305	21.6
0.8000	45	1.619	-.724	-.075	-1.446	.293	18.9
0.8000	90	1.656	-.496	-.085	-1.578	.259	11.8
0.8000	135	1.823	-.618	-.172	-1.706	.236	7.7
0.8250	0	1.510	-1.233	.232	-.840	.330	26.8
0.8250	45	1.304	-.546	.002	-1.184	.374	23.8
0.8250	90	1.361	-.139	.029	-1.354	.319	16.5
0.8250	135	1.894	-.424	-.247	-1.829	.552	18.2

x/R	ψ, deg	\bar{v}_R/v_o	\bar{v}_x/v_o	\bar{v}_y/v_o	\bar{v}_z/v_o	σ_{v_R}/v_o	$\sigma_\epsilon, \text{deg}$
0.8500	0	.677	-.528	-.001	-.424	.240	32.9
0.8500	45	1.012	.120	-.022	-1.005	.535	34.5
0.8500	90	.834	.466	-.143	-.677	.468	36.1
0.8500	135	.745	-.522	-.438	-.300	.573	49.1
0.9000	0	.299	-.126	-.267	-.047	.153	27.7
0.9000	45	.326	.041	-.323	-.019	.283	32.6
0.9000	90	.430	-.071	-.421	.051	.301	33.2
0.9000	135	.436	-.149	-.405	.064	.184	27.9
1.0000	0	.278	-.143	-.168	.169	.032	16.3
1.0000	45	.276	-.087	-.243	.098	.048	12.4
1.0000	90	.298	-.119	-.236	.137	.042	15.0
1.0000	135	.323	-.151	-.218	.184	.039	14.6
1.1000	0	.280	-.166	-.188	.124	.012	7.0
1.1000	45	.280	-.135	-.211	.125	.016	8.9
1.1000	90	.288	-.154	-.210	.123	.017	9.3
1.1000	135	.301	-.187	-.201	.124	.015	6.9
1.2000	0	.263	-.180	-.181	.061	.010	6.2
1.2000	45	.269	-.171	-.197	.064	.015	7.2
1.2000	90	.261	-.173	-.188	.056	.014	7.4
1.2000	135	.272	-.196	-.181	.055	.016	4.9
1.3000	0	.322	-.205	-.248	.018	.424	11.3
1.3000	45	.334	-.213	-.257	.024	.447	11.8
1.3000	90	.343	-.224	-.259	.018	.506	12.3
1.3000	135	.351	-.240	-.255	.024	.586	13.3
1.4000	0	.223	-.146	-.168	-.018	.015	8.5
1.4000	45	.234	-.151	-.178	-.015	.016	7.9
1.4000	90	.226	-.143	-.174	-.020	.012	8.3
1.4000	135	.223	-.151	-.163	-.022	.016	9.2
1.5000	0	.214	-.134	-.159	-.052	.015	4.1
1.5000	45	.229	-.143	-.170	-.055	.012	3.7
1.5000	90	.213	-.133	-.158	-.051	.015	3.6
1.5000	135	.204	-.132	-.144	-.059	.014	4.0

TEST CONDITION 1, $z/R = -0.20$
 $\Omega R = 628 \text{ ft/sec}$, $\theta_{75} = 6.04 \text{ deg}$, $C_T = 0.0017$

x/R	ψ, deg	\bar{V}_R/v_o	\bar{V}_x/v_o	\bar{V}_y/v_o	\bar{V}_z/v_o	σ_{V_R}/v_o	$\sigma_\epsilon, \text{deg}$
0.3125	0	.969	-.017	-.172	-.954	.287	11.7
0.3125	45	.960	.059	-.035	-.958	.327	15.7
0.3125	90	.950	.043	-.117	-.941	.308	12.9
0.3125	135	.905	-.003	-.186	-.886	.267	11.8
0.4000	0	1.189	.019	-.103	-1.184	.285	4.5
0.4000	45	1.160	-.057	-.178	-1.145	.298	4.2
0.4000	90	1.115	-.056	-.087	-1.110	.320	8.6
0.4000	135	1.154	-.014	-.108	-1.149	.283	6.1
0.5000	0	1.356	-.124	-.160	-1.340	.280	5.5
0.5000	45	1.348	-.131	-.184	-1.329	.332	6.2
0.5000	90	1.319	-.053	-.136	-1.311	.324	8.7
0.5000	135	1.322	-.094	-.163	-1.309	.314	3.6
0.6000	0	1.434	-.224	-.089	-1.414	.262	4.7
0.6000	45	1.437	-.228	-.088	-1.416	.285	5.5
0.6000	90	1.396	-.239	-.035	-1.374	.258	7.3
0.6000	135	1.418	-.236	-.103	-1.394	.302	3.6
0.7000	0	1.482	-.293	-.039	-1.452	.281	5.8
0.7000	45	1.487	-.273	-.074	-1.459	.302	7.0
0.7000	90	1.464	-.238	-.136	-1.438	.278	4.6
0.7000	135	1.463	-.244	-.113	-1.438	.293	5.0
0.7500	0	1.556	-.291	.050	-1.528	.334	7.7
0.7500	45	1.550	-.326	-.119	-1.511	.312	4.7
0.7500	90	1.511	-.323	-.085	-1.474	.278	6.8
0.7500	135	1.532	-.318	-.098	-1.495	.286	4.9
0.7750	0	1.565	-.372	-.010	-1.520	.355	5.1
0.7750	45	1.489	-.332	.082	-1.449	.316	14.0
0.7750	90	1.566	-.300	-.004	-1.537	.267	5.4
0.7750	135	1.568	-.298	.011	-1.540	.254	4.6
0.7875	0	1.578	-.389	-.094	-1.526	.371	6.6
0.7875	45	1.531	-.292	-.091	-1.500	.284	9.7
0.7875	90	1.522	-.270	-.082	-1.495	.276	8.8
0.7875	135	1.571	-.318	-.107	-1.535	.265	6.7
0.8000	0	1.611	-.427	-.049	-1.552	.525	17.0
0.8000	45	1.428	-.353	-.037	-1.383	.406	10.8
0.8000	90	1.445	-.251	-.125	-1.418	.284	9.3
0.8000	135	1.601	-.307	-.056	-1.570	.258	8.0

x/R	ψ, deg	\bar{v}_R/v_o	\bar{v}_x/v_o	\bar{v}_y/v_o	\bar{v}_z/v_o	σ_{v_R}/v_o	$\sigma_\epsilon, \text{deg}$
0.8125	0	1.569	-.612	.062	-1.444	.621	21.0
0.8125	45	1.353	-.455	-.040	-1.273	.419	25.0
0.8125	90	1.361	-.152	.003	-1.353	.315	16.8
0.8125	135	1.580	-.400	.011	-1.528	.270	16.3
0.8250	0	1.365	-.562	.150	-1.236	.440	25.3
0.8250	45	1.295	-.088	.140	-1.285	.327	16.5
0.8250	90	1.553	-.096	.141	-1.544	.282	12.6
0.8250	135	1.586	-.507	.037	-1.502	.338	23.6
0.8375	0	.636	-.519	-.211	-.302	1.039	51.1
0.8375	45	.802	-.128	-.043	-.791	.481	39.1
0.8375	90	.818	.408	-.079	-.704	.636	43.3
0.8375	135	.523	-.115	.035	-.509	.907	64.8
0.8500	0	.610	-.381	-.104	-.465	.375	40.7
0.8500	45	.763	.015	.103	-.756	.437	37.2
0.8500	90	.793	.444	.108	-.648	.616	48.8
0.8500	135	.479	-.151	-.066	-.450	.629	64.5
0.8625	0	.253	-.090	.039	-.233	.271	50.8
0.8625	45	.405	.003	.094	-.394	.398	49.6
0.8625	90	.255	.000	.081	-.242	.408	52.1
0.8625	135	.228	-.064	.062	-.210	.249	59.3
0.8750	0	.213	-.066	-.177	-.097	.323	59.4
0.8750	45	.236	-.006	-.162	-.171	.362	58.9
0.8750	90	.248	.014	-.215	-.123	.344	54.1
0.8750	135	.265	-.027	-.222	-.141	.313	55.2
0.9000	0	.187	-.055	-.175	-.039	.166	52.0
0.9000	45	.229	-.034	-.224	-.039	.202	46.9
0.9000	90	.227	-.037	-.224	-.009	.204	51.1
0.9000	135	.246	-.042	-.243	-.011	.186	43.6
0.9500	0	.331	-.016	-.296	.147	.105	17.2
0.9500	45	.350	.012	-.312	.158	.108	13.7
0.9500	90	.352	-.022	-.311	.164	.101	13.8
0.9500	135	.332	-.026	-.300	.140	.093	12.7
1.000	0	.372	-.112	-.340	.102	.098	4.6
1.000	45	.380	-.117	-.347	.101	.098	4.9
1.000	90	.388	-.130	-.354	.091	.101	4.4
1.000	135	.376	-.123	-.343	.091	.096	4.2

x/R	ψ , deg	\bar{v}_R/v_o	\bar{v}_x/v_o	\bar{v}_y/v_o	\bar{v}_z/v_o	σ_{v_R}/v_o	σ_ϵ , deg
1.1000	0	.323	-.101	-.290	.100	.084	5.1
1.1000	45	.324	-.093	-.294	.101	.085	3.4
1.1000	90	.326	-.106	-.284	.119	.085	6.3
1.1000	135	.323	-.102	-.284	.114	.083	6.2
1.2000	0	.324	-.123	-.294	.058	.083	3.3
1.2000	45	.326	-.126	-.296	.054	.083	3.3
1.2000	90	.328	-.122	-.298	.062	.086	3.3
1.2000	135	.327	-.121	-.298	.062	.082	3.4
1.3000	0	.329	-.148	-.292	.025	.088	2.9
1.3000	45	.337	-.151	-.300	.027	.088	2.9
1.3000	90	.332	-.151	-.295	.023	.088	2.8
1.3000	135	.328	-.148	-.291	.024	.080	2.9
1.4000	0	.332	-.140	-.289	.083	.211	17.5
1.4000	45	.336	-.138	-.293	.090	.227	17.6
1.4000	90	.344	-.144	-.299	.091	.240	17.7
1.4000	135	.343	-.140	-.298	.098	.260	18.1

TEST CONDITION 2, $z/R = -0.20$

$\Omega R = 449$ ft/sec, $\theta_{75} = 9.79$ deg, $C_T = 0.0042$

x/R	ψ , deg	\bar{v}_R/v_o	\bar{v}_x/v_o	\bar{v}_y/v_o	\bar{v}_z/v_o	σ_{v_R}/v_o	σ_ϵ , deg
0.3125	0	1.110	-.065	-.212	-1.088	.118	4.0
0.3125	45	1.124	-.238	-.296	-1.057	.107	3.0
0.3125	90	1.020	-.095	-.218	-.992	.123	9.5
0.3125	135	1.117	.162	-.207	-1.086	.111	7.5
0.4000	0	1.281	-.192	-.180	-1.254	.119	3.2
0.4000	45	1.303	-.014	-.054	-1.302	.139	6.3
0.4000	90	1.351	.019	-.213	-1.334	.105	3.3
0.4000	135	1.302	-.046	-.214	-1.284	.113	2.9
0.5000	0	1.423	-.194	-.125	-1.404	.029	3.1
0.5000	45	1.549	-.045	-.198	-1.535	.030	2.7
0.5000	90	1.492	-.094	-.215	-1.474	.034	2.6
0.5000	135	1.414	-.149	-.198	-1.393	.037	2.6
0.6000	0	1.479	-.186	.047	-1.466	.102	5.7
0.6000	45	1.647	-.145	-.199	-1.628	.122	3.4
0.6000	90	1.608	-.186	-.220	-1.582	.099	2.6
0.6000	135	1.548	-.227	-.196	-1.519	.105	2.8

x/R	ψ, deg	\bar{v}_R/v_o	\bar{v}_x/v_o	\bar{v}_y/v_o	\bar{v}_z/v_o	σ_{VR}/v_o	$\sigma_\epsilon, \text{deg}$
0.7000	0	1.583	-.142	.183	-1.566	.143	7.0
0.7000	45	1.786	-.149	-.231	-1.765	.119	2.7
0.7000	90	1.774	-.214	-.242	-1.745	.135	3.1
0.7000	135	1.724	-.250	-.233	-1.690	.124	3.5
0.7500	0	1.659	-.117	.023	-1.655	.112	5.0
0.7500	45	1.909	-.195	-.182	-1.890	.039	3.2
0.7500	90	1.889	-.238	-.195	-1.864	.045	2.7
0.7500	135	1.808	-.293	-.168	-1.776	.077	4.2
0.8000	0	2.085	.106	.022	-2.082	.127	6.3
0.8000	45	2.233	-.384	-.196	-2.191	.079	4.9
0.8000	90	1.836	-.257	-.195	-1.808	.097	3.5
0.8000	135	2.291	.261	.054	-2.276	.131	6.6
0.8125	0	2.179	.441	-.077	-2.132	.228	5.5
0.8125	45	2.572	-.584	-.303	-2.486	.129	7.7
0.8125	90	1.762	-.387	-.321	-1.689	.157	12.5
0.8125	135	1.916	.454	-.072	-1.860	.217	10.3
0.8250	0	2.168	.487	.047	-2.112	.294	4.8
0.8250	45	2.673	-.571	-.225	-2.602	.219	11.1
0.8250	90	1.717	-.386	-.290	-1.647	.161	10.5
0.8250	135	1.712	.787	-.052	-1.519	.317	13.3
0.8375	0	2.029	.935	.081	-1.799	.435	14.5
0.8375	45	2.966	-1.185	-.091	-2.718	.718	21.7
0.8375	90	1.540	-.494	-.414	-1.399	.308	17.7
0.8375	135	1.130	.615	-.257	-.913	.315	22.9
0.8500	0	1.768	1.535	.156	-.865	.371	22.7
0.8500	45	3.059	-2.929	-.017	-.884	1.044	20.4
0.8500	90	1.201	-.452	-.524	-.982	.224	17.4
0.8500	135	.834	.500	-.297	-.599	.440	39.1
0.8625	0	2.149	1.785	.355	-1.143	.248	11.1
0.8625	45	3.118	-2.657	-.014	-1.632	.784	15.7
0.8625	90	1.266	-.487	-.481	-1.065	.172	17.3
0.8625	135	.802	.477	-.542	-.350	.220	30.0
0.8750	0	.987	.949	-.102	.250	.259	29.8
0.8750	45	1.154	-.800	-.658	.508	.212	25.0
0.8750	90	.722	-.380	-.504	-.352	.303	33.9
0.8750	135	.553	.045	-.534	-.139	.434	37.9

x/R	ψ, deg	\bar{v}_R/v_o	\bar{v}_x/v_o	\bar{v}_y/v_o	\bar{v}_z/v_o	σ_{v_R}/v_o	$\sigma_\epsilon, \text{deg}$
0.8875	0	.463	.438	-.131	.074	.509	57.1
0.8875	45	.652	-.240	-.439	.418	.294	41.9
0.8875	90	.475	-.326	-.344	.030	.213	43.3
0.8875	135	.459	-.149	-.426	.082	.247	40.1
0.9000	0	.451	.243	-.372	.079	.294	40.1
0.9000	45	.639	-.016	-.622	.147	.273	31.0
0.9000	90	.501	-.195	-.459	.054	.299	38.1
0.9000	135	.507	-.161	-.467	.112	.317	38.9
0.9500	0	.387	-.040	-.362	.131	.184	28.6
0.9500	45	.412	.005	-.399	.103	.149	35.4
0.9500	90	.481	-.048	-.453	.156	.129	27.3
0.9500	135	.506	-.122	-.451	.193	.151	27.9
1.0000	0	.393	-.124	-.345	.141	.045	10.0
1.0000	45	.422	-.084	-.390	.138	.047	14.6
1.0000	90	.442	-.136	-.397	.138	.058	12.9
1.0000	135	.467	-.161	-.409	.158	.061	10.0
1.1000	0	.337	-.123	-.286	.129	.037	14.4
1.1000	45	.350	-.068	-.315	.137	.044	13.6
1.1000	90	.357	-.098	-.316	.135	.052	14.3
1.1000	135	.355	-.135	-.306	.120	.044	14.6
1.2000	0	.313	-.120	-.264	.119	.063	16.9
1.2000	45	.331	-.115	-.295	.096	.071	16.3
1.2000	90	.335	-.123	-.294	.102	.053	15.9
1.2000	135	.325	-.132	-.267	.130	.058	20.0
1.3000	0	.409	-.193	-.333	.138	.213	26.0
1.3000	45	.410	-.143	-.326	.203	.257	24.7
1.3000	90	.417	-.168	-.332	.188	.292	24.5
1.3000	135	.468	-.254	-.371	.131	.322	21.2
1.4000	0	.287	-.117	-.241	.105	.040	13.1
1.4000	45	.295	-.101	-.256	.107	.038	13.7
1.4000	90	.287	-.104	-.247	.100	.040	13.8
1.4000	135	.285	-.113	-.242	.100	.043	14.2
1.5000	0	.333	-.129	-.302	.055	.030	5.9
1.5000	45	.339	-.120	-.309	.071	.027	5.6
1.5000	90	.319	-.118	-.291	.059	.024	5.7
1.5000	135	.317	-.123	-.287	.052	.030	5.2

TEST CONDITION 3, $z/R = -0.20$
 $\Omega R = 450 \text{ ft/sec}$, $\theta_{75} = 6.20 \text{ deg}$, $C_T = 0.0019$

x/R	ψ, deg	\bar{v}_R/v_o	\bar{v}_x/v_o	\bar{v}_y/v_o	\bar{v}_z/v_o	σ_{v_R}/v_o	σ_e, deg
0.3125	0	1.106	.027	-.404	-1.029	.167	8.9
0.3125	45	1.094	.086	-.395	-1.017	.160	14.8
0.3125	90	1.141	.050	-.433	-1.054	.182	10.7
0.3125	135	1.141	.081	-.522	-1.012	.216	9.7
0.4000	0	1.450	.035	-.279	-1.422	.076	4.5
0.4000	45	1.487	-.113	-.434	-1.418	.075	4.7
0.4000	90	1.345	-.179	-.417	-1.266	.081	7.0
0.4000	135	1.360	.079	-.101	-1.354	.122	6.8
0.5000	0	1.683	-.109	-.338	-1.645	.178	4.4
0.5000	45	1.739	-.228	-.364	-1.685	.186	3.1
0.5000	90	1.705	-.151	-.335	-1.665	.193	6.0
0.5000	135	1.694	-.187	-.340	-1.649	.180	3.7
0.6000	0	1.808	-.088	-.246	-1.789	.047	4.0
0.6000	45	1.866	-.101	-.280	-1.842	.048	3.7
0.6000	90	1.833	-.185	-.297	-1.799	.045	4.0
0.6000	135	1.788	-.202	-.310	-1.749	.044	3.9
0.7000	0	1.872	-.221	-.197	-1.849	.048	5.1
0.7000	45	1.906	-.258	-.248	-1.872	.070	4.7
0.7000	90	1.858	-.246	-.299	-1.817	.062	4.7
0.7000	135	1.823	-.283	-.279	-1.779	.047	4.2
0.7500	0	1.884	-.135	-.214	-1.867	.189	3.6
0.7500	45	1.907	-.105	.011	-1.904	.196	5.7
0.7500	90	1.880	-.107	-.275	-1.857	.173	3.5
0.7500	135	1.856	-.130	-.266	-1.833	.174	3.9
0.8000	0	1.873	-.149	-.217	-1.855	.173	5.5
0.8000	45	1.869	-.048	-.151	-1.863	.160	9.0
0.8000	90	1.928	-.092	-.237	-1.911	.167	5.5
0.8000	135	1.909	-.095	-.264	-1.888	.176	4.6
0.8250	0	1.848	-.117	-.219	-1.831	.174	5.5
0.8250	45	1.837	.008	-.075	-1.836	.173	6.0
0.8250	90	1.940	.018	-.199	-1.930	.193	4.6
0.8250	135	1.930	-.013	-.222	-1.917	.163	4.2
0.8375	0	1.850	-.289	-.261	-1.808	.057	5.2
0.8375	45	1.843	.016	.055	-1.842	.147	5.9
0.8375	90	2.021	-.038	-.243	-2.006	.034	2.8
0.8375	135	2.020	-.103	-.264	-2.000	.023	3.2

x/R	ψ, deg	\bar{v}_R/v_0	\bar{v}_x/v_0	\bar{v}_y/v_0	\bar{v}_z/v_0	σ_{v_R}/v_0	$\sigma_\epsilon, \text{deg}$
0.8500	0	1.710	-.537	-.173	-1.615	.173	20.5
0.8500	45	1.820	-.021	.021	-1.820	.229	13.0
0.8500	90	1.931	.026	-.114	-1.928	.236	10.3
0.8500	135	1.954	-.104	-.237	-1.937	.244	12.2
0.8625	0	1.561	-.555	-.334	-1.420	.235	20.2
0.8625	45	1.474	.066	.022	-1.473	.366	21.5
0.8625	90	1.932	.278	-.138	-1.907	.180	14.2
0.8625	135	2.057	-.255	-.169	-2.034	.313	21.8
0.8750	0	1.507	-.282	-.280	-1.454	.344	18.7
0.8750	45	1.820	.529	-.224	-1.727	.187	14.0
0.8750	90	2.160	.048	-.296	-2.139	.621	23.3
0.8750	135	1.872	-.532	-.460	-1.735	.362	24.8
0.8875	0	1.279	-.118	-.254	-1.248	.436	24.3
0.8875	45	1.594	.543	-.306	-1.468	.431	17.6
0.8875	90	1.512	.625	-.110	-1.372	.877	44.6
0.8875	135	1.218	-.488	-.358	-1.057	.796	43.6
0.9000	0	.509	-.091	-.316	-.389	.291	42.5
0.9000	45	.672	.240	-.364	-.511	.407	43.5
0.9000	90	.464	.197	-.391	-.156	.360	49.0
0.9000	135	.652	-.238	-.595	-.121	.299	36.2
0.9125	0	.744	-.189	-.273	-.666	.293	29.3
0.9125	45	.798	.281	-.149	-.732	.453	38.9
0.9125	90	.894	.820	-.343	-.097	.529	39.2
0.9125	135	.624	-.437	-.412	.168	.889	44.3
0.9250	0	.387	-.083	-.365	-.098	.240	46.7
0.9250	45	.492	-.004	-.488	-.063	.237	38.7
0.9250	90	.481	.038	-.477	-.043	.285	39.8
0.9250	135	.452	-.018	-.451	-.013	.243	44.0
0.9500	0	.503	-.328	-.381	.034	.377	39.9
0.9500	45	.475	-.164	-.438	.083	.469	39.2
0.9500	90	.454	-.147	-.426	.054	.584	44.5
0.9500	135	.506	-.157	-.451	.168	.595	44.3
1.0000	0	.692	-.073	-.676	.128	.091	11.3
1.0000	45	.727	-.013	-.720	.101	.102	12.1
1.0000	90	.736	-.053	-.723	.124	.105	10.3
1.0000	135	.736	-.062	-.718	.152	.111	10.7

x/R	ψ, deg	\bar{v}_R/v_o	\bar{v}_x/v_o	\bar{v}_y/v_o	\bar{v}_z/v_o	σ_{v_R}/v_o	$\sigma_\epsilon, \text{deg}$
1.1000	0	.376	-.080	-.347	.120	.089	15.8
1.1000	45	.392	-.041	-.369	.126	.099	16.7
1.1000	90	.393	-.062	-.366	.127	.098	15.8
1.1000	135	.400	-.083	-.371	.126	.094	14.1
1.2000	0	.375	-.100	-.354	.075	.062	16.9
1.2000	45	.383	-.079	-.361	.102	.068	14.6
1.2000	90	.377	-.086	-.355	.094	.067	15.1
1.2000	135	.394	-.110	-.367	.094	.070	14.8
1.3000	0	.344	-.007	-.338	.064	.057	14.8
1.3000	45	.348	-.006	-.341	.069	.065	16.0
1.3000	90	.336	.002	-.329	.067	.062	16.3
1.3000	135	.324	-.007	-.318	.059	.058	18.1
1.4000	0	.422	-.068	-.406	.094	.045	14.6
1.4000	45	.436	-.046	-.424	.089	.051	15.3
1.4000	90	.433	-.057	-.421	.087	.054	14.3
1.4000	135	.424	-.039	-.411	.095	.053	14.6
1.5000	0	.343	.122	-.318	.047	.034	8.9
1.5000	45	.345	.129	-.317	.045	.037	9.2
1.5000	90	.344	.135	-.313	.045	.035	8.8
1.5000	135	.343	.142	-.311	.030	.038	8.6

TEST CONDITION 1, $z/R = -0.25$
 $\Omega R = 625 \text{ ft/sec}$, $\theta_{75} = 6.27 \text{ deg}$, $C_T = 0.0022$

x/R	ψ, deg	\bar{v}_R/v_o	\bar{v}_x/v_o	\bar{v}_y/v_o	\bar{v}_z/v_o	σ_{v_R}/v_o	$\sigma_\epsilon, \text{deg}$
0.3125	0	.987	-.091	.093	-.979	.296	7.3
0.3125	45	1.013	-.055	.113	-1.005	.278	7.0
0.3125	90	.975	-.099	.090	-.965	.273	5.7
0.3125	135	.936	-.127	.102	-.922	.277	6.2
0.4000	0	1.205	-.137	.186	-1.182	.249	6.5
0.4000	45	1.173	-.173	.127	-1.153	.286	5.9
0.4000	90	1.174	-.145	.173	-1.152	.333	7.5
0.4000	135	1.167	-.149	.267	-1.126	.271	8.4
0.5000	0	1.395	-.252	.185	-1.360	.286	5.1
0.5000	45	1.383	-.269	.204	-1.341	.298	7.7
0.5000	90	1.374	-.219	.195	-1.343	.300	4.4
0.5000	135	1.386	-.226	.203	-1.353	.270	3.5

x/R	$\psi, \text{ } ^\circ$	\bar{v}_R/v_o	\bar{v}_x/v_o	\bar{v}_y/v_o	\bar{v}_z/v_o	σ_{v_R}/v_o	$\sigma_\epsilon, \text{deg}$
0.6000	0	1.458	-.209	.127	-1.438	.282	4.2
0.6000	45	1.420	-.206	.189	-1.393	.287	8.1
0.6000	90	1.411	-.203	.116	-1.392	.273	3.6
0.6000	135	1.430	-.179	.219	-1.402	.275	6.8
0.7000	0	1.621	-.327	.047	-1.587	.350	7.4
0.7000	45	1.639	-.367	.050	-1.597	.335	10.9
0.7000	90	1.609	-.343	.105	-1.569	.341	9.8
0.7000	135	1.618	-.382	-.064	-1.571	.317	4.0
0.7500	0	1.704	-.306	.037	-1.676	.426	6.5
0.7500	45	1.589	-.321	.102	-1.553	.348	10.7
0.7500	90	1.555	-.232	.109	-1.534	.268	7.3
0.7500	135	1.632	-.226	.055	-1.615	.234	4.4
0.7625	0	1.649	-.417	-.073	-1.594	.460	15.8
0.7625	45	1.509	-.318	-.080	-1.473	.346	11.1
0.7625	90	1.568	-.222	-.153	-1.544	.322	10.4
0.7625	135	1.670	-.347	-.128	-1.629	.258	13.9
0.7750	0	1.679	-.383	.021	-1.635	.512	16.5
0.7750	45	1.596	-.449	.020	-1.532	.481	18.3
0.7750	90	1.508	-.213	-.083	-1.490	.335	13.6
0.7750	135	1.583	-.253	-.054	-1.562	.339	10.1
0.7875	0	1.594	-.548	.274	-1.471	.690	27.9
0.7875	45	1.454	-.315	.093	-1.416	.424	20.3
0.7875	90	1.485	-.091	.140	-1.476	.512	22.9
0.7875	135	1.649	-.280	.105	-1.622	.630	34.7
0.8000	0	1.689	-.640	-.085	-1.561	.551	18.1
0.8000	45	1.512	-.338	-.204	-1.459	.349	18.7
0.8000	90	1.710	-.206	-.094	-1.695	.363	18.0
0.8000	135	1.668	-.235	-.132	-1.646	.405	18.6
0.8125	0	.950	-.408	.093	-.852	.577	42.6
0.8125	45	.914	-.327	.029	-.853	.421	38.6
0.8125	90	.914	.032	.139	-.903	.462	41.6
0.8125	135	.811	-.121	.261	-.758	.735	52.1
0.8250	0	1.105	-.224	.106	-1.077	.534	37.8
0.8250	45	1.207	-.251	.132	-1.174	.412	29.0
0.8250	90	1.185	-.064	.000	-1.183	.502	28.6
0.8250	135	1.147	-.015	-.138	-1.139	.458	32.4

x/R	ψ, deg	\bar{v}_R/v_o	\bar{v}_x/v_o	\bar{v}_y/v_o	\bar{v}_z/v_o	σ_{v_R}/v_o	$\sigma_\epsilon, \text{deg}$
0.8375	0	.682	-.498	.103	-.454	.465	41.9
0.8375	45	.638	-.156	.010	-.618	.474	41.3
0.8375	90	.774	.193	.087	-.744	.703	51.7
0.8375	135	.570	.059	-.094	-.559	.842	57.9
0.8500	0	.820	.037	.317	-.756	.508	43.0
0.8500	45	.988	.022	.246	-.957	.581	41.6
0.8500	90	.916	.037	.283	-.870	.493	39.2
0.8500	135	.775	.140	.148	-.748	.447	40.3
0.9000	0	.325	-.110	.216	-.216	.545	56.9
0.9000	45	.452	.094	.181	-.403	.543	55.7
0.9000	90	.360	.027	.272	-.234	.433	56.7
0.9000	135	.352	.046	.149	-.316	.500	56.9
0.9500	0	.229	-.130	.186	.027	.144	42.6
0.9500	45	.206	-.123	.164	.004	.149	44.4
0.9500	90	.220	-.116	.180	.050	.138	42.9
0.9500	135	.212	-.067	.182	.086	.165	46.6
1.0000	0	.044	-.038	.015	.017	.100	61.4
1.0000	45	.029	-.024	.000	.016	.130	61.1
1.0000	90	.057	-.051	.001	.024	.115	54.1
1.0000	135	.037	-.024	-.002	.029	.124	57.6
1.1000	0	.127	-.073	.076	.070	.044	24.0
1.1000	45	.121	-.077	.070	.062	.040	24.4
1.1000	90	.130	-.079	.082	.064	.038	19.1
1.1000	135	.127	-.087	.067	.064	.035	21.2
1.2000	0	.127	-.092	.075	.044	.040	14.9
1.2000	45	.127	-.093	.075	.043	.038	15.9
1.2000	90	.134	-.094	.083	.047	.040	13.6
1.2000	135	.130	-.095	.077	.045	.039	14.3
1.3000	0	.134	-.049	-.119	.039	.053	15.6
1.3000	45	.132	-.045	-.118	.039	.054	20.7
1.3000	90	.134	-.048	-.120	.037	.050	17.8
1.3000	135	.132	-.043	-.121	.031	.050	17.9
1.4000	0	.060	.002	.043	-.042	.036	51.0
1.4000	45	.060	.002	.039	-.046	.035	48.3
1.4000	90	.065	-.001	.037	-.053	.034	42.8
1.4000	135	.067	-.001	.043	-.051	.035	41.6

x/R	ψ, deg	\bar{v}_R/v_o	\bar{v}_x/v_o	\bar{v}_y/v_o	\bar{v}_z/v_o	σ_{v_R}/v_o	$\sigma_\epsilon, \text{deg}$
1.5000	0	.023	.019	.012	-.002	.034	55.0
1.5000	45	.022	.020	.009	-.002	.035	58.4
1.5000	90	.012	.010	.006	.001	.045	52.0
1.5000	135	.015	.010	.010	.006	.041	40.7

TEST CONDITION 2, $z/R = -0.25$

$\Omega R = 439 \text{ ft/sec}$, $\theta_{75} = 9.90 \text{ deg}$, $C_T = 0.0044$

x/R	ψ, deg	\bar{v}_R/v_o	\bar{v}_x/v_o	\bar{v}_y/v_o	\bar{v}_z/v_o	σ_{v_R}/v_o	$\sigma_\epsilon, \text{deg}$
0.3125	0	.984	.090	.247	-.949	.136	12.6
0.3125	45	1.007	-.066	.098	-1.000	.144	10.3
0.3125	90	.938	-.041	-.044	-.936	.073	7.8
0.3125	135	.809	-.016	-.037	-.808	.076	7.6
0.4000	0	1.326	-.018	.065	-1.324	.026	2.6
0.4000	45	1.283	-.130	.001	-1.276	.032	2.7
0.4000	90	1.337	.040	.102	-1.333	.060	4.0
0.4000	135	1.342	.098	.021	-1.338	.034	2.6
0.5000	0	1.436	-.119	.098	-1.428	.021	2.6
0.5000	45	1.467	-.103	.230	-1.445	.075	4.7
0.5000	90	1.483	-.010	.028	-1.483	.032	2.7
0.5000	135	1.413	-.033	.039	-1.412	.035	2.6
0.6000	0	1.577	-.199	.108	-1.560	.024	2.6
0.6000	45	1.615	-.076	.125	-1.608	.085	3.3
0.6000	90	1.596	-.086	.029	-1.593	.044	2.6
0.6000	135	1.566	-.144	.037	-1.559	.051	2.6
0.7000	0	1.638	-.197	.023	-1.626	.039	2.8
0.7000	45	1.787	-.000	-.039	-1.787	.051	3.0
0.7000	90	1.757	-.062	-.049	-1.756	.047	2.9
0.7000	135	1.765	-.117	-.045	-1.760	.045	2.6
0.7500	0	1.622	-.176	.007	-1.613	.091	6.1
0.7500	45	1.819	.121	.176	-1.806	.126	7.0
0.7500	90	1.757	.031	.040	-1.756	.101	5.0
0.7500	135	1.816	-.039	.023	-1.815	.090	5.3
0.8000	0	1.866	-.158	.273	-1.839	.247	7.9
0.8000	45	1.957	-.123	.142	-1.947	.142	6.6
0.8000	90	1.897	-.215	.154	-1.879	.171	6.6
0.8000	135	1.982	-.118	.029	-1.978	.251	9.2

x/R	ψ, deg	\bar{v}_R/v_o	\bar{v}_x/v_o	\bar{v}_y/v_o	\bar{v}_z/v_o	σ_{v_R}/v_o	$\sigma_\epsilon, \text{deg}$
0.8125	0	1.828	-.031	.077	-1.826	.227	7.2
0.8125	45	2.155	-.018	-.061	-2.154	.181	6.0
0.8125	90	1.885	-.262	-.017	-1.866	.153	6.9
0.8125	135	1.782	.014	-.123	-1.778	.203	10.1
0.8250	0	1.851	.145	.158	-1.839	.148	7.0
0.8250	45	2.290	-.140	.030	-2.285	.104	5.6
0.8250	90	1.860	-.232	.029	-1.845	.070	3.4
0.8250	135	1.745	.148	-.115	-1.735	.100	4.6
0.8375	0	1.847	.207	.076	-1.834	.191	5.2
0.8375	45	2.333	-.115	-.030	-2.330	.227	13.3
0.8375	90	1.822	-.296	-.069	-1.797	.218	9.6
0.8375	135	1.570	.146	-.070	-1.562	.236	8.0
0.8500	0	1.628	.352	.011	-1.590	.216	8.1
0.8500	45	2.732	-.037	.098	-2.730	.575	5.1
0.8500	90	1.805	-.529	-.133	-1.720	.282	10.3
0.8500	135	1.230	.068	-.163	-1.217	.189	12.4
0.8625	0	1.415	.466	-.145	-1.328	.151	12.9
0.8625	45	3.063	.975	-.261	-2.892	.495	8.1
0.8625	90	2.022	-.827	-.361	-1.810	.240	19.2
0.8625	135	1.009	-.046	-.350	-.945	.257	18.6
0.8750	0	1.444	.679	-.245	-1.250	.079	10.0
0.8750	45	4.989	.335	-.327	-4.967	.836	10.6
0.8750	90	1.657	-.751	-.338	-1.438	.132	7.2
0.8750	135	.783	-.044	-.276	-.731	.131	21.9
0.8875	0	1.210	1.055	.038	-.593	.148	16.7
0.8875	45	1.790	-.930	.163	1.521	1.286	45.0
0.8875	90	1.006	-.674	-.176	-.725	.301	25.6
0.8875	135	.571	.038	-.203	-.532	.246	31.4
0.9000	0	1.036	.791	-.240	-.624	.114	15.1
0.9000	45	2.501	.830	-.113	2.356	.931	38.3
0.9000	90	1.309	-1.094	-.382	-.608	.144	11.5
0.9000	135	.578	-.265	-.273	-.435	.092	18.3
0.9125	0	.793	.712	-.245	-.249	.146	21.2
0.9125	45	1.216	-.162	-.264	1.175	.179	19.3
0.9125	90	.835	-.784	-.280	-.057	.127	16.0
0.9125	135	.513	-.385	-.280	-.191	.124	21.9

x/R	ψ, deg	\bar{v}_R/v_o	\bar{v}_x/v_o	\bar{v}_y/v_o	\bar{v}_z/v_o	σ_{V_R}/v_o	$\sigma_\epsilon, \text{deg}$
0.9250	0	.552	.472	-.260	-.120	.188	26.6
0.9250	45	.725	-.281	-.440	.503	.166	22.3
0.9250	90	.574	-.504	-.269	.050	.148	16.1
0.9250	135	.438	-.315	-.291	-.085	.148	23.7
0.9500	0	.290	.143	-.238	-.084	.205	34.4
0.9500	45	.379	.016	-.361	.116	.125	33.2
0.9500	90	.450	-.224	-.384	.071	.140	30.2
0.9500	135	.451	-.295	-.341	-.003	.079	23.5
1.0000	0	.238	-.011	-.238	.012	.055	16.3
1.0000	45	.328	.039	-.316	.080	.083	15.7
1.0000	90	.381	-.132	-.348	.082	.051	11.3
1.0000	135	.403	-.212	-.323	.115	.057	14.0
1.1000	0	.327	-.143	-.294	.020	.018	5.8
1.1000	45	.355	-.079	-.345	.028	.020	7.5
1.1000	90	.370	-.138	-.339	.053	.020	6.8
1.1000	135	.379	-.183	-.332	.010	.018	5.4
1.2000	0	.316	-.088	-.303	.017	.011	6.2
1.2000	45	.337	-.036	-.335	.009	.016	3.1
1.2000	90	.341	-.074	-.332	.021	.014	3.8
1.2000	135	.337	-.114	-.316	.029	.014	5.8
1.3000	0	.251	-.081	-.237	-.008	.053	21.2
1.3000	45	.252	-.053	-.246	.009	.058	24.1
1.3000	90	.257	-.067	-.248	.004	.057	24.8
1.3000	135	.260	-.086	-.245	-.009	.065	22.8
1.4000	0	.276	-.084	-.263	-.003	.040	13.7
1.4000	45	.280	-.070	-.271	.015	.035	13.8
1.4000	90	.279	-.074	-.268	.005	.035	14.2
1.4000	135	.281	-.076	-.271	.002	.044	14.1
1.5000	0	.279	-.020	-.278	-.003	.013	3.4
1.5000	45	.275	-.014	-.274	.001	.013	3.7
1.5000	90	.275	-.020	-.274	.003	.014	3.2
1.5000	135	.275	-.020	-.275	.000	.013	3.1

TEST CONDITION 3, $z/R = -0.25$
 $\Omega R = 444 \text{ ft/sec}$, $\theta_{75} = 6.27 \text{ deg}$, $C_T = 0.0021$

x/R	ψ, deg	\bar{v}_R/v_o	\bar{v}_x/v_o	\bar{v}_y/v_o	\bar{v}_z/v_o	σ_{v_R}/v_o	$\sigma_\epsilon, \text{deg}$
0.3125	0	1.034	-.090	-.119	-1.024	.116	8.1
0.3125	45	1.091	-.073	-.230	-1.064	.080	6.4
0.3125	90	1.023	-.068	-.093	-1.016	.085	7.8
0.3125	135	1.037	.060	-.177	-1.020	.118	11.1
0.4000	0	1.270	-.080	-.142	-1.260	.068	5.4
0.4000	45	1.490	.123	-.196	-1.472	.082	5.4
0.4000	90	1.417	.020	-.330	-1.378	.075	3.5
0.4000	135	1.299	-.036	-.290	-1.265	.068	3.1
0.5000	0	1.716	.067	-.164	-1.707	.033	2.8
0.5000	45	1.743	-.026	-.192	-1.732	.028	2.9
0.5000	90	1.712	-.135	-.227	-1.691	.040	2.7
0.5000	135	1.728	.016	-.138	-1.723	.046	2.9
0.6000	0	1.781	-.024	-.150	-1.774	.170	2.8
0.6000	45	1.808	-.060	-.185	-1.798	.170	2.8
0.6000	90	1.779	-.063	-.167	-1.770	.183	3.5
0.6000	135	1.766	-.092	-.149	-1.757	.153	3.4
0.7000	0	1.880	-.092	-.176	-1.869	.022	2.6
0.7000	45	1.906	-.115	-.217	-1.891	.031	2.6
0.7000	90	1.828	-.123	-.229	-1.809	.032	3.4
0.7000	135	1.827	-.064	-.193	-1.816	.044	2.6
0.7500	0	1.912	-.180	-.187	-1.894	.183	3.1
0.7500	45	1.911	-.186	-.220	-1.889	.197	2.9
0.7500	90	1.834	-.123	.075	-1.828	.167	6.7
0.7500	135	1.833	-.126	-.199	-1.818	.167	3.1
0.7125	0	1.964	-.194	-.184	-1.946	.029	2.8
0.7125	45	1.957	-.213	-.224	-1.932	.035	3.4
0.7125	90	1.811	-.153	.011	-1.804	.094	6.4
0.7125	135	1.872	-.105	-.266	-1.850	.050	2.7
0.7250	0	1.978	-.211	-.180	-1.958	.037	2.7
0.7250	45	1.951	-.199	-.241	-1.926	.025	2.7
0.7250	90	1.814	-.114	.152	-1.804	.082	6.3
0.7250	135	1.865	-.088	-.236	-1.848	.045	2.6
0.7375	0	2.013	-.228	.011	-2.000	.097	7.1
0.7375	45	1.946	-.269	-.108	-1.924	.071	8.8
0.7375	90	1.872	-.190	.027	-1.862	.151	7.8
0.7375	135	1.874	-.112	-.151	-1.864	.120	5.2

x/R	ψ, deg	\bar{v}_R/v_o	\bar{v}_x/v_o	\bar{v}_y/v_o	\bar{v}_z/v_o	σ_{v_R}/v_o	$\sigma_\epsilon, \text{deg}$
0.8000	0	2.042	-.274	.174	-2.016	.207	9.4
0.8000	45	1.897	-.318	-.060	-1.869	.174	7.8
0.8000	90	1.702	-.183	.007	-1.692	.187	10.2
0.8000	135	1.798	-.106	-.118	-1.791	.137	6.0
0.8125	0	1.970	-.399	-.120	-1.926	.183	11.2
0.8125	45	1.870	-.385	-.219	-1.817	.098	9.2
0.8125	90	1.742	-.172	-.086	-1.732	.117	7.4
0.8125	135	1.856	-.022	-.201	-1.845	.046	2.6
0.8250	0	1.920	-.421	-.050	-1.873	.107	12.7
0.8250	45	1.840	-.342	-.247	-1.791	.090	7.6
0.8250	90	1.771	-.052	.111	-1.767	.106	5.9
0.8250	135	1.858	.024	-.199	-1.847	.053	2.6
0.8325	0	1.840	-.573	-.193	-1.738	.169	14.1
0.8325	45	1.763	-.321	-.203	-1.721	.164	11.6
0.8325	90	1.689	-.005	.041	-1.688	.112	7.6
0.8325	135	1.858	.075	-.148	-1.850	.062	2.7
0.8500	0	1.769	-.611	-.161	-1.652	.201	17.9
0.8500	45	1.737	-.403	-.326	-1.658	.180	13.6
0.8500	90	1.715	.020	-.029	-1.714	.204	9.2
0.8500	135	1.865	.103	-.160	-1.856	.114	3.0
0.9000	0	1.318	-.594	-.439	-1.091	.314	18.6
0.9000	45	1.292	-.304	-.325	-1.213	.334	22.2
0.9000	90	1.128	.058	-.127	-1.119	.306	26.0
0.9000	135	1.434	.547	-.272	-1.297	.250	13.2
0.9500	0	.526	-.315	-.281	-.313	.381	44.8
0.9500	45	.561	-.048	-.260	-.495	.346	44.3
0.9500	90	.508	.096	-.273	-.418	.460	44.4
0.9500	135	.342	.192	-.213	-.186	.514	55.0
1.0000	0	.366	-.161	-.314	-.099	.133	34.4
1.0000	45	.349	-.077	-.324	-.106	.148	32.9
1.0000	90	.361	-.010	-.342	-.117	.267	38.1
1.0000	135	.312	-.020	-.309	-.037	.239	42.0
1.1000	0	.318	-.138	-.285	.032	.027	5.6
1.1000	45	.324	-.098	-.300	.071	.030	6.8
1.1000	90	.323	-.113	-.296	.064	.022	6.0
1.1000	135	.327	-.124	-.298	.050	.028	6.9

x/R	ψ, deg	\bar{V}_R/v_o	\bar{v}_x/v_o	\bar{v}_y/v_o	\bar{v}_z/v_o	σ_{V_R}/v_o	$\sigma_\epsilon, \text{deg}$
1.2000	0	.276	-.086	-.254	.065	.027	6.1
1.2000	45	.284	-.067	-.266	.072	.029	6.8
1.2000	90	.288	-.085	-.264	.075	.031	5.2
1.2000	135	.287	-.099	-.262	.064	.029	4.4
1.3000	0	.319	.023	-.318	.007	.023	3.4
1.3000	45	.326	.028	-.324	.008	.024	4.4
1.3000	90	.319	.018	-.319	.008	.024	3.7
1.3000	135	.316	.023	-.315	.006	.025	3.7
1.4000	0	.188	.002	-.187	.012	.061	31.1
1.4000	45	.184	.012	-.184	.005	.061	35.3
1.4000	90	.186	-.005	-.186	.005	.058	31.3
1.4000	135	.181	-.001	-.181	.004	.064	34.8
1.5000	0	.246	.073	-.234	-.021	.043	19.3
1.5000	45	.253	.072	-.241	-.027	.035	15.0
1.5000	90	.251	.063	-.242	-.026	.045	17.5
1.5000	135	.249	.056	-.241	-.034	.037	17.1

TEST CONDITION 1, $z/R = -0.30$

$\Omega R = 628 \text{ ft/sec}$, $\theta_{75} = 6.00 \text{ deg}$, $C_T = 0.0016$

x/R	ψ, deg	\bar{V}_R/v_o	\bar{v}_x/v_o	\bar{v}_y/v_o	\bar{v}_z/v_o	σ_{V_R}/v_o	$\sigma_\epsilon, \text{deg}$
0.3125	0	1.044	-.158	.018	-1.032	.369	9.2
0.3125	45	1.028	-.138	-.015	-1.018	.373	7.5
0.3125	90	1.013	-.159	-.002	-1.000	.359	8.2
0.3125	135	1.008	-.195	-.010	-.999	.368	9.5
0.4000	0	1.364	-.267	.023	-1.337	.372	6.4
0.4000	45	1.358	-.249	-.018	-1.335	.374	7.2
0.4000	90	1.358	-.208	-.043	-1.341	.408	5.4
0.4000	135	1.345	-.243	-.007	-1.323	.404	6.3
0.5000	0	1.416	-.150	.092	-1.405	.348	4.6
0.5000	45	1.411	-.128	.101	-1.401	.390	5.0
0.5000	90	1.386	-.143	.089	-1.376	.392	5.2
0.5000	135	1.393	-.160	.114	-1.379	.401	6.0
0.6000	0	1.569	-.197	.376	-1.511	.388	8.9
0.6000	45	1.544	-.330	.204	-1.494	.384	8.1
0.6000	90	1.515	-.317	.211	-1.466	.363	6.9
0.6000	135	1.523	-.232	.317	-1.471	.362	10.9

x/R	ψ, deg	\bar{V}_R/v_o	\bar{V}_x/v_o	\bar{V}_y/v_o	\bar{V}_z/v_o	σ_{V_R}/v_o	$\sigma_\epsilon, \text{deg}$
0.7000	0	1.536	-.316	-.293	-1.475	.348	9.4
0.7000	45	1.550	-.322	-.390	-1.465	.387	8.4
0.7000	90	1.552	-.295	-.409	-1.468	.388	8.3
0.7000	135	1.538	-.288	-.314	-1.478	.369	8.1
0.7500	0	1.523	.140	-.023	-1.517	.422	8.2
0.7500	45	1.543	.148	-.187	-1.524	.429	7.6
0.7500	90	1.512	.099	-.153	-1.501	.398	11.5
0.7500	135	1.499	.116	-.081	-1.492	.386	10.0
0.7750	0	1.666	.041	-.008	-1.666	.443	7.4
0.7750	45	1.663	-.028	-.005	-1.663	.457	6.9
0.7750	90	1.605	-.008	.063	-1.604	.453	9.8
0.7750	135	1.633	-.020	-.014	-1.632	.391	10.2
0.7875	0	1.557	-.117	.350	-1.513	.374	12.0
0.7875	45	1.571	-.047	.217	-1.556	.411	11.4
0.7875	90	1.449	-.152	.197	-1.428	.500	15.5
0.7875	135	1.463	-.113	.322	-1.423	.460	13.4
0.8000	0	1.559	-.138	.031	-1.552	.474	4.7
0.8000	45	1.549	-.189	.028	-1.538	.475	3.9
0.8000	90	1.524	-.201	.038	-1.510	.406	16.5
0.8000	135	1.532	-.128	.092	-1.524	.396	5.9
0.8125	0	1.711	-.072	.335	-1.676	.458	8.4
0.8125	45	1.685	-.080	.331	-1.650	.450	7.4
0.8125	90	1.658	-.053	.417	-1.604	.416	8.4
0.8125	135	1.648	-.097	.326	-1.612	.329	7.2
0.8250	0	1.729	-.156	.218	-1.708	.572	13.1
0.8250	45	1.755	-.329	.164	-1.716	.628	17.1
0.8250	90	1.664	-.262	.222	-1.628	.460	15.1
0.8250	135	1.615	-.112	.251	-1.591	.350	10.4
0.8375	0	1.654	-.035	-.029	-1.653	.388	5.5
0.8375	45	1.647	-.028	-.053	-1.646	.388	4.7
0.8375	90	1.600	-.019	.002	-1.600	.364	8.0
0.8375	135	1.633	-.036	.070	-1.631	.339	7.4
0.8500	0	1.142	.274	.211	-1.089	.540	33.4
0.8500	45	1.214	-.040	.131	-1.206	.478	29.2
0.8500	90	1.037	-.352	.431	-.875	.837	39.8
0.8500	135	1.248	-.194	.005	-1.233	.512	33.0

x/R	ψ, deg	\bar{v}_R/v_o	\bar{v}_x/v_o	\bar{v}_y/v_o	\bar{v}_z/v_o	σ_{v_R}/v_o	$\sigma_\epsilon, \text{deg}$
0.8625	0	1.215	-.137	.088	-1.204	.466	23.3
0.8625	45	1.127	-.390	-.022	-1.057	.310	26.4
0.8625	90	1.394	-.339	.092	-1.349	.234	15.5
0.8625	135	1.222	-.123	.049	-1.215	.299	17.4
0.8750	0	1.326	-.385	.052	-1.268	.978	28.3
0.8750	45	.901	-.309	-.093	-.841	.597	39.9
0.8750	90	.932	-.312	-.052	-.877	.452	40.0
0.8750	135	1.076	-.331	.016	-1.024	.467	32.9
0.9000	0	.145	-.130	-.064	-.012	.335	47.7
0.9000	45	.200	-.185	-.056	-.049	.241	50.9
0.9000	90	.223	-.170	-.054	-.134	.202	47.9
0.9000	135	.199	-.104	-.055	-.161	.205	53.1
0.9500	0	.137	-.062	-.120	-.018	.082	41.0
0.9500	45	.159	-.056	-.147	-.023	.114	40.9
0.9500	90	.176	-.103	-.143	.011	.103	35.9
0.9500	135	.162	-.098	-.126	-.031	.115	41.2
1.0000	0	.114	-.004	-.083	-.077	.265	52.6
1.0000	45	.129	-.049	-.066	-.100	.203	59.1
1.0000	90	.121	-.037	-.087	-.075	.208	55.4
1.0000	135	.144	-.009	-.108	-.095	.193	50.3
1.1000	0	.163	-.089	-.112	.078	.091	39.2
1.1000	45	.157	-.085	-.110	.074	.090	37.0
1.1000	90	.165	-.096	-.101	.088	.097	36.8
1.1000	135	.171	-.112	-.108	.070	.098	35.2
1.2000	0	.197	-.061	.089	-.165	.071	16.4
1.2000	45	.192	-.052	.086	-.163	.069	19.6
1.2000	90	.192	-.055	.083	-.164	.070	18.0
1.2000	135	.193	-.057	.083	-.164	.067	16.7
1.3000	0	.270	-.017	-.166	-.212	.099	17.4
1.3000	45	.267	-.007	-.158	-.215	.092	16.0
1.3000	90	.265	-.022	-.153	-.216	.094	14.8
1.3000	135	.272	-.017	-.167	-.214	.095	14.2
1.4000	0	.111	-.078	.078	.011	.043	28.5
1.4000	45	.114	-.081	.079	.012	.045	27.4
1.4000	90	.119	-.086	.082	.013	.045	19.7
1.4000	135	.115	-.085	.076	.012	.045	22.3

x/R	ψ, deg	\bar{v}_R/v_o	\bar{v}_x/v_o	\bar{v}_y/v_o	\bar{v}_z/v_o	σ_{v_R}/v_o	$\sigma_\epsilon, \text{deg}$
1.5000	0	.122	-.012	.044	-.113	.077	37.8
1.5000	45	.114	-.021	.045	-.102	.084	45.6
1.5000	90	.120	-.017	.038	-.113	.082	39.8
1.5000	135	.121	-.032	.049	-.106	.080	40.8

TEST CONDITION 2, $z/R = -0.30$
 $\Omega R = 450 \text{ ft/sec}$, $\theta_{75} = 9.69 \text{ deg}$, $C_T = 0.0040$

x/R	ψ, deg	\bar{v}_R/v_o	\bar{v}_x/v_o	\bar{v}_y/v_o	\bar{v}_z/v_o	σ_{v_R}/v_o	$\sigma_\epsilon, \text{deg}$
0.3125	0	.619	.005	.407	-.467	.090	21.0
0.3125	45	.630	.009	.345	-.527	.058	12.2
0.3125	90	.593	.005	.307	-.508	.079	17.1
0.3125	135	.546	.100	.317	-.433	.080	22.3
0.4000	0	1.092	.127	.459	-.983	.071	7.4
0.4000	45	.933	.005	.369	-.857	.083	10.5
0.4000	90	1.153	.113	.404	-1.074	.056	7.5
0.4000	135	1.142	.114	.451	-1.043	.065	7.7
0.5000	0	1.447	.136	.285	-1.412	.021	2.7
0.5000	45	1.425	.070	.271	-1.397	.030	3.6
0.5000	90	1.345	.009	.261	-1.319	.034	3.1
0.5000	135	1.387	.143	.353	-1.334	.070	5.1
0.6000	0	1.566	.105	.292	-1.535	.035	2.7
0.6000	45	1.551	.054	.233	-1.532	.028	2.6
0.6000	90	1.640	.160	.398	-1.582	.068	3.5
0.6000	135	1.557	.136	.213	-1.536	.035	2.6
0.7000	0	1.654	.069	.295	-1.626	.031	2.6
0.7000	45	1.666	.056	.232	-1.648	.030	2.6
0.7000	90	1.695	.185	.234	-1.668	.044	3.2
0.7000	135	1.683	.130	.210	-1.665	.047	2.6
0.8000	0	1.502	.039	.232	-1.483	.254	12.7
0.8000	45	1.662	.072	.326	-1.629	.300	12.8
0.8000	90	1.649	.165	.129	-1.635	.268	12.5
0.8000	135	1.692	.135	.125	-1.682	.274	13.0
0.9000	0	1.672	.226	.197	-1.645	.109	5.3
0.9000	45	1.991	.293	.091	-1.968	.096	6.9
0.9000	90	1.942	.279	.082	-1.920	.179	4.1
0.9000	135	1.941	.480	-.031	-1.881	.220	6.3

x/R	ψ, deg	\bar{v}_R/v_0	\bar{v}_x/v_0	\bar{v}_y/v_0	\bar{v}_z/v_0	σ_{v_R}/v_0	$\sigma_\epsilon, \text{deg}$
0.9250	0	1.503	.329	.232	-1.447	.271	15.8
0.9250	45	1.940	.486	-.014	-1.879	.478	15.9
0.9250	90	1.896	.189	-.028	-1.886	.353	15.3
0.9250	135	1.628	.370	-.091	-1.583	.292	17.0
0.9375	0	1.420	.346	.105	-1.373	.142	9.1
0.9375	45	2.168	.937	-.243	-1.941	.467	10.0
0.9375	90	2.308	.079	-.204	-2.297	.397	20.4
0.9375	135	1.498	.110	-.160	-1.485	.302	18.7
0.9500	0	1.357	.501	.044	-1.261	.172	15.0
0.9500	45	2.288	1.777	.133	-1.434	1.083	29.3
0.9500	90	2.308	.019	.107	-2.306	.630	25.6
0.9500	135	1.431	.063	-.160	-1.420	.334	25.1
0.9625	0	1.172	.368	.204	-1.094	.255	19.0
0.9625	45	1.798	1.167	-.161	-1.358	.447	18.7
0.9625	90	2.874	.448	-.455	-2.802	.520	17.7
0.9625	135	1.530	-.110	-.159	-1.518	.227	18.6
0.9750	0	.837	.207	.184	-.790	.332	29.0
0.9750	45	1.060	.886	.066	-.579	.364	25.2
0.9750	90	1.901	1.885	-.218	-.101	1.568	45.1
0.9750	135	1.426	-.697	-.460	-1.156	1.167	46.8
0.9875	0	.636	.189	.134	-.593	.240	20.1
0.9875	45	.976	.934	.122	-.257	.313	24.2
0.9875	90	1.264	.711	-.214	1.023	.714	48.1
0.9875	135	1.646	-1.633	-.022	-.207	.664	30.6
1.0000	0	.549	.119	.154	-.513	.161	22.4
1.0000	45	.722	.672	.163	-.205	.305	27.3
1.0000	90	.976	.513	.050	.829	.312	38.7
1.0000	135	1.379	-1.323	.028	.386	.578	30.7
1.1000	0	.160	-.075	.085	-.114	.041	26.6
1.1000	45	.113	-.007	.049	-.101	.032	25.5
1.1000	90	.066	-.024	.046	-.041	.052	26.1
1.1000	135	.128	-.096	.067	.053	.048	35.7
1.2000	0	.104	-.007	.083	-.062	.044	36.4
1.2000	45	.086	.002	.056	-.065	.030	30.4
1.2000	90	.087	.004	.059	-.064	.028	31.1
1.2000	135	.099	-.009	.077	-.063	.034	35.3

x/R	ψ, deg	\bar{v}_R/v_o	\bar{v}_x/v_o	\bar{v}_y/v_o	\bar{v}_z/v_o	σ_{v_R}/v_o	$\sigma_\epsilon, \text{deg}$
1.3000	0	.025	.019	.015	-.006	.087	69.0
1.3000	45	.030	.026	-.004	-.015	.087	71.9
1.3000	90	.030	.022	-.005	-.019	.085	70.8
1.3000	135	.029	.027	.004	-.011	.076	71.5
1.4000	0	.067	.015	.045	-.047	.070	58.1
1.4000	45	.062	.021	.043	-.039	.075	50.2
1.4000	90	.060	.022	.043	-.036	.067	53.5
1.4000	135	.064	.012	.053	-.034	.067	55.9
1.5000	0	.028	-.022	.014	-.010	.091	65.5
1.5000	45	.018	-.016	.007	-.003	.099	71.7
1.5000	90	.018	-.017	.006	-.001	.100	74.7
1.5000	135	.034	-.022	.020	-.017	.089	61.4

TEST CONDITION 3, $z/R = -0.30$
 $\Omega R = 448 \text{ ft/sec}$, $\theta_{75} = 6.35 \text{ deg}$, $C_T = 0.0023$

x/R	ψ, deg	\bar{v}_R/v_o	\bar{v}_x/v_o	\bar{v}_y/v_o	\bar{v}_z/v_o	σ_{v_R}/v_o	$\sigma_\epsilon, \text{deg}$
0.3125	0	.919	.032	.493	-.775	.102	10.3
0.3125	45	.875	.047	.437	-.757	.093	10.9
0.3125	90	.892	.088	.438	-.772	.102	9.4
0.3125	135	.935	.080	.481	-.797	.108	11.6
0.4000	0	1.359	.270	.491	-1.238	.089	6.1
0.4000	45	1.318	.152	.401	-1.246	.065	4.1
0.4000	90	1.256	.107	.368	-1.196	.084	3.5
0.4000	135	1.421	.312	.424	-1.320	.090	4.3
0.5000	0	1.650	.062	.502	-1.570	.196	7.1
0.5000	45	1.714	.144	.276	-1.686	.169	4.5
0.5000	90	1.628	.061	.301	-1.599	.200	5.4
0.5000	135	1.571	.000	.370	-1.526	.229	6.4
0.6000	0	1.936	.167	.358	-1.895	.030	4.3
0.6000	45	1.918	.126	.301	-1.890	.032	4.4
0.6000	90	1.882	.101	.307	-1.854	.042	5.2
0.6000	135	1.904	.148	.546	-1.818	.082	7.7
0.7000	0	2.044	-.098	.214	-2.031	.046	3.9
0.7000	45	2.004	-.099	.175	-1.994	.055	3.7
0.7000	90	1.940	-.109	.154	-1.931	.044	3.8
0.7000	135	1.957	-.012	.511	-1.889	.081	6.8

x/R	ψ, deg	\bar{v}_R/v_o	\bar{v}_x/v_o	\bar{v}_y/v_o	\bar{v}_z/v_o	σ_{v_R/v_o}	$\sigma_\epsilon, \text{deg}$
0.7500	0	2.202	-.253	.258	-2.172	.252	5.1
0.7500	45	2.037	-.289	.208	-2.006	.230	6.3
0.7500	90	1.881	-.242	.198	-1.854	.177	7.2
0.7500	135	1.885	-.036	.519	-1.811	.153	7.4
0.7625	0	2.103	-.209	.227	-2.080	.051	2.8
0.7625	45	1.999	-.185	.174	-1.983	.048	2.7
0.7625	90	1.918	-.135	.175	-1.905	.038	3.1
0.7625	135	1.909	-.007	.331	-1.880	.072	4.6
0.7750	0	2.269	-.205	.326	-2.236	.077	6.6
0.7750	45	2.066	-.198	.300	-2.034	.061	3.0
0.7750	90	1.923	-.164	.284	-1.894	.043	4.2
0.7750	135	1.908	-.004	.593	-1.813	.124	6.7
0.7875	0	2.592	-.538	.777	-2.413	.535	22.5
0.7875	45	1.957	-.494	.075	-1.892	.186	12.3
0.7875	90	1.830	-.457	-.082	-1.770	.114	10.0
0.7875	135	1.681	-.090	.124	-1.674	.191	16.1
0.8000	0	1.358	-1.116	.699	-.331	.666	34.5
0.8000	45	1.638	-.857	.190	-1.383	.320	24.7
0.8000	90	1.743	-.552	.134	-1.647	.228	16.9
0.8000	135	1.684	-.116	.410	-1.630	.245	15.6
0.8125	0	.889	.013	.477	-.750	.559	45.8
0.8125	45	1.564	-.707	.460	-1.317	.425	27.5
0.8125	90	1.593	-.647	.353	-1.413	.356	22.2
0.8125	135	1.568	-.370	.410	-1.468	.313	23.6
0.8250	0	.988	-.723	.095	-.666	.424	36.5
0.8250	45	1.214	-.875	.072	-.839	.400	30.5
0.8250	90	1.309	-.482	.250	-1.191	.386	22.8
0.8250	135	1.364	-.109	.303	-1.326	.356	24.5
0.8375	0	.721	-.593	.356	-.205	.435	45.4
0.8375	45	.876	-.756	.129	-.424	.274	32.0
0.8375	90	.878	-.410	.045	-.775	.237	30.4
0.8375	135	.920	-.151	.189	-.888	.413	30.4
0.8500	0	1.062	-.933	.339	-.377	.432	32.1
0.8500	45	1.129	-.743	.247	-.814	.360	26.6
0.8500	90	1.171	-.264	.292	-1.103	.295	17.8
0.8500	135	1.186	.138	.364	-1.120	.336	21.1

x/R	ψ, deg	\bar{v}_R/v_0	\bar{v}_x/v_0	\bar{v}_y/v_0	\bar{v}_z/v_0	σ_{v_R}/v_0	$\sigma_\epsilon, \text{deg}$
0.9000	0	.366	-.226	.237	.162	.138	32.0
0.9000	45	.357	-.241	.248	.090	.114	31.1
0.9000	90	.320	-.204	.246	.017	.115	37.2
0.9000	135	.284	-.158	.235	.013	.129	38.5
0.9500	0	.335	-.150	.250	.164	.041	21.5
0.9500	45	.283	-.151	.212	.111	.047	25.6
0.9500	90	.288	-.180	.198	.107	.041	24.9
0.9500	135	.300	-.171	.206	.135	.038	23.4
1.0000	0	.322	-.169	.227	.154	.037	20.4
1.0000	45	.269	-.161	.180	.120	.044	24.4
1.0000	90	.284	-.152	.189	.147	.044	23.5
1.0000	135	.298	-.148	.204	.160	.039	22.2
1.1000	0	.237	-.220	.051	.072	.016	7.8
1.1000	45	.205	-.189	.043	.067	.017	9.8
1.1000	90	.227	-.215	.037	.063	.019	9.0
1.1000	135	.246	-.231	.047	.071	.019	9.0
1.2000	0	.252	-.237	.052	.066	.014	7.9
1.2000	45	.230	-.217	.048	.059	.014	11.7
1.2000	90	.244	-.232	.046	.058	.013	10.5
1.2000	135	.253	-.243	.041	.058	.015	6.7
1.3000	0	.249	-.199	.005	.149	.370	23.6
1.3000	45	.248	-.186	-.010	.164	.407	24.7
1.3000	90	.259	-.190	-.001	.176	.440	24.6
1.3000	135	.266	-.202	-.000	.173	.500	27.0
1.4000	0	.221	-.219	.010	.027	.029	8.6
1.4000	45	.212	-.210	.012	.026	.027	9.7
1.4000	90	.214	-.211	.010	.029	.026	11.4
1.4000	135	.223	-.222	.004	.024	.027	9.9
1.5000	0	.174	-.168	-.024	-.040	.037	30.2
1.5000	45	.168	-.163	-.022	-.032	.033	31.9
1.5000	90	.169	-.164	-.020	-.035	.036	32.5
1.5000	135	.164	-.157	-.019	-.042	.038	34.9